

## **INFORMATION TO USERS**

This manuscript has been reproduced from the microfilm master. UMI films the text directly from the original or copy submitted. Thus, some thesis and dissertation copies are in typewriter face, while others may be from any type of computer printer.

**The quality of this reproduction is dependent upon the quality of the copy submitted. Broken or indistinct print, colored or poor quality illustrations and photographs, print bleedthrough, substandard margins, and improper alignment can adversely affect reproduction.**

In the unlikely event that the author did not send UMI a complete manuscript and there are missing pages, these will be noted. Also, if unauthorized copyright material had to be removed, a note will indicate the deletion.

Oversize materials (e.g., maps, drawings, charts) are reproduced by sectioning the original, beginning at the upper left-hand corner and continuing from left to right in equal sections with small overlaps.

Photographs included in the original manuscript have been reproduced xerographically in this copy. Higher quality 6" x 9" black and white photographic prints are available for any photographs or illustrations appearing in this copy for an additional charge. Contact UMI directly to order.

Bell & Howell Information and Learning  
300 North Zeeb Road, Ann Arbor, MI 48106-1346 USA  
800-521-0600

**UMI<sup>®</sup>**



A new multiplexed absorbance detection approach for high-throughput PCR analysis,  
enzyme assay, peptide mapping and combinatorial homogeneous catalysis screening using  
96-capillary array electrophoresis

by

Xiaoyi Gong

A dissertation submitted to the graduate faculty  
in partial fulfillment of the requirements for the degree of  
DOCTOR OF PHILOSOPHY

Major: Analytical Chemistry

Major Professor: Edward S. Yeung

Iowa State University

Ames, Iowa

2000

**UMI Number: 9990446**

**UMI<sup>®</sup>**

---

**UMI Microform 9990446**

**Copyright 2001 by Bell & Howell Information and Learning Company.**

**All rights reserved. This microform edition is protected against  
unauthorized copying under Title 17, United States Code.**

---

**Bell & Howell Information and Learning Company  
300 North Zeeb Road  
P.O. Box 1346  
Ann Arbor, MI 48106-1346**

Graduate College  
Iowa State University

This is to certify that the Doctoral dissertation of

**Xiaoyi Gong**

has met the dissertation requirements of Iowa State University

Signature was redacted for privacy.

---

**Major Professor**

Signature was redacted for privacy.

---

**For the Major Program**

Signature was redacted for privacy.

---

**For the Graduate College**

**To my late father**

## TABLE OF CONTENTS

<b>ABSTRACT .....</b>	<b>vi</b>
<b>CHAPTER 1. GENERAL INTRODUCTION.....</b>	<b>1</b>
Dissertation Organization.....	1
Capillary Electrophoresis, a Brief Introduction .....	1
Detection in Capillary Electrophoresis.....	5
High-throughput Analysis Techniques.....	12
Our Goal .....	19
References .....	20
<b>CHAPTER 2. NOVEL ABSORPTION DETECTION APPROACH FOR MULTIPLEXED CAPILLARY ELECTROPHORESIS USING A LINEAR PHOTODIODE ARRAY .....</b>	<b>29</b>
Abstract .....	29
Introduction .....	29
Experimental Section .....	32
Results and Discussion.....	35
Conclusions .....	40
Acknowledgement.....	43
References .....	43
<b>CHAPTER 3. GENETIC TYPING AND HIV-1 DIAGNOSIS BY USING 96 CAPILLARY ARRAY ELECTROPHORESIS AND UV ABSORPTION DETECTION .....</b>	<b>54</b>
Abstract .....	54
Introduction .....	54
Experimental Section .....	56
Results and Discussion.....	59
Conclusions .....	60
Acknowledgement.....	61
References .....	62
<b>CHAPTER 4. COMBINATORIAL SCREENING OF ENZYME ACTIVITY BY USING MULTIPLEXED CAPILLARY ELECTROPHORESIS .....</b>	<b>70</b>
Abstract .....	70
Introduction .....	70

Experimental Section .....	73
Results and Discussion.....	76
Acknowledgement.....	80
References .....	80
<b>CHAPTER 5. HIGH-THROUGHPUT COMPREHENSIVE PEPTIDE MAPPING OF PROTEINS BY MULTIPLEXED CAPILLARY ELECTROPHORESIS .....</b>	<b>91</b>
Abstract .....	91
Introduction .....	91
Experimental Section .....	93
Results and Discussion.....	96
Conclusions .....	102
Acknowledgement.....	103
References .....	103
<b>CHAPTER 6. COMBINATORIAL SCREENING OF HOMOGENEOUS CATALYSIS AND REACTION OPTIMIZATION BASED ON MULTIPLEXED CAPILLARY ELECTROPHORESIS.....</b>	<b>118</b>
Acknowledgement.....	122
Supporting Information .....	122
References .....	122
<b>CHAPTER 7. GENERAL CONCLUSIONS .....</b>	<b>129</b>
<b>APPENDIX A. SUPPORTING INFORMATION FOR CHAPTER 6 .....</b>	<b>131</b>
<b>APPENDIX B. DATA ACQUISITION AND PROCESSING SOFTWARE FOR PHOTODIODE ARRAY .....</b>	<b>135</b>
<b>ACKNOWLEDGEMENT.....</b>	<b>142</b>

## ABSTRACT

The purpose of this research was to develop a UV-vis absorbance detection approach for multiplexed capillary electrophoresis and to explore the use of multiplexed capillary electrophoresis with UV-vis absorbance detection as a high-throughput analysis technique for various applications.

We first introduced a novel absorbance detection approach for 96-capillary array electrophoresis. The approach involved the use of a 1024-pixel linear photodiode array on which a 96-capillary array was imaged by a camera lens. Either a tungsten lamp or a mercury lamp was used as the light source such that all common wavelengths for absorption detection were accessible by simply interchanging narrow-band filters. The detection limit for Rhodamine 6G for each capillary in the multiplexed array was  $1.8 \times 10^{-8}$  M (S/N=2). The cross talk between adjacent capillaries was less than 0.2%. Simultaneous analysis of 96 samples using capillary zone electrophoresis (CZE) was demonstrated.

We further applied the 96-capillary array electrophoresis system with UV-vis absorbance detection for high-throughput PCR analysis, enzyme assay, protein analysis by peptide mapping, and combinatorial screening of homogeneous catalytic reactions.

For PCR analysis, we showed that capillary array electrophoresis could be applied to HIV-1 diagnosis and D1S80 VNTR genetic typing based simply on UV absorption detection. Not only was the use of specialized and potentially toxic fluorescent labels eliminated, but also the complexity and cost of the instrumentation were greatly reduced.

Efficient and comprehensive screening of LDH-1 enzymatic activity was accomplished in a combinatorial array of 96 reaction micro-vials. Quantitation of the

extent of the reaction at well-defined time intervals was achieved by using 96-capillary array electrophoresis coupled with the multiplexed absorption detector. Capillary electrophoresis provides high separation resolution to isolate the product from the reactants. For the conversion of NADH to NAD<sup>+</sup>, the catalytic activity of LDH was confirmed to be the highest at pH 7.

A novel multi-modal method for peptide mapping of proteins by 96-capillary array electrophoresis was presented. By combining capillary zone electrophoresis for charge to size separations in four different pH conditions and micellar electrokinetic chromatography for hydrophobicity-based separations in two different conditions in a 96-capillary array, peptide fragments of digested proteins were readily resolved and showed unique fingerprints. This demonstrated the possibility to rapidly screen proteins as well as to efficiently optimize separation conditions in CE by a combinatorial approach.

We further developed a new methodology, nonaqueous capillary array electrophoresis coupled with microreaction, to address the throughput needs of combinatorial approaches to homogeneous catalysis screening and reaction optimization. Catalytic activity, selectivity and kinetics of the various combinations for a new a new palladium-catalyzed annulation reaction were determined quickly.

## **CHAPTER 1. GENERAL INTRODUCTION**

### **Dissertation Organization**

This dissertation begins with a general introduction. The following chapters are presented as five complete scientific manuscripts. General conclusions summarize the work and provide some prospective for future research. Appendices include the information of hardware and software in detail.

### **Capillary Electrophoresis**

The ability to separate the individual components of a mixture is a critical requirement in the chemical or biochemical sciences. From a historical perspective, the pioneering experiments of Tiselius in 1937<sup>1</sup> that showed the electrophoretic separation of proteins provided the first practical demonstration of the use of electrophoresis as a separation technique. One of the early problems encountered when utilizing the Tiselius' approach was severe band broadening due to the convection currents generated by Joule heating. An important solution to this problem has been carrying out electrophoresis in buffer utilizing anticonvective supporting media such as paper,<sup>2</sup> starch,<sup>3</sup> agarose,<sup>4</sup> and most recently and importantly, polyacrylamide.<sup>5</sup> Today, polyacrylamide gel electrophoresis remains one of the most popular techniques for separation and characterization of proteins and nucleic acids in virtually every biochemistry laboratory.

Capillary electrophoresis (CE) is the most recently introduced electrophoretic separation technique. In 1967 Hjerten<sup>6</sup> recognized that carrying out electrophoresis in narrow diameter tubes reduced thermal effects. Hjerten also showed that it was possible to carry out electrophoretic separations using capillaries of 300- $\mu\text{m}$  internal diameter and to detect separated bands by ultraviolet (UV) absorbance detection. In 1974, Virtanen<sup>7</sup>

described a potentiometric detection method for zone electrophoresis using small diameter Pyrex<sup>®</sup> tubing (internal diameter 200 to 500  $\mu\text{m}$ ). Alkali cations,  $\text{Li}^+$ ,  $\text{Na}^+$  and  $\text{K}^+$  were successfully separated and detected. Virtinen also mentioned the importance of electroosmotic flow in influencing electrophoretic separations. In 1979 Mikkers *et al.*<sup>8</sup> carried out zone electrophoresis in Teflon<sup>®</sup> tubing of 200- $\mu\text{m}$  internal diameter in order to reduce convection problems. A number of both inorganic and organic anions were resolved in less than 10 minutes, using both UV and conductometric detection. Jorgenson and Lukacs<sup>9</sup> were the first to demonstrate that the use of even narrower capillaries (< 100- $\mu\text{m}$  internal diameter) produced highly efficient electrophoretic separations. Voltages as high as 30 kV were used. The large surface-to-volume ratio of capillary columns with such small internal diameters allowed for very efficient dissipation of Joule heat generated from the large applied electric fields. Separation efficiencies as high as  $4 \times 10^5$  number of theoretical plates were achieved by these authors.

The work by Jorgenson and Lukacs was effectively the beginning of the rapid development of CE techniques. In the last two decades, research groups throughout the world have expanded the horizons of CE. Today, "capillary electrophoresis" has become a collective name that is constituted of a family of specialized separation techniques using capillaries as separation channels and electric field as separation driving force. The main modes of CE that have been developed include capillary zone electrophoresis (CZE), micellar electrokinetic capillary chromatography (MEKC), capillary isoelectric focusing (CIEF), capillary gel electrophoresis (CGE), and capillary isotacophoresis (CITP).

CZE is also called free-zone capillary electrophoresis. In common cases, an open tube fused-silica capillary of 10-100  $\mu\text{m}$  internal diameter and 150-360  $\mu\text{m}$  outer diameter is

cut to a 20-100 cm length. The capillary is filled with the selected running buffer. The two ends of the capillary are immersed in two buffer reservoirs. A high voltage from several kilovolts up to 50 kV is applied across the capillary. Samples are injected from one end of the capillary by either hydrodynamic or electrokinetic injection. The analytes running through the capillary under the high electric field are separated usually based upon their differences in mass to charge ratio. CZE has been used to separate a wide range of charged simple organic molecules, inorganic ions, peptides, and proteins. DNA molecules have almost the same mass to charge ratio regardless of their sizes, so it is impossible to separate them directly by CZE. However, Drouin *et al.*<sup>10</sup> proposed that by attaching an uncharged friction-generating label at the end of DNA molecules prior to electrophoresis, DNA separations by CZE could be achieved because larger DNA molecules are less affected by the dragging of the end label and elute faster. Addition of different additives to the running buffer solutions can further expand the separation power of CZE. For example, cyclodextrins<sup>11</sup> as well as other chiral discriminating agents<sup>12</sup> have been added to the separation buffers as chiral selectors to perform chiral separations by CZE. In all cases of chiral separations transient complexes are formed between one or both of the enantiomers and the added chiral selector, and differences in the free energy of formation of these complexes lead to enantiomeric separation.

MEKC was first introduced by Terabe<sup>13</sup> in 1984. The use of MEKC, unlike CZE, allows the separation of both charged and uncharged molecules. In this mode of operation of CE, usually a certain surfactant is added to the buffer solutions at a concentration above its critical micelle concentration, so that micelles are formed in the buffer solution as a pseudo phase. To resolve neutral compounds, micelles are required to be charged and thus have an

electrophoretic mobility. Neutral analytes are separated based on differences in their partitioning characteristics between the solution phase and the micellar phase. In MEKC, the most often used surfactant is sodium dodecyl sulfate (SDS)<sup>14</sup> although a lot of other surfactants have been studied.<sup>15</sup>

CGE has been developed mainly for the separation of large biological molecules like nucleic acids and proteins. In this technique, the capillary is filled with polymer gel, which forms a sieving matrix that has characteristic pore sizes. When ions move through the sieving matrix, larger ions are obstructed more than the smaller ones and therefore move slower. The separation is thus based upon the differences in size of analyte ions. Various polymers have been studied as the sieving matrices in CGE for the analysis of nucleic acids and proteins. Linear polyacrylamide (LPA) and its derivatives,<sup>16</sup> poly(ethylene oxide) (PEO),<sup>17</sup> and polyvinylpyrrolidone (PVP)<sup>18</sup> were used for DNA sequencing, separation of DNA fragments, PCR product analysis, genotyping, and DNA mutation detection. LPA,<sup>19</sup> dextrans<sup>20</sup>, PEO,<sup>21</sup> and polyvinyl alcohol<sup>22</sup> were employed in the appropriate concentrations required to yield molecular sieving of the SDS-protein complexes. Compared to conventional slab gel DNA analysis or SDS-PAGE protein analysis methods, these CGE techniques usually provide the benefits of shorter analysis time, higher separation efficiency, lower sample consumption, and full automation of the analysis process including sample introduction, separation, and data reduction.

CIEF and CITP are less explored modes of CE operation. The latter technique has been primarily used as an on-capillary preconcentration method for dilute mixture of analytes,<sup>23</sup> although it has the potential for being a separate analytical mode of CE. In CIEF a pH gradient under the influence of an electric field is set up along a capillary using

ampholytes. Within the pH gradient, analytes, usually polypeptides, are focused to the position where their net charge is zero, i.e., where  $\text{pH} = \text{pI}$ . Focused analyte bands are usually transported slowly to the detect window to be detected. CIEF is particularly useful for characterization of protein mixtures and determination of protein isoelectric points.

Another separation technique that is related to CE is capillary electrochromatography (CEC), which is a hybrid method between capillary HPLC and CE. In CEC, solvent is driven through capillary tubes by electroosmotic flow (EOF) induced by the applied electric field across the capillary instead of hydraulic flow induced by pressure in HPLC. The main advantages of using EOF include a gain in separation efficiency through the plug flow profile and the usage of particles much smaller than in column HPLC. The latter is possible in CEC because of the absence of column back pressure when the solvents are moved by EOF. Excellent reviews about CEC can be found in Reference 24.

## **Detection in Capillary Electrophoresis**

### **Overview**

The high separation power of CE could not be exploited fully if there were no compatible detectors. While the small internal diameter of capillaries provide the benefits of efficient heat dissipation and low sample and solvent consumption, it also brings about the challenge to develop sensitive detection methods because very low amounts of analytes are generally used in CE separation processes. In most cases, the detectors used for HPLC cannot be borrowed for CE without substantial modification.

The challenge to detect very low amounts of analytes separated in CE leads to a lot of efforts to develop state-of-art detection systems. A wide variety of detection schemes now

have been coupled to CE with varying degrees of success. In general, the development of CE detectors can be classified into three major categories: optical, electrochemical, and mass spectrometric. Among these three categories, optical detectors are by far the most widely used in both commercial CE instruments and homemade CE systems in research labs. One of the major reasons is optical detection is contactless, so it is less affected by the interference of the high applied electric field. In addition, optical detection can be used with a wide range of aqueous, organic and polymer buffers as well as many buffer additives. Therefore, another advantage of the optical detection schemes for CE is they can be employed in different modes of CE operation (i.e., CZE, MEKC, CGE, CIEF, and CEC) with very little or no modification. Because of the limit of space and the relevance to the work in this dissertation, the following text only covers some optical detection schemes. A lot of emphasis is put on UV-vis absorbance detection, while laser induced fluorescence (LIF) detection is briefly discussed for comparison. General reviews about CE optical detection schemes can be found in reference.<sup>25</sup> Reviews of electrochemical detectors and mass spectrometric detectors for CE can be found elsewhere.<sup>26,27</sup>

### **UV-vis absorbance detection**

UV-vis absorbance detectors are the most commonly used detectors for CE. All commercial CE instruments are provided with an absorbance detector. As with HPLC, the primary reason for the popularity of the absorbance detection schemes is simply that the majority of compounds analyzed absorb somewhere in the UV region. In most CE UV-vis absorbance detector designs, light from a lamp is collected and imaged onto the capillary, and either a monochromator or a filter is used to isolate a specific wavelength band for the absorbance measurement. The transmitted intensity is detected with a photodetector and

electronics and computers are used to convert the transmitted intensity to an absorbance reading.

The Lambert-Beer law ultimately controls the performance of absorbance detection:

$$A = \text{Log } I_0/I = \epsilon bc$$

where A is the measured sample absorbance,  $I_0$  is the intensity of radiation incident upon the sample, I is the intensity of radiation emergent from the sample,  $\epsilon$  is the molar extinction coefficient of the sample at the selected wavelength, b is the optical path-length, and c is the molar concentration of the sample.

The primary disadvantage of absorbance detection for CE is the relatively high concentration limit of detection (LOD). As seen from the Lambert-Beer law, for a certain analyte ( $\epsilon$ ) and a certain analyte molar concentration (c), the measured absorbance (A) signal is directly proportional to the optical path-length (b). For trans-column CE absorbance detection, the optical path-length is restricted by the internal diameter of capillaries, which is usually in the range of 20-100  $\mu\text{m}$ . Because the capillary is cylindrical, the effective optical path-length is somewhat less than the capillary internal diameter. The mean trans-column path-length can be approximated by  $(\pi \times \text{internal diameter})/4$ . Note for a 75- $\mu\text{m}$  internal diameter capillary, this would result in an mean optical path-length of 59  $\mu\text{m}$  and an absorbance signal less than 1/150 of that measured on a standard HPLC detection flow cell of 1 cm optical path-length.

To improve the absorbance signal in CE detection, one obvious choice is to extend effective light path-length. As shown in Figure 1, several attempts have been made by using rectangular capillaries,<sup>28</sup> bending capillaries to make Z-shaped flow cells,<sup>29</sup> employing axial

illumination or whole column illumination,<sup>30,31</sup> constructing multireflection cells,<sup>32</sup> or forming "bubble cells"<sup>33</sup> at the detection region of capillaries. Two to forty fold improvement in LOD have been reported. Bubble-cell design and Z-type flow cell design have been available in some commercial CE machines from Agilent Technologies (formerly Hewlett-Packard).<sup>34</sup>

Certain problems still exist when putting these path-length extended absorbance detection schemes into practical uses. Capillaries in rectangular format or with bubble cells are either not commercially available or much more expensive. Z-shaped flow cells increase the signal level at the expense of separation efficiency, although the length of flow cells can be limited to around 1 mm to minimize the extra band broadening while still keeping the substantial signal improvement. Axial illumination needs precise alignment of the light source, capillary and the detector to maximize the amount of light reaching the detector. Whole column illumination by total internal reflection needs special high refractive index separation media such as dimethyl sulfoxide or low refractive index Teflon<sup>®</sup> capillaries, neither of which are commonly used in research labs or industry. Multi-reflection cells bring about the greatest improvement in LOD, but capillaries need to be specially treated and coated by silver. Also lasers need to be used as the light source and precise alignment is critical. The problems of using lasers in absorbance detection are that lasers are usually one or two orders of magnitude noisier than the conventional light sources, and deep UV wavelengths are not available at moderate costs.

In our lab, we found an easy way to extend the optical path-length.<sup>35</sup> As shown in Figure 2, two prisms are used to "sandwich" a capillary. Light beams that pass through the prisms will travel along the inside core of the capillary at a certain angle  $\beta$ . The angle  $\beta$  is

controlled by the incident angle  $\alpha$ , the prism angle  $\gamma$ , and the refractive indexes of the prism, the capillary wall, and the solution inside the capillary. When  $\beta$  is smaller than 90 degrees (trans-column), certain levels of light path-length extension should be expected. In our preliminary experiments, 6 fold improvement of LOD for Rhodamine 6-G was observed. This optical path-length extension approach does not require specially treated capillaries, exotic buffer solutions, or lasers, so it should be easier to be put into practical uses.

The LOD can also be improved by reduction of detector noise. The major noise sources in CE absorbance detection are flicker noise and shot noise. Flicker noise is due to the intensity fluctuation of light sources. Different light sources have different level of intensity fluctuation. Jorgenson *et al.*<sup>36</sup> compared the performance of Zn (214nm), Cd (229nm), and As (200 nm) lamps and found that the zinc lamp is the best choice. Battery-operated tungsten lamps provide the full spectrum of visible light and have superb stability. Low-pressure mercury lamps produce a sharp line at 254 nm that is very useful for nucleic acid detection. We found in our lab that DC- powered low-pressure mercury lamps are more stable than the AC-powered ones. We also found that double-beam detection schemes can substantially reduce the flicker noise from both types of low-pressure mercury lamps.<sup>37</sup>

Shot noise is generally defined as the combined noise associated with the random generation of photons from the light source and the random generation of photoelectrons in the photodetector. The relative shot noise level is inversely proportional to the square root of the number of photons reaching the photodetector at any given point of time. As a result, the detector shot noise level can be reduced simply by increasing the optical throughput of the system. Using lasers as the light source can substantially increase the optical throughput because not only are lasers 2 to 4 orders of magnitude brighter than conventional light

sources, but also the laser output can be efficiently focused into the capillary. Lasers are, therefore, theoretically capable of superior shot noise limited performance. In practice, however, lasers can be quite noisy, with typical intensity fluctuation in the 1% range. Our group<sup>38</sup> proposed a noise-cancellation circuit with a double-beam laser absorbance detection scheme for CE. The extra flicker noise from lasers was substantially reduced by the double-beam noise-cancellation. A 25-fold of improvement in LOD was obtained over typical commercial CE absorbance detectors.

Recently Jorgenson *et al.*<sup>39</sup> reported a new approach for lowering the CE absorbance detection noise. This approach involved the use of a photodiode array in which each of the diodes in the array was treated as an independent absorbance detector. Averaging the electropherograms generated from 1500 diodes in the diode array resulted in a noise 85 times lower than that of an electropherogram generated from any one diode in the array. The array detector was reported to improve the CE absorbance detection limit by a factor of 3.8 over the typical commercial CE absorbance detectors.

### **Indirect UV-vis absorbance detection**

While direct UV-vis absorbance detection is applicable to an abundance of analytes, it is not truly universal. Compounds whose structures do not include  $\pi$  bonds (i.e. small inorganic ions, carbohydrates, etc.) usually have very small molar extinction coefficients even at very low wavelengths. An alternative way to detect molecules that do not possess appreciable absorptivities is to use indirect absorbance detection. In this technique, as shown in Figure 3, an ionic additive of high molar extinction coefficient is introduced to the buffer system. In the absence of analyte, the continually eluting buffer generates a high background

absorbance level. Because of the condition of constant electric field, the presence of ionic analyte (having a lower absorbance than the buffer additive) in the capillary leads to the displacement of the buffer additive ions and thus a decrease in the concentration of highly absorbing buffer additive ions. As a result, elution of analyte is accompanied by a decrease in the absorbance of buffer. This decrease in absorbance, or negative absorbance signal, is proportional to the amount of analyte present. The best performance of indirect absorbance detection requires careful selection of the signal-generating chromophore and optimization of the chromophore and buffer concentrations according to the types and concentrations of the analytes. Therefore, indirect detection is best suited for application-specific analysis in which all critical parameters may be optimized and then remain unchanged from run to run. The LODs for an well-optimized indirect CE absorbance measurement can reach the  $10^{-6}$  -  $10^{-5}$  M range.<sup>40</sup>

### **Laser Induced Fluorescence Detection**

LIF is the most sensitive detection mode available for CE. The signal in fluorescence measurements is much smaller than that in absorbance detection since only a portion of absorbed photons generate fluorescence photons.<sup>41</sup> However, the energy of the fluorescence photons generated from an excited molecule is generally different than the photons absorbed by the molecule. In optical measurement, this means the fluorescence signal can be differentiated from the excitation background by various types of wavelength discrimination. By careful selection of optical arrangements and wavelength filters, the background in LIF detection can be pushed to a negligible level. Therefore a very low LOD can be achieved by using LIF detection in CE since LOD is determined by signal to noise

ratio rather than the absolute signal level. The lowest LODs for the CE/LIF detection are below  $10^{-13}$  M<sup>42</sup> or mass LODs of less than 10 molecules.<sup>43</sup>

While LIF detection provides the superior sensitivities for fluorescence dyes and properly labeled molecules, its application is limited largely to large biopolymers such as nucleic acids and proteins, for which fluorescence labeling chemistry is well developed. Most small organic and inorganic molecules do not have strong enough native fluorescence for sensitive detection. Development of fluorescence derivation chemistry for these smaller molecules tends to be labor intensive since no universal solution is available for a wide variety of molecules. Environmental effects of some toxic fluorescence dyes are also a concern.

### **High-throughput Analysis Techniques**

#### **Overview**

Analytical chemists always hope that analyses can be performed in a timely fashion as long as accuracy and cost are not compromised for speed. The real pressure for high-throughput analysis, however, came along with the Human Genome Project (HGP) initiated in 1990. As stated in the 1993 version of five-year plans of HGP (FY1994 through FY1998),<sup>44</sup> one of major goals under "DNA sequencing" category is "...to develop technology for high-throughput sequencing..." The answer of analytical chemists for this goal is the development of massively multiplexed CGE systems coupled with sensitive LIF detection. With the validation and use of such multiplexed CE DNA sequencing systems, the project to sequence the whole human genome has been much accelerated.

All human genetic codes could be sequenced by the end of 2001 or even earlier.<sup>45</sup> However, the human genome is only one of almost one hundred genomes being sequenced around the world. In addition, comparative genomics, single nucleotide polymorphism (SNP), and other genome-related issues are examples of applications that will continue to seek new advances in high-throughput analysis technologies.

Combinatorial chemistry has advanced to a stage that it could revolutionize the discovery of new drugs,<sup>46</sup> novel materials, and efficient catalysts.<sup>47</sup> It aims to substantially increase the throughput of discovery by scanning and testing vast number of possibilities in a parallel fashion. Combinatorial chemists have developed and keep developing novel methods to synthesize a large number of compounds simultaneously. Characterization and screening of all the compounds produced by these parallel synthesis methods impose new pressure on analytical chemists for the development of high-throughput analysis technologies.

Optimization of experiment conditions is routinely performed in every chemistry research lab. Even with careful planning, this could still be very time-consuming. An organic graduate student could spend months or even years in trying all the different solvent, catalyst, temperature, and reaction time combinations to improve the yield of a synthesis from 60 to 95 percent. An analytical graduate student, meanwhile, could be working overnight to test different buffers, pHs, and column lengths to resolve a shoulder peak to baseline resolution. The reason for the low-throughput is that conventionally every condition needs to be tried and analyzed sequentially. If high-throughput analysis techniques can be adapted for optimization processes, as shown in Chapter 6 in this dissertation for example, the whole optimization throughput could be drastically improved.

## **Multiplexed Capillary Electrophoresis**

In the past few years, several research groups have been involved in developing multiplexed CE systems with several to hundreds of capillaries, thus greatly increasing system analysis throughput. To date, this work has been driven almost exclusively by efforts to accommodate capillary gel electrophoresis with LIF detection for the high-throughput DNA sequencing,<sup>48</sup> although recently multiplexed CE have been used for high-throughput PCR analysis,<sup>49</sup> genotyping,<sup>50</sup> and mutation detection.<sup>51</sup>

The major difference among various multiplexed capillary electrophoresis systems with LIF detection lies in the detection scheme. Generally, the LIF detection modes fall into two categories: scanning and imaging. For the scanning detection mode, either capillaries or the single channel detection systems translate along the scan axis, so each capillary can be detected sequentially and repetitively. In an imaging detection system, all capillaries are illuminated and detected simultaneously.

Mathies *et al.*<sup>52</sup> first developed confocal scanning LIF detection for multiplexed CE. The optical system utilized a planar array of 25 capillaries attached to a precision translation stage. As the translation stage was swept back and forth beneath the stationary microscope objective, the individual capillaries were interrogated in an epi-illumination format. In this format, the laser excitation beam was focused onto the capillaries by a microscope objective, and the emitted fluorescence was collected by the same objective using a 180-degree geometry, followed by detection using a PMT. The small local illumination region enabled the use of a modest laser power and elimination of cross talk among adjacent capillaries. High repetition rate scan systems with sensitive closed feedback loops were required and

therefore limited the number of capillaries that may be scanned. Recent development included using a rotating objective instead of horizontal sweeping the capillary array. This allowed up to 1000 capillaries be detected in one system.<sup>53</sup>

The imaging LIF detection systems have used multi-sheath flow cells, on-column illumination, and fiber-optic array illumination.

Kambara *et al.*<sup>54</sup> developed an approach of multicapillary LIF detection that involves the use of a multi-sheath flow cell. In this approach, a linear array of capillaries terminated in a multi-sheath flow cell through which the excitation laser beams were directed in a side illumination fashion. Sample eluted from the capillaries into the sheath flow cell. The fluorescence emission was monitored using a cooled CCD camera. Because the DNA sample was illuminated in the gel-free region, background fluorescence and scattering light were minimized. Therefore, better signal-to-noise ratio was achieved in this system. Two-dimensional packing of the capillary array is possible using the detection scheme, as claimed by the authors.

Our group first developed the on-column illumination LIF detection scheme for multiplexed capillary array electrophoresis.<sup>55</sup> 100 capillaries are densely packed. The laser beam was shined across the capillary array using cylindrical lenses and the fluorescence emission was monitored using a cooled CCD system. This design has no moving parts and can provide 100% duty cycle. However, relatively high laser power is required to excite the capillary array since the laser beam is dispersed. Recently, Heller *et al.*<sup>56</sup> reported a laser line generator that was able to produce a laser line to uniformly illuminate 96 capillaries, yet used a low power laser (~30mW).

An alternative excitation approach not requiring high laser power was side illumination.<sup>57</sup> This approach involved directing the laser excitation beam through the edge of a linear array of capillaries. The transmitted laser beam through one capillary could be reused by the next one. A wave-guide was used to achieve uniform illumination. The drawback of this design was that precise optical alignment was required, which limited the number of capillaries in the array.

Zhang *et al.*<sup>58</sup> developed an approach using fiber-optic illumination. Laser excitation and fluorescence collection were performed through optic fibers in a 90-degree arrangement. The low light collection efficiency of the optical fibers was compensated by the use of an intensified CCD. However, the optical fiber illumination required a high-powered laser to excite a large number of capillaries. For this reason, the authors switched to the use of a single beam to illuminate all capillaries.<sup>59</sup> Difficult alignment of the fiber-capillary junction still limited the application of this approach to a large capillary array.

Today, there are three commercial versions of multiplexed capillary electrophoresis DNA sequencers. At the XII International Symposium on High Performance Capillary Electrophoresis & Related Techniques (HPCE'99), all three commercial instruments were presented. The three commercial instruments all feature 96 capillaries. ABI PRISM<sup>®</sup> 3700<sup>60</sup> from PE Biosystems originated from the design of Kambara and employed postcolumn detection with liquid sheath flow. MegaBACE 1000<sup>61</sup> from Molecule Dynamics (Sunnyvale, CA) was based on the prototypes of Mathies and scanning LIF detection. SCE9610<sup>62</sup> from SpectruMedix (State College, PA) used Yeung's on-column illumination/LIF imaging detection approach. An expansion to 384 capillaries was foreseen by the company.

## Microchip

Microchips are miniaturized devices with microfabricated channels. The first instrument on a microchip was an integrated gas chromatograph on a 5-cm diameter silicon wafer.<sup>63</sup> While this device never commercially succeeded, it nonetheless initiated the application of micromachining technology to constructing chemical analysis devices. Liquid phase separation techniques are more suitable to miniaturization than gas chromatography, since many liquid phase separations such as CE, capillary LC, and MEKC have already been practiced in capillary tubes with internal diameters (5-200  $\mu\text{m}$ ) of one to two orders of magnitude smaller than those in gas chromatography. In addition, separation lengths tend to be much shorter for liquid phase separation techniques. These smaller dimensions allow the fabrication of a column in a proportionately smaller area. Furthermore, electroosmotic flow allows transporting liquid solutions in microfabricated channels without band-broadening issues associated with the parabolic flow-rate pattern of hydraulic flow. For CE related separation techniques, there is an additional benefit to use microchips. Microchips have better heat dissipation efficiencies than do capillaries, so higher electric fields can be applied without causing significant Joule heating problems. When band-broadening in CE separations are dominated by axial diffusion, which is usually true when Joule heating can be neglected and the injection plug is small, CE separation efficiency is not a function of separation length but of applied voltage. Therefore, when very high electric field strength is used, the separation length and thus the analysis time can be substantially shortened without sacrifice of the separation efficiency. For example, Ramsey *et al.*<sup>64</sup> reported that electrophoretic separation of a binary mixture was achieved with baseline resolution in less

than 150 ms with an electric-field strength of 1.5 kV/cm and a 0.9-mm long separation channel.

LIF detection is so far the most popular detection schemes for microchips because of its high sensitivity. Basically the same optical arrangement can be borrowed from conventional CE LIF detection systems. Absorbance detectors have been less employed on microchips due to both the concern of limited sensitivity and many popular glass and polymer chip substrates not being UV-transparent. Harrison *et al.*<sup>65</sup> used a 140- $\mu\text{m}$  U-shaped detection cell fabricated on a microchip to improve the absorbance detection limit. 6  $\mu\text{M}$  of fluorescein could be detected. Optical fibers were used to guide the source light to the U-cell and the transmitted light to a photodetector. Other detection schemes such as mass spectrometry,<sup>66</sup> Roman spectroscopy,<sup>67</sup> refractive index detection,<sup>68</sup> and electrochemical detection<sup>69</sup> have also been explored for microchip systems. Electrochemical detectors are particularly attractive for microchips because microelectrodes can be fabricated on chips along with separation channels.<sup>70</sup>

To simultaneously analyze large number of samples in high-throughput fashion, arrays of separation channels have been designed on microchips. Mathies *et al.*<sup>71</sup> have reported a microchip device with 48 parallel separation channels to separate 96 genotyping samples in two runs in less than 8 minutes. A microchip with 96 radial separation channels has also been designed by the authors. Combining the massively parallel separation channels and ultra-fast separation speed, microchip technology is very promising to push high-throughput analysis to the next level.

## **Other High-throughput Analysis Techniques**

So far there are several non-separation based parallel assays for high-throughput homogeneous catalysis screening. Modifications of UV absorption,<sup>72,73</sup> fluorescence,<sup>74</sup> color,<sup>75</sup> and temperature<sup>76</sup> induced by the catalytic reactions are indicators of catalytic activity. In these approaches, although the relative activity of the catalyst is determined quickly, no quantitative information about the regioselectivity and stereoselectivity of the catalytic reaction can be obtained. It is also necessary that analysts have very different measurable properties compared to sample matrices. In most cases, secondary screening is necessary.

Multiplex HPLC is another interesting approach,<sup>77,78</sup> but achieving the high-density bundle like 96 capillaries in multiplexed CE is not trivial due to column size and mass transfer and separation mechanisms. Thin-layer chromatography and slab gel electrophoresis, on the other hand, are difficult for complete automation.

## **Our Goal**

Multiplexed capillary electrophoresis coupled with laser induced fluorescence detection is a very successful high-throughput analysis technique for DNA sequencing. While LIF detection provides the desired sensitivity for DNA sequencing, UV-vis absorbance detection has remained very useful because of its ease of implementation and wide applicability. Our goal is to develop an UV-vis absorbance detection approach for multiplexed capillary electrophoresis and apply the absorbance-detection based multiplexed capillary electrophoresis to perform high-throughput analysis for various applications other than DNA sequencing.

**References:**

1. Tiselius, A., *Trans. Faraday Soc.*, **1937**, 33, 524.
2. Consden, R., Gordon, A. H., and Martin, A. J. P., *J. Biochem.*, **1944**, 38, 244.
3. Smithies, O., *J. Biochem.*, **1955**, 61, 629.
4. Hjerten, S., *Biochem. Biophys. Acta*, **1961**, 53, 514.
5. Raymond, S. and Weintraub, L., *Science*, **1959**, 130, 711.
6. Hjerten, S., *Chromatogr. Rev.*, **1967**, 9, 122.
7. Virtanen, R., *Vol 123 Acta Polytechnica Scandinavia (Helsinki)*, **1974**.
8. Mikkers, F. E. P., Everaerts, F. M., and Verheggen, T. P. E. M., *J. Chromatogr.*, **1979**, 169, 11.
9. Jorgenson, J. and Lukacs, K. D., *Anal. Chem.*, **1981**, 53, 1298.
10. Mayer, G., Slater, G. W., and Drouin, G., *Anal. Chem.*, **1994**, 66, 1777.
11. Zhao, Z., Malik, A., and Lee, M.L., *J. Microcol. Sep.*, **1992**, 4, 411.
12. Otsuka, K. and Terabe, S., *J. Chromatogr.*, **1990**, 515, 221.
13. Terabe, S., Otsuka, K., Ichikawa, K., Tsuchuya, A., and Ando, T., *Anal. Chem.*, **1984**, 56, 111.
14. Nielen, N. M., *J. High Resolut. Chromatogr.*, **1993**, 16, 62.
15. Muijselaar, P.G., Otsuka, K., and Terabe, S., *J. Chromatogr. A*, **1997**, 780, 41.
16. Ruiz-Martinez, M.C., Berka, J., and Belenkii, A., *Anal. Chem.*, **1993**, 65, 2851.
17. Fung, E., and Yeung, E. S., *Anal. Chem.*, **1995**, 67, 1913.
18. Gao, Q., and Yeung, E. S., *Anal. Chem.*, **1998**, 70, 1382.
19. Widhalm, A., Schwer, C., Blass, D., Kenndler, E., *J. Chromatogr.*, **1991**, 546, 446.

20. Ganzler, K., Greve, K., Cohen, A. S., Karger, B. L., Guttman, A., and Cooke, N. C., *Anal. Chem.*, **1992**, 64, 2665.
21. Guttman, A., Nolan, J., and Cooke, N., *J. Chromatogr.*, **1993**, 632, 171.
22. Simo-Alfonso, E., Conti, M., Gelfi, C., and Righetti, P. G., *J. Chromatogr. A*, **1995**, 689, 85.
23. Foret, F., Szoko, E., and Karger, B. L., *J. Chromatogr.*, **1992**, 608, 3.
24. Dermaux, A., and Sandra, P., *Electrophoresis*, **1999**, 20, 3027.
25. Pentoney, S. L., Sweedler, J. V., *Handbook of Capillary Electrophoresis (2nd Ed.)*, **1997**, 379.
26. Kappes, T., Hauser, P. C., *Electroanalysis*, **2000**, 12, 165.
27. Ding, J., Vouros, P., *Anal. Chem.*, **1999**, 71, 378A.
28. Tsuda, T., Sweedler, J. V., and Zare, R. N., *Anal. Chem.*, **1990**, 62, 2149.
29. Bruin, G. J. M., Stegeman, G., Van Asten, A. c., Xu, X., Draak, J. C., and Poppe, H., *J. Chromatogr.*, **1991**, 559, 163.
30. Taylor, J. A., and Yeung, E. S., *J. Chromatogr.*, **1991**, 550, 831.
31. Xi, X., and Yeung, E. S., *Appl. Spectrosc.*, **1991**, 45, 1199.
32. Wang, t., Aiken, J. H., Huie, C. W., Hartwick, R. A., *Anal. Chem.*, **1991**, 63, 1372.
33. Heiger, D. N., *Paper Presented, HPCE '93, Orlando Florida, 1993*.
34. Product information, Agilent Technologies, <http://www.agilent.com>
35. Gong, X., and Yeung, E. S., *Unpublished results*.
36. Green J. S., and Jorgenson J. W., *J. Liq. Chromatogr.*, **1989**, 12, 2527.
37. Gong, X., and Yeung, E. S., *Anal. Chem.*, **1999**, 71, 4989.
38. Xue, Y., and Yeung, E. S., *J. Am. Chem. Soc.*, **1993**, 65, 15.

39. Culbertson, C. T., and Jorgenson, J. W., *Anal. Chem.*, **1998**, 70, 2629.
40. Weinberger, R., *Practical Capillary Electrophoresis*, **1993**.
41. Ingle, D., Crouch S. R., *Spectrochemical Analysis*, **1988**.
42. Timperman, A. T., Khatib, K., and Sweedler, J. V., *Anal. Chem.*, **1995**, 67, 139.
43. Chen., D. Y., Aldelhelm, K., Cheng, X. L., Dovichi, N. J., *Analyst*, **1994**, 119, 349.
44. Collins, F., and Galas, D., *Science*, **1993**, 262, 42.
45. Press release, Celera Corp., <http://www.celera.com>.
46. Xu, R., Greiveldinger, G., Marenus, L., Cooper, A., Ellman, J., *J. Am. Chem. Soc.*, **1999**, 121, 4898.
47. Brocchini, S., James, K., Tangpasuthadol, V., and Kohn, J., *J. Am. Chem. Soc.*, **1997**, 119, 4553.
48. Carrilho E., *Electrophoresis*, **2000**, 21, 55.
49. Madabhushi, R. S., Vainer, M., Dolnik, V., Enad, S., Barker, D. L., Harris, D. W., and Mansfield, E. S., *Electrophoresis*, **1997**, 18, 104.
50. Gao, Q., Pang, H., and Yeung, E. S., *Electrophoresis*, **1999**, 20, 1518.
51. Gao, Q., *Doctoral Dissertation*, **1999**.
52. Huang, X. C., Quesada, M. A., and Mathies, R. A., *Anal. Chem.*, **1992**, 64, 2149.
53. Kheterpal, I., and Mathies, R. A., *Anal. Chem.*, **1999**, 71, 31.
54. Kambara, H., and Takahashi, S., *Nature*, **1993**, 361, 565.
55. Ueno, K., and Yeung, E. S., *Anal. Chem.*, **1994**, 66, 1424.
56. Behr, S., Matzig, M., Levin, A., Eickhoff, H., and Heller, C., *Electrophoresis*, **1999**, 20, 1492.
57. Lu, X., and Yeung, E. S., *Applied Spectroscopy*, **1995**, 49, 605.

58. Quesada, M. A., and Zhang, S., *Electrophoresis*, **1996**, 17, 1841.
59. Quesada, M. A., dhadwal, H. S., Fisk, D., and Studier, F. W., *Electrophoresis*, **1998**, 19, 1415.
60. Product Information, PE Biosystems. <http://www.pebio.com>.
61. Product Information, Molecular Dynamics, <http://www.mdyn.com>.
62. Product Information, SpectruMedix, <http://www.spectrumedix.com>.
63. Terry, S. C., Jerman, J., and Angell, J. B., *IEEE Trans. Electron Dev.*, **1979**, 26, 880.
64. Jacobson, S. C., Hergenroder, R., and Ramsey, J. M., *Anal. Chem.*, **1994**, 66, 1114.
65. Liang, Z. H., Chiem, N., Ocvirk, G., Tang, T., Fluri, K., and Harrison, D. J., *Anal. Chem.*, **1996**, 68, 1040.
66. Ramsey, R. S., and Ramsey, J. M., *Anal. Chem.*, **1997**, 69, 1174.
67. Walker, P. A., Morris, M. D., Burns, M. A., and Johnson, B. N., *Anal. Chem.*, **1998**, 70, 3766.
68. Burggraf, N., Krattiger, B., Demello, A. J., Derooij, N. F., and Manz, A., *Analyst*, **1998**, 123, 1443.
69. Gavin, P. F., and Ewing, A. G., *J. Am. Chem. Soc.*, **1996**, 118, 8932.
70. Dolnik, V., Liu, S., Jovanovich, S., *Electrophoresis*, **2000**, 21, 41.
71. Simpson, P. C., Roach, D., Woolley, A. T., Thorsen, T., Johnston, R., Sensabaugh, G. F., and Mathies, R. A., *Proc. Natl. Acad. Sci. USA*, **1998**, 95, 2256.
72. Wagner, J., Lerner, R., and Barbas, C., *Science*, **1995**, 270, 1797.
73. Menger, F., Ding, J., and Barragan, V., *J. Org. Chem.*, **1998**, 63, 7578.
74. Cooper, A., McAlexander, L., Lee, D., Torres, M., and Crabtree, R., *J. Am. Chem. Soc.*, **1998**, 120, 9971.

75. Lavastre, O., and Morken, J., *Angew. Chem. Int. Ed.*, **1999**, 38, 3163.
76. Taylor, S., and Morken, J., *Science*, **1998**, 280, 267.
77. Zhang, Y., Tan, H., and Yeung, E. S., *Anal. Chem.*, **1999**, 71, 5018.
78. Zeng, L., and Kassel, D., *Anal. Chem.*, **1998**, 70, 4380.

**FIGURE CAPTIONS**

**FIGURE 1.** Several methods to extend the pathlength in absorbance detection in CE

(A) Standard trans-column geometry

(B) Z-shaped flow cell

(C) Rectangular capillary

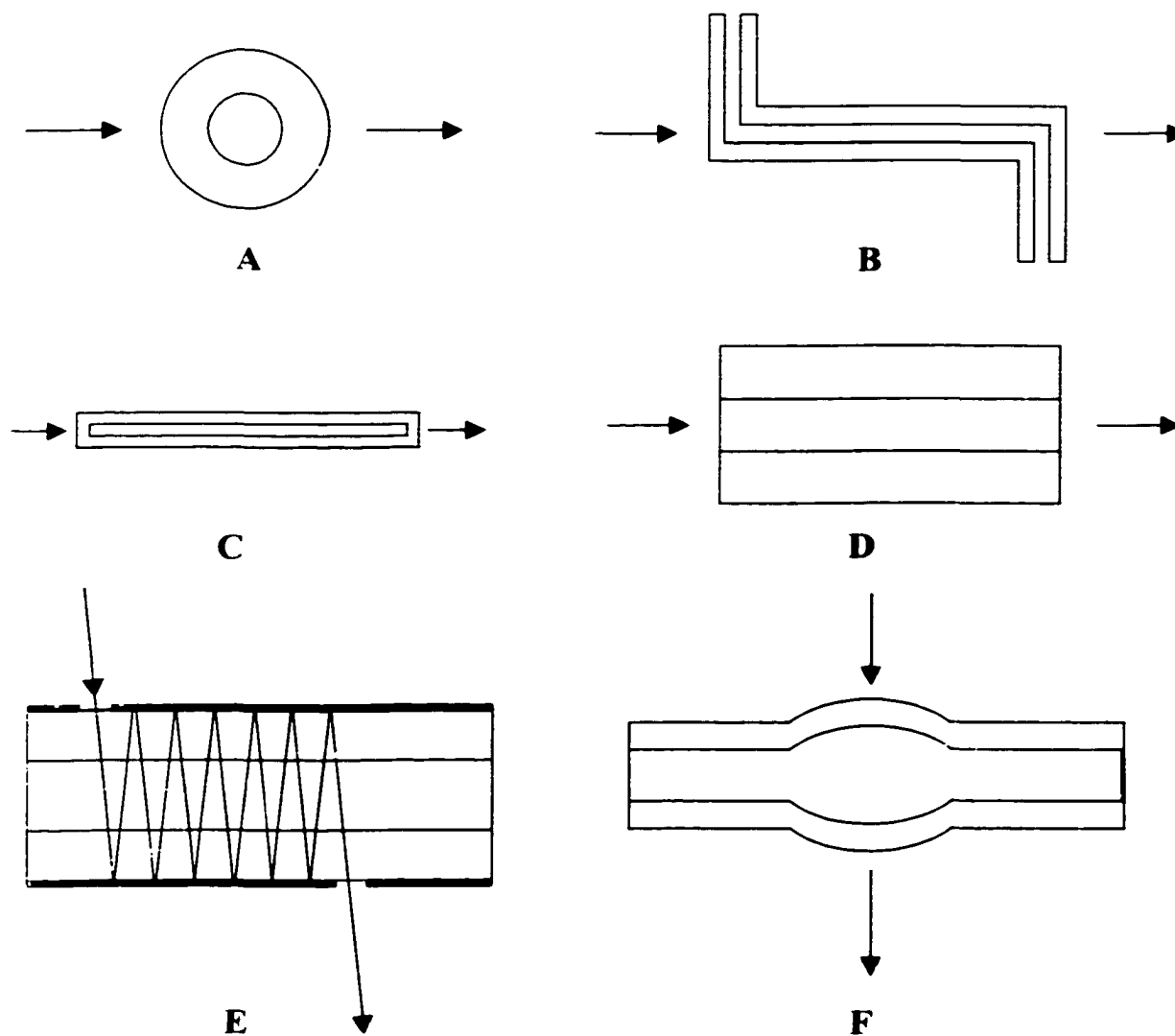
(D) Axial illumination

(E) Multi-reflection cell

(F) "Bubble" cell

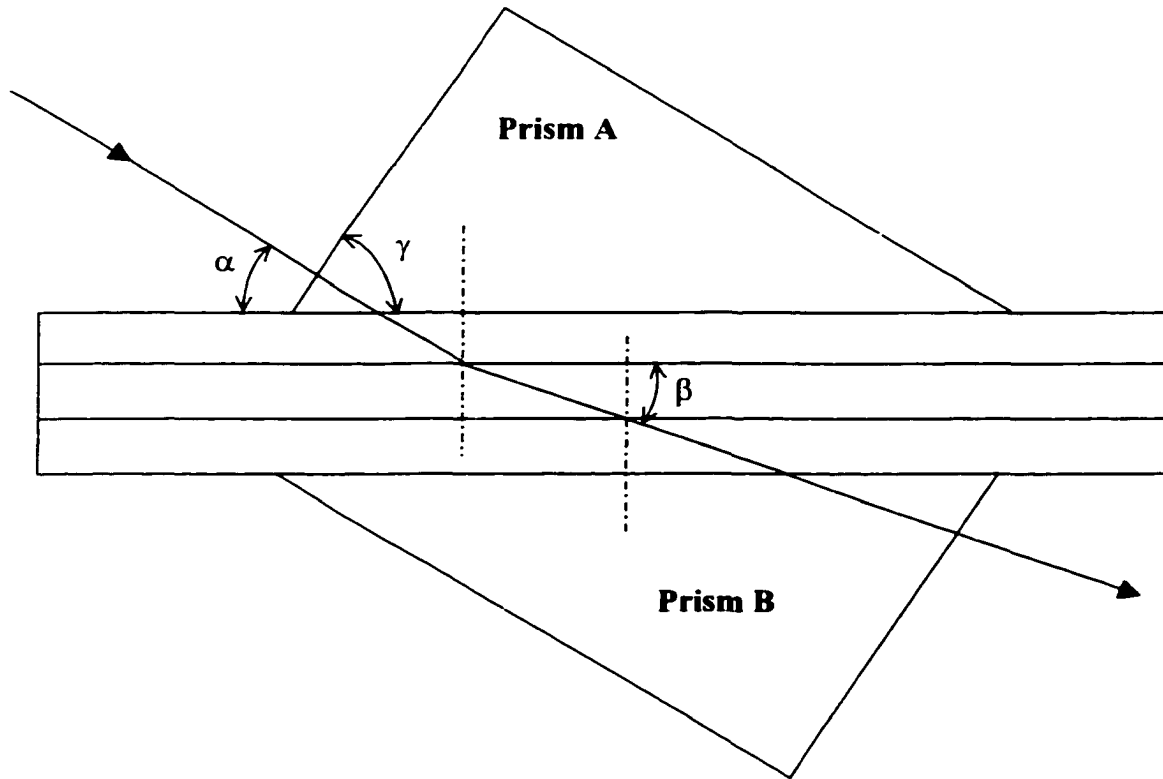
**FIGURE 2.** An alternative approach to path-length extension

**FIGURE 3.** Diagram illustrating the principle of indirect detection. Shaded circles represent buffer additive ions. In (B), the analyte ions are represented by open circles and have displaced some of buffer additive ions.

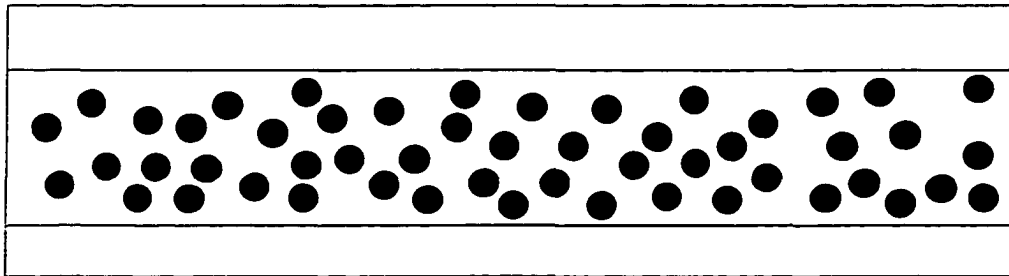
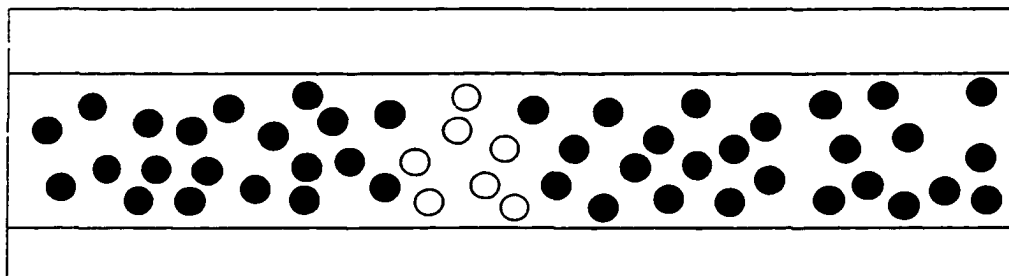


**FIGURE 1.** Several methods to extend the pathlength in absorbance detection for CE.

- (A) Standard trans-column geometry
- (B) Z-shaped flow cell
- (C) Rectangular capillary
- (D) Axial illumination
- (E) Multireflection cell
- (F) "Bubble" cell



**FIGURE 2.** An alternative approach to path-length extension

**A****B**

**FIGURE 3.** Diagram illustrating the principle of indirect detection. Shaded circles represent buffer additive ions. In (B), the analyte ions are represented by open circles and have displaced some of buffer additive ions.

## CHAPTER 2. AN ABSORBANCE DETECTION APPROACH FOR MULTIPLEXED CAPILLARY ELECTROPHORESIS USING A LINEAR PHOTODIODE ARRAY

A paper published in Analytical Chemistry \*

Xiaoyi Gong and Edward S. Yeung

### Abstract

A novel absorption detection method for highly multiplexed capillary electrophoresis is presented for zone electrophoresis and for micellar electrokinetic chromatography. The approach involves the use of a linear photodiode array on which a capillary array is imaged by a camera lens. Either a tungsten lamp or a mercury lamp can be used as the light source such that all common wavelengths for absorption detection are accessible by simply interchanging narrow-band filters. Each capillary spans several diodes in the photodiode array for absorption measurements. Over 100 densely packed capillaries can be monitored by a single photodiode array element with 1024 diodes. The detection limit for rhodamine 6G for each capillary in the multiplexed array is about  $1.8 \times 10^{-8}$  M injected (S/N=2). The cross talk between adjacent capillaries is less than 0.2%. Simultaneous analysis of 96 samples is demonstrated.

### Introduction

Rapid development of biological and pharmaceutical technology has posed a challenge for high-throughput analytical methods. For one example, current development of

---

\* Reprinted with permission from Analytical Chemistry 1999, 71, 4989

combinatorial chemistry has made it possible to synthesize hundreds or even thousands of compounds per day in one batch.<sup>1</sup> Characterization and analysis of such huge numbers of compounds have become the bottleneck. Parallel processing (i.e. simultaneous multisample analysis) is a natural way to increase the throughput. However, due to limitations related to column size, pressure requirement, detector and stationary phase material, it will be very difficult to build a highly multiplexed high-performance liquid chromatography (HPLC) system. The same goes for building a highly multiplexed gas chromatography (GC) system.

High performance capillary electrophoresis (CE) has rapidly become an important analytical tool for the separation of a large variety of compounds, ranging from small inorganic ions to large biological molecules.<sup>2,3</sup> With attractive features such as rapid analysis time, high separation efficiency, small sample size and low solvent consumption, CE has been increasingly used as an alternative or complementary technique to HPLC. Capillary gel electrophoresis<sup>4</sup> in highly multiplexed capillary tubes has been demonstrated for high-speed, high-throughput DNA analysis. A 96-capillary array electrophoresis system has been successfully used in our group<sup>5,6</sup> and in other groups<sup>7-11</sup> to perform DNA sequencing and other DNA analysis. In these multiplexed CE systems, laser-induced fluorescence is exclusively employed as the detection method. While fluorescence detection is suitable for DNA sequencing applications because of its high sensitivity and special labeling protocols, UV absorption detection has remained very useful because of its ease of implementation and wide applicability, especially for the deep-UV (200-220 nm) detection of organic and biologically important compounds.

Wu and Pawliszyn reported a capillary isoelectric focusing system using a two-dimensional CCD detector in which one dimension represented the capillary length while the second dimension recorded the absorption spectrum.<sup>12</sup> With the trade of wavelength resolution in the second CCD dimension, isoelectric focusing in two capillary tubes was simultaneously monitored according to their report.<sup>12</sup> The use of optical fibers for

illumination led to low light intensities and poor UV transmission. So, only visible wavelengths have been employed for the detection of certain proteins.<sup>12</sup> Because the CCD has a very small electron well capacity (about 0.3 million electrons), the limit of detection (LOD) of that system is limited by the high shot noise in absorption detection. The use of the CCD produced an overwhelming amount of data per exposure, limiting the data rate to one frame every 15 s. Also, the imaging scheme utilized is not suitable for densely packed capillary arrays because of the presence of mechanical slits to restrict the light paths. Further, in order to avoid cross talk, only square capillaries can be used.

Photodiode arrays (PDA) are used in many commercial CE and HPLC systems for providing absorption spectra of the analytes in real time. Transmitted light from a single point in the flow stream is dispersed by a grating and recorded across the linear array. Jorgenson and coworkers reported a capillary zone electrophoresis system using a photodiode array as the imaging absorption detector.<sup>13</sup> Different elements in the array were used to image different axial locations in one capillary tube to follow the progress of the separation. Because the PDA has a much larger electron well capacity (tens of million electrons), it is superior to the CCD for absorption detection. Time-correlated integration was applied to improve the signal-to-noise ratio (S/N).<sup>13</sup> In this paper, we present a novel absorbance detection approach for multiplexed CE using a single linear photodiode array detector. 96-capillary array zone electrophoresis or micellar electrokinetic chromatography (MEKC) were performed and the analytes were detected simultaneously by the PDA detector. Uniform separation efficiency and S/N were obtained using this system. An analysis throughput that is 100 times higher than the conventional single-capillary electrophoresis instruments can thus be achieved.

## **Experimental Section**

### **96-Capillary Array Electrophoresis System**

Figure 1 shows the experimental setup. 96 fused-silica capillaries (75  $\mu\text{m}$  i.d., 150  $\mu\text{m}$  o.d.; Polymicro Technologies, Phoenix, AZ) with 35 cm effective length and 55 cm total length were packed side by side at the detection windows. A uniform window region was created after packing by using an excimer laser beam to burn off the polyimide coating. At the ground (exit) end of the capillary array, the capillaries were bundled together to allow simultaneously buffer filling and rinsing. At the injection end, the capillary array was spread out and mounted on a copper plate to form an 8  $\times$  12 format with dimensions that fitted into a 96-well microtiter plate for sample introduction. In addition, 96 gold-coated pins (Mill-Max Mfg. Corp.) were located next to the capillary tips to serve as individual electrodes. Sample and buffer trays were moved and aligned under the capillary inlets. This way, the capillary array is never physically moved. A high-voltage DC power supply from Spellman provided power for electrophoresis. All 96 electrodes were connected to the same power supply. Similar 96-capillary array electrophoresis systems with fluorescence detection were used in our laboratory for DNA sequencing<sup>14</sup> and genetic typing,<sup>15</sup> as reported elsewhere.

### **Array Detection System**

As shown in Figure 1, the light source, filter, capillary array holder, camera lens and PDA detector were all contained in a light-tight metal box attached to an optical table. All optical components were centered 12.6 cm above the optical table. As the light source, a 12-V tungsten lamp or a 254-nm hand-held mercury lamp (model E-09816-02; Cole-Parmer) was used for visible or UV absorption detection, respectively. In the case of the tungsten lamp (with a filament length of 1.1 cm) the light was first expanded through a cylindrical lens to uniformly cover the detection windows of the entire array that had a combined width

of 1.5 cm. The hand-held mercury lamp proved to have a long enough emission length (7 cm), thus no light expansion optics was needed for illuminating the whole array. The transmitted light from the capillary array passed through an interference filter (Oriel) and a quartz lens (Nikon; f.l. = 105 mm; F# = 4.5). The interference filter was employed to define the absorption wavelength. An inverted image of the capillary array, at a nominal magnification factor of 1.5, was created by the quartz lens on the face of the PDA. The PDA (model S5964, Hamamatsu) incorporated a linear image sensor chip, a driver/amplifier circuit and a temperature controller. The linear image sensor chip had 1024 diodes, each of which was 25  $\mu\text{m}$  in width and 2500  $\mu\text{m}$  in height. The temperature controller thermoelectrically cooled the sensor chip to 0 °C to lower the dark count and to minimize temperature drift, thus enabling reliable measurements to be made over a wide dynamic range. The built-in driver/amplifier circuit was interfaced to an IBM-compatible computer (233 MHz Pentium, Packard Bell) via a National Instrument PCI E Series multifunction 16-bit I/O board. The I/O board also served as a pulse generator to provide a master clock pulse and a master start pulse required by the linear image sensor. All code used to operate the PDA and to acquire the data were written in house using National Instruments Labview 4.1 software.

### **Data Acquisition and Treatment**

A very large amount of data were generated for each CE run using the 1024-element PDA detector. A run of one hour with a data acquisition rate of 10 Hz generated 70 Mb of data. All the data were therefore written directly to the hard disk in real time. Signals from up to ten elements of the PDA could be displayed in real time in the Labview program. Real-time monitoring of more pixels was limited by the video speed of our computer. The raw data sets were extracted into single-diode electropherogram data by another in-house Labview program. Data treatment and analysis were performed using Microsoft Excel 97

and GRAMS/32 5.05 (Galactic Industries). The transmitted light intensities collected at the PDA were converted to absorbance values using the tenth capillary (buffer solution only) as a continuous blank reference. The root-mean-squared (rms) noise in all of the electropherograms was obtained using a section of baseline near one of the analyte peaks. This baseline section was of about the same width as the peaks of interest.

### **Separation Conditions**

For the capillary zone electrophoresis experiments, the capillary array was first flushed with methanol and then water for clean up. pH 8.0 1×TBE buffer with 0.2% (w/w) polyvinylpyrrolidone (PVP) was filled into the capillary array while the injection end was immersed into a buffer tray. After buffer filling, the filling ends were immersed into a second buffer tray. The analytes were put into a 96-well microtiter sample plate (1 µl/well) and injected at the cathode for 6 s at 11 kV (100 V/cm). The running voltage was also 11 kV. For the CE experiments, the capillaries were washed for 1 min with buffer in between runs. For the MEKC experiments, the capillary array was first flushed with 0.1 M HCl and then water. The buffer additive used was Brij-S made by sulfonation of Brij-30 with chlorosulfonic acid.<sup>16</sup> The analytes were injected at the cathode for 3 s at 10 kV and run at the same voltage.

### **Reagents and Chemicals**

Fluorescein (F), rhodamine 6G and 5(6)-carboxyfluorescein (5CF, 6CF) were obtained from Sigma. 2,7-diacetate,dichloro-fluorescein (DADCF) was obtained from Acros. The sample solutions for CZE were prepared by dissolving the appropriate amounts of these fluoresceins in 1×TBE buffer with 0.2% (w/w) PVP. For the MEKC experiments, the analytes and buffer additives were purchased from Aldrich, J. T. Baker and Sigma. The running buffer was prepared by adding appropriate aliquots of 1.0 M HCl, 250 mM Brij-S

stock solutions, acetonitrile and 2-propanol into water. The pH was adjusted to 2.4 using 0.1 M HCl or 0.1 M NaOH stock solutions and confirmed by a pH meter.

## **Results and Discussion**

### **Capillary Array Images**

A typical 96-capillary array image obtained using a tungsten lamp and the PDA is shown in Figure 2A. As can be seen in Figure 2B, the center of each capillary corresponds to a 'peak' in the image. Between two adjacent capillaries, there is normally a spacing that also creates a transmission 'peak'. These 'spacing peaks' are usually a bit broader and have larger intensities (saturated in this case) than the 'center peaks' in this imaging system, as shown in Figure 2B. If the array packing is not even, two adjacent capillaries can overlap each other so that the 'spacing peak' between them was not observed (data not shown). Including the spacing, each capillary was imaged upon 9-11 diodes in the PDA. The 96-capillary array covered 912 pixels in total. As can be seen in Figure 2B, between the 'center peak' and the 'spacing peak', there is a 'valley' which corresponds to the wall of the capillary. When the capillary array image was well focused onto the PDA, the intensities of these valleys became minimized. This feature was used to produce the best focusing. The diodes that corresponded to the center peaks were used as the absorption detectors for the corresponding capillaries. Their intensities are about 40% to 90% of the saturation value of the diodes. To maintain the relatively uniform intensity distribution over the capillary array, we found that the emission length of the light source should be at least two times larger than the width of the capillary array (1.5 cm). The hand-held mercury lamp (7-cm emission length) that was used as the UV light source was long enough for uniform illumination of the entire array. The tungsten lamp used as the visible light source, however, had only a 1-cm emission length, so a cylindrical lens needs to be added to magnify the light source to

meet the illumination requirement. Figure 2A shows a  $2\times$  variation in optical throughput from the center to the edge of the array. This means that the detection limit will vary by  $\sqrt{2} \times$  across the array. The sensitivity (signal) however will vary by  $2\times$  unless the intensities are first ratioed to the blank (buffer) and a log scale is used (Beer's Law). As seen from Figure 1, the Hg lamp is placed very far from the array. The intensity distribution is thus much more uniform than that in Figure 2A.

We note that unlike previous reports,<sup>12,13</sup> there are no mechanical slits to define the image. This is quite surprising. The cylindrical capillaries do refract light onto other diodes in the array. However, the distance to the camera lens is much larger than the radius of curvature. Each diode receives a low level of stray light averaged over all capillaries. This sets the limit on the "valleys" in Fig. 2 but contributes negligibly to cross talk. The rays of light crossing the diameters of the capillaries will travel straight and are properly imaged at the PDA. Sensitivity (absorption path length) is thus also optimized. The facts that there are no mechanical slits and that each capillary spans 9 pixels mean that the system is extremely stable. No realignment or refocusing is needed over a period of a week.

### **Signal-to-Noise Considerations**

A clear understanding of the noise sources for the array detector is important, as the noise will ultimately determine the minimum baseline fluctuation level and thus the LOD of the system. Dark noise of the PDA can be attributed to dark current shot noise, diode reset noise and circuit noise, which are not dependent on the number of photoelectrons generated in the diodes (i.e. the input light intensity). According to the data given by the manufacturer, the dark noise ( $s_d$ ) of the PDA is about 3200 electrons at 0 °C. Shot noise is generally defined as the combined noise associated with the random generation of photons from the excitation source and the random generation of photoelectrons in the diode junction, and is equal to the square root of the number of photoelectrons counted in each diode,  $(n_e)^{1/2}$ . The

total rms noise level ( $s$ ) of the PDA in the absence of flicker noise (see below) can be expressed using the equation

$$s = s_d + (n_e)^{1/2}. \quad (1)$$

Therefore, it is desirable to have as high a photon count as possible. The electron well capacity of a diode is generally proportional to the area of the sensing junction. A long but narrow diode will maximize the dynamic range and the spatial resolution (in one dimension) at the same time. This comes with an increase in dark current such that cooling becomes mandatory.

For the PDA used in this work, the saturation charge for each diode is about 25 pC, or 156 million electrons. This is almost three times as high as the PDA used in previous work.<sup>13</sup> In real absorption detection, however, the diodes should only be 85-90% saturated to allow room for baseline drift due to uncontrollable variables over the period of data acquisition. The total rms noise for an 85% saturated diode was calculated to be 14700 electrons according to Equation (1), given  $s_d$  to be equal to 3200 electrons. Conversion of this value into absorbance units gave an absorbance noise limit of  $4.7 \times 10^{-5}$ .

Actual noise was measured from single-diode electropherograms. The tungsten lamp was used as the light source and was moved back and forth behind the capillary array to control the input light intensity, and thus the number of photoelectrons generated at the diode junction. The measured rms noise level of one diode is linearly proportional to the square root of the number of photoelectrons generated at the diode junction. The intercept of the linear regression of the curve can be related to the rms dark noise according to Equation (1). The measured intercept value was 3266 electrons, which was close to what was given by the manufacturer, 3200 electrons. Also the measured slope, 0.92, was close to the theoretical value of 1. When the diode was more than 25% saturated with the tungsten lamp as the light source, the major noise source was shot noise. This could be attributed to the relatively low dark noise of the thermoelectrically cooled PDA and the superior stability of

the battery-powered DC tungsten lamp (thus a negligible flicker noise). When a PDA was used at room temperature (results not shown), the rms noise level was at least 5 times higher. The measured rms noise of the diode at 85% saturation level can be converted to an absorbance unit of  $4.8 \times 10^{-5}$ , which is close to the expected noise limit of  $4.7 \times 10^{-5}$ . When the hand-held mercury lamp was used, the average measured rms noise for one diode was  $9.0 \times 10^{-5}$  at 85% saturation level, which was about two times higher than the expected value. This is believed to be due to the additional intensity flicker noise associated with the mercury lamp.

Mathematical smoothing can reduce the noise significantly without distorting the signal if properly used. To ensure that more data points can be used for smoothing, without sacrificing temporal response, a higher data acquisition rate needs to be employed. For the PDA detector, data acquisition rate is limited by the digitization rate and the exposure time. The A/D converter in our system is capable of functioning at 25 kHz. So, 40 ms is the minimum exposure time for each data point in the 1024 array. With the tungsten or mercury lamp as the light source in this experiment, a 40-ms exposure time was more than sufficient to attain around 85% saturation level for all diodes. Normally an analyte peak is more than 10 s in width, and 9 data points are enough to represent a typical chromatographic or electrophoretic peak. So, up to 25 data points (1 s in time) can be used for smoothing with little sacrifice of the width of the analyte peaks. Different kinds of smoothing approaches were compared, and boxcar smoothing proved to be the most efficient method to suppress the noise here (data not shown). After 25-point boxcar smoothing, the average rms noise was lowered to  $1.33 \times 10^{-5}$  AU at 85% saturation level with the tungsten lamp as the light source. One can consider smoothing as increasing the dynamic range (electron well depth) of the diodes after the fact. The observed enhancement factor is close to the factor of 5 predicted by Equation (1).

To probe the actual detection limits achievable using this capillary array absorption

detection system, electrophoresis of rhodamine 6G, at the concentration of  $4 \times 10^{-7}$  M in  $1 \times$ TBE buffer solution was performed using  $1 \times$ TBE as the running buffer. The sample was hydrodynamically injected for 6 s at a height difference of 8 cm. No sample stacking is expected under these conditions. Capillary electrophoresis was run at 250 V/cm. Detection was performed at a wavelength of 552 nm, defined by an interference filter with 10-nm bandwidth. The electropherogram from one capillary in the array is shown in Figure 3(A). The S/N for the rhodamine 6G peak was about 8 (based on a peak height of 0.0002 and a rms noise between frame 1950 and frame 2250 of  $2.6 \times 10^{-5}$ ), which was near the detection limit predicted by Eq. (1). After 25-point boxcar smoothing, the S/N ratio was improved to about 45, as shown in Figure 3(B). The resulting  $1.8 \times 10^{-8}$  M LOD (S/N = 2) for Rhodamine 6G injected is comparable to what most commercial single-capillary machines could achieve.

The hand-held mercury lamp used in this experiment had much more fluctuation than the tungsten lamp did, but less than the pen-light mercury lamp used in previous work.<sup>13</sup> This is inherent to the discharge nature of the mercury source as compared to Joule heating in the tungsten source. While the battery-operated tungsten lamp provided negligible flicker noise in the system, a double-beam scheme was employed to cancel the flicker noise due to the mercury lamp. Certain capillaries in this 96-capillary array were injected with blank samples (buffer solution), and the signals from them were used as reference signals. Signals from other capillaries were normalized to the level of the reference signal from the nearest reference capillary, and then the reference signal was subtracted from the normalized signals. Figure 4 shows the effect of the noise cancellation scheme for a signal at about 85% saturation level. The baseline drift and the intermediate-term noise (i.e. those on the time scale of the signal peaks) were reduced. After normalization to the reference signal, the rms noise of the signal was lowered to  $6.0 \times 10^{-5}$  AU from  $9.1 \times 10^{-5}$  AU. The short-term (high frequency) noise is actually a bit higher. However, these are adequately smoothed out by the

boxcar algorithm described above. It was found that in this 96-capillary array, the blank signal from one capillary could act well enough as the reference for signals from ten capillaries on each side. So only five reference capillaries were needed in the entire 96-capillary array. We note that since the data in each diode was acquired consecutively by the digitizer, true temporal correlation of the flicker noise still does not exist between the reference and the measurement channels. This contributes to the short-term noise. This aspect of the system could potentially be improved in the future with more sophisticated diode arrays with flexible clock functions.

Figure 5 shows the result of the MEKC separation of five neutral compounds. The separation was modeled after a recent study on single-capillary separations.<sup>16</sup> The separation resolution and S/N are relatively good compared to that in ref. 16. The molar absorptivities of the PAH are lower and the peak widths are larger. The injected concentration of 9,10-diphenylanthracene was  $9 \times 10^{-5}$  M. The LOD (S/N = 2) is  $1.9 \times 10^{-6}$  M before smoothing and  $9.2 \times 10^{-7}$  M after smoothing. The final noise level was higher by about 2 fold compared to the CZE separation experiment due to the higher intensity fluctuation of the hand-held mercury lamp, as discussed above.

The MEKC separation also generated very high current, which is 30  $\mu$ A per capillary and about 3 mA for the whole array. Therefore a large amount of heat was produced during the separation. Some cooling approaches needed to be employed to help the heat dissipation. It was found the hottest part in this setup during the separation was the detection window. This was because all the capillaries were densely packed together in this region. To avoid mechanical vibrations in the capillary array, which would bring about excess amounts of noise, a laminar flow of nitrogen gas was created in parallel to the detection window of the capillary array to carry away the heat generated in this region. After the nitrogen cooling approach was employed, heat dissipation was not a problem in this setup.

## **Cross talk**

To minimize the cross talk between adjacent capillaries, the image of a capillary on the face of the PDA needs to be big enough to ensure that the diode corresponding to the center of the capillary receives minimal stray light from adjacent capillaries. It was found if the image of one capillary covers more than 8 diodes in the PDA, cross talk was less than 0.2%, which is negligible for the multiplexed analysis. Cross talk was also found to be related to the spatial alignment of the capillary array. We found that the image of each capillary in the array needs to be parallel to the diodes in the PDA. Otherwise the signal from more than one capillary may cross over each diode (which is narrow but long) and cause more cross talk. The array also needs to be confined to a plane, or else imaging will not be uniform for each capillary. Finally, vibrations in the capillaries, especially when high voltage is applied or when cooling fans are improperly situated, will cause additional flicker noise in the system. Rigid mounting of the array and of the optics is therefore critical.

## **96-Capillary Array Results**

Figure 6 shows the result of CZE separation of four visible dyes in the 96-capillary array. The horizontal direction represents the capillary array arrangement while the vertical direction represents the migration time. Relatively uniform separation resolution and S/N distribution can be observed from the reconstructed image file. Cross talk between adjacent capillaries was not observable, as expected for this analyte concentration range. This is the first demonstration of a very high-throughput multiplex capillary electrophoresis system using an absorption detector.

The results for multiplexed CE indicate that the migration times are highly nonuniform among the capillaries. This is to be expected from the absence of temperature regulation and variations in the column surfaces. We have demonstrated that an internal standardization scheme can be employed to normalize the results among the capillaries so

that the migration times and the peak areas are reliable enough for high-throughput applications.<sup>17</sup> Figure 7 confirms that by using the first and the last peaks as the two internal standards,<sup>18-20</sup> both the migration times and the peak areas become uniform across the array. For the second and third peaks the relative standard deviations (RSDs) of migration times were reduced from 17% and 22% to 1.9% and 2.0%, and the RSDs of peak areas were reduced from 65% and 87% to 3.8% and 8.8%, respectively. In the case of peak areas, two capillaries (#23 and #45, see Figure 7B) dominated the contributions to the RSDs. If these two were omitted from the statistical analysis, the RSDs were lowered to 2.9% and 5.3%, respectively. The fact that this normalization scheme<sup>17</sup> works equally well with the absorption detector here shows that the data in Figure 7B are all within the linear range of the detector. This is not surprising since at no time did the intensity decrease by more than 15% (Fig. 6). For larger absorptions, a logarithmic correction will need to be applied to maintain a linear response.

### **Conclusions**

For the first time, a high-throughput 96-capillary array electrophoresis system using absorption detection was demonstrated. Uniform separation efficiency and good S/N can be obtained. The LOD achievable for this setup is comparable to those for commercial single-capillary electrophoresis machines using absorption detection. The separation of ionic and of neutral analytes were demonstrated by zone electrophoresis and by MEKC respectively. Consequently, the capillary array electrophoresis system can do everything single-capillary electrophoresis absorption instruments can do, only with much higher throughput. Potentially, it can also serve as an alternative to HPLC in many applications. No moving parts were used in this setup. Once the positions of all components are fixed, the only thing that needs to be adjusted is the focal point of the camera lens, just like taking a picture, to get

the best focused image of the capillary array. One focused, no noticeable changes in the system were observed over many days. Also, no lasers are used, thus the system should be smaller, more cost effective and easier to use and maintain than the multiplexed laser-induced fluorescence CE systems. Besides, the analytes do not have to be fluorescent to be detected. The absorption wavelength can be selected by simply changing a filter. Since the sample injection process involves only moving different microtiter plates under the injection block and can be fully automated, it should be possible to obtain a true throughput that is 100 times higher than what conventional single CE absorption determinations can achieve.

### **Acknowledgement**

The authors thank Dr. H.-M. Pang for assistance in setting up the 96-capillary array. The Ames Laboratory is operated for the U.S. Department of Energy by Iowa State University under Contract No. W-7405-Eng-82. This work was supported by the Director of Science, Office of Biological and Environmental Research and Office of Basic Energy Sciences, Division of Chemical Sciences, and by the National Institutes of Health.

### **References:**

1. Borman, S., *C&E News*, **1998**, April 6, 47-67.
2. Jorgenson, J. W., and Lukacs, K. D., *Anal. Chem.*, **1981**, *53*, 1298-1302.
3. Jorgenson, J. W., and Lukacs, K. D., *Anal. Chem.*, **1981**, *53*, 209-216.
4. Cohen, A. S., Najarian, D. R., Paulus, A., Guttman, A., Smith, J. A., and Karger, B. L., *Proc. Natl. Acad. Sci. (USA)*, **1988**, *85*, 9660-9663.
5. Taylor, J. A., and Yeung, E. S., *Anal. Chem.*, **1993**, *65*, 956-960.
6. Ueno, K., and Yeung, E. S., *Anal. Chem.*, **1994**, *66*, 1424-1431.

7. Huang, X. C., Quesada, M. A., and Mathies, R. A., *Anal. Chem.*, **1992**, *64*, 967-972.
8. Mathies, R. A., Huang, X. C., and Quesada, M. A., *Anal. Chem.*, **1992**, *64*, 2149-2154.
9. Kambara, H., and Takahashi, S., *Nature*, **1993**, *361*, 565-566.
10. Takahashi, S., Murakami, K., Anazawa, T., and Kambara, H., *Anal. Chem.*, **1994**, *66*, 1021-1026.
11. Dovichi, N. J., Zhang, J., Zhao, J., Rong, J., Liu, R., Elliott, J., Bay, S., Roos, P., and Coulson, L., DOE Human Genome Workshop IV, Santa Fe, NM, November 13-17, **1994**, Abstract #131.
12. Wu, J., and Pawliszyn, J., *Analyst (Cambridge)*, **1995**, *120*, 1567-1571.
13. Culbertson, C. T., and Jorgenson, J. W., *Anal. Chem.*, **1998**, *70*, 2629-2638.
14. Pang, H.-M., Pavski, V., and Yeung, E. S., submitted.
15. Gao, Q., Pang, H.-M., and Yeung, E. S., *J. Chromatogr.*, **1999**, accepted.
16. Ding, W., and Fritz, J. S., *Anal. Chem.*, **1998**, *70*, 1859-1865.
17. Xue, G., Pang, H.-M., and Yeung, E. S., *Anal. Chem.*, **1999**, accepted [AC990062B].
18. Dose, E. V., and Guiochon, G. A., *Anal. Chem.*, **1991**, *63*, 1154-1158.
19. Lee, T. T., and Yeung, E. S., *Anal. Chem.*, **1991**, *63*, 2842-2848.
20. Lee, T. T., and Yeung, E. S. *Anal. Chem.*, **1992**, *64*, 1226-1231.

**FIGURE CAPTIONS**

- FIGURE 1. Photograph of the experimental setup. Center: 96-well microtiter plate injection block. Left: capillaries bundled into 8 groups and finally into a single union for simultaneous fill and flush. Extreme left: mercury lamp. Background: automobile battery for tungsten lamp (not in use as shown). Right: camera lens with interference filter and light shield. Extreme right: cooled photodiode array detector. The optical tube has 1" centered mounting holes.
- FIGURE 2. (A) Image on the PDA of the whole 96-capillary array. (B) Image on the PDA of one region of the 96-capillary array. a: a 'center peak'; b: a 'spacing peak'; and c: a 'valley'.
- FIGURE 3. Electropherograms of rhodamine 6G injected at  $4 \times 10^{-7}$  M. (A) raw data and (B) data with 25-point boxcar smoothing. The two plots were offset for clarity.
- FIGURE 4. Noise cancellation using a double-beam scheme for the UV light source. (A) electropherogram before noise cancellation, (B) reference signal from a blank capillary, and (C) electropherogram after noise cancellation.
- FIGURE 5. Separation of 6 polyaromatic hydrocarbons monitored by the diode-array absorption detection system. In order, these are 9,10-diphenylanthracene ( $9 \times 10^{-5}$  M), benzo[ghi]perylene ( $1 \times 10^{-4}$  M), benzo[a]pyrene ( $6 \times 10^{-5}$  M), benz[a]anthracene ( $4 \times 10^{-5}$  M), fluoranthene ( $1 \times 10^{-4}$  M) and anthracene ( $5 \times 10^{-5}$  M).

FIGURE 6. Result of CZE separation of 4 visible dyes in the 96-capillary array. In order, these are 5CF ( $4 \times 10^{-5}$  M), 6CF ( $4 \times 10^{-5}$  M), F ( $8 \times 10^{-5}$  M) and DADCF ( $1.2 \times 10^{-4}$  M). The horizontal direction represents the location of the capillaries. The vertical direction represents migration time from 5.3 to 7.0 min. Top plot: intensity across the array. Left plot: intensity along one of the capillaries.

FIGURE 7. Reproducibility of (A) migration times and (B) peak areas across the capillary array for the raw data (open symbols) and data normalized by two internal standards (filled symbols) for two fluoresceins.

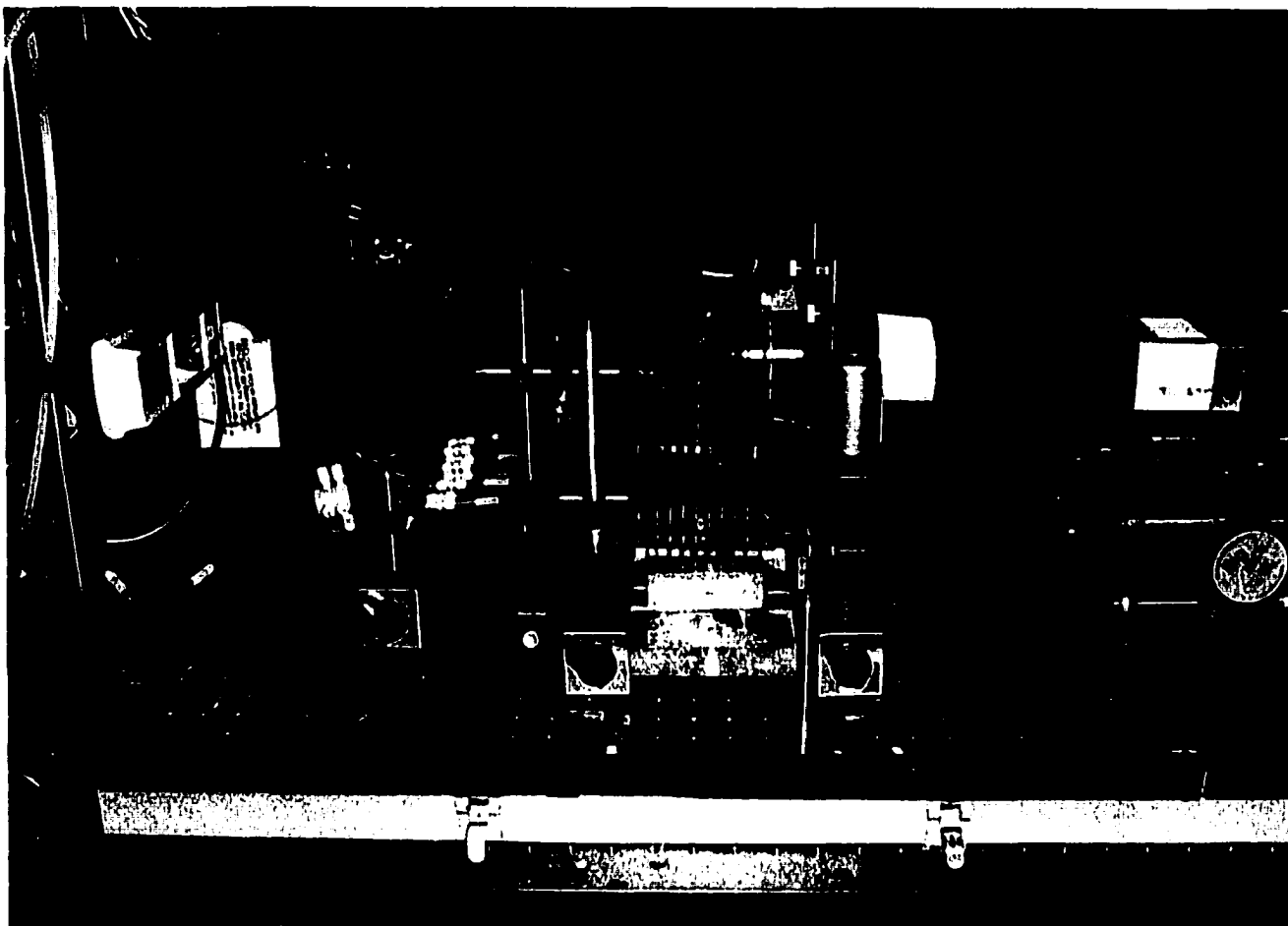


**FIGURE 1**

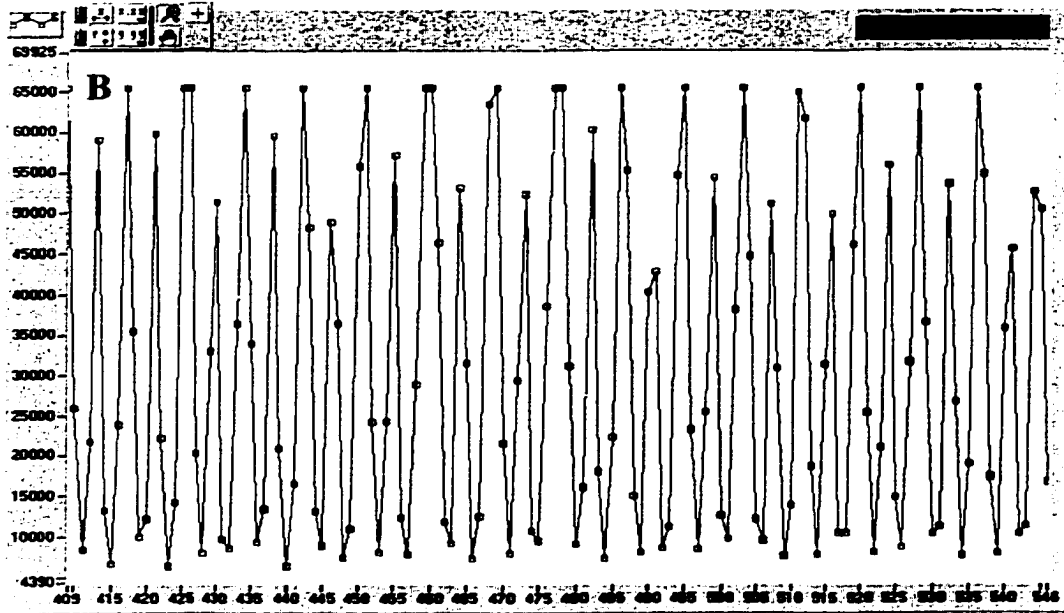
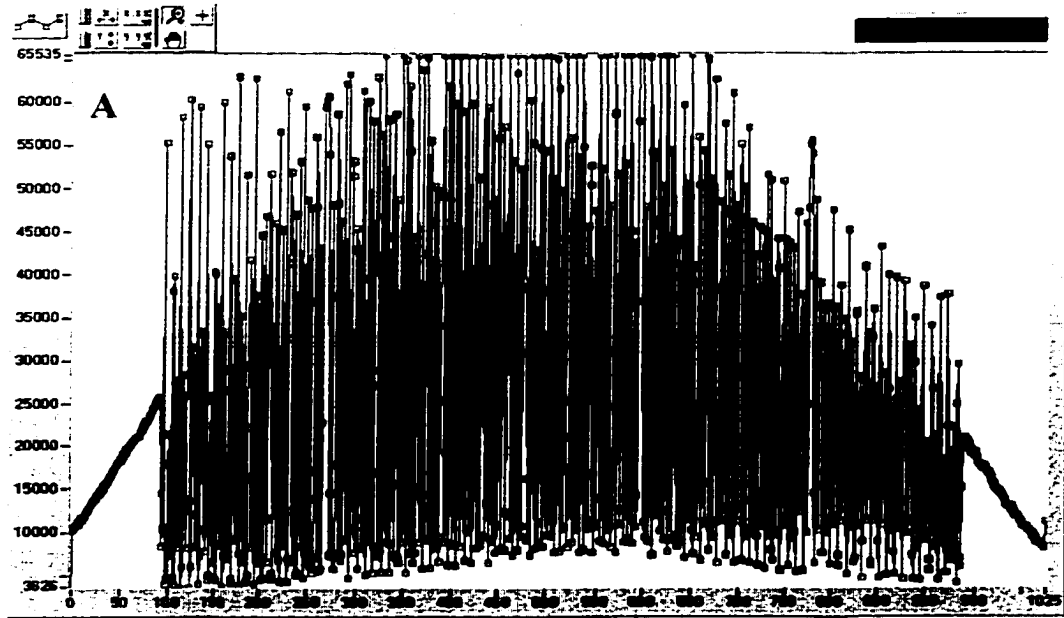
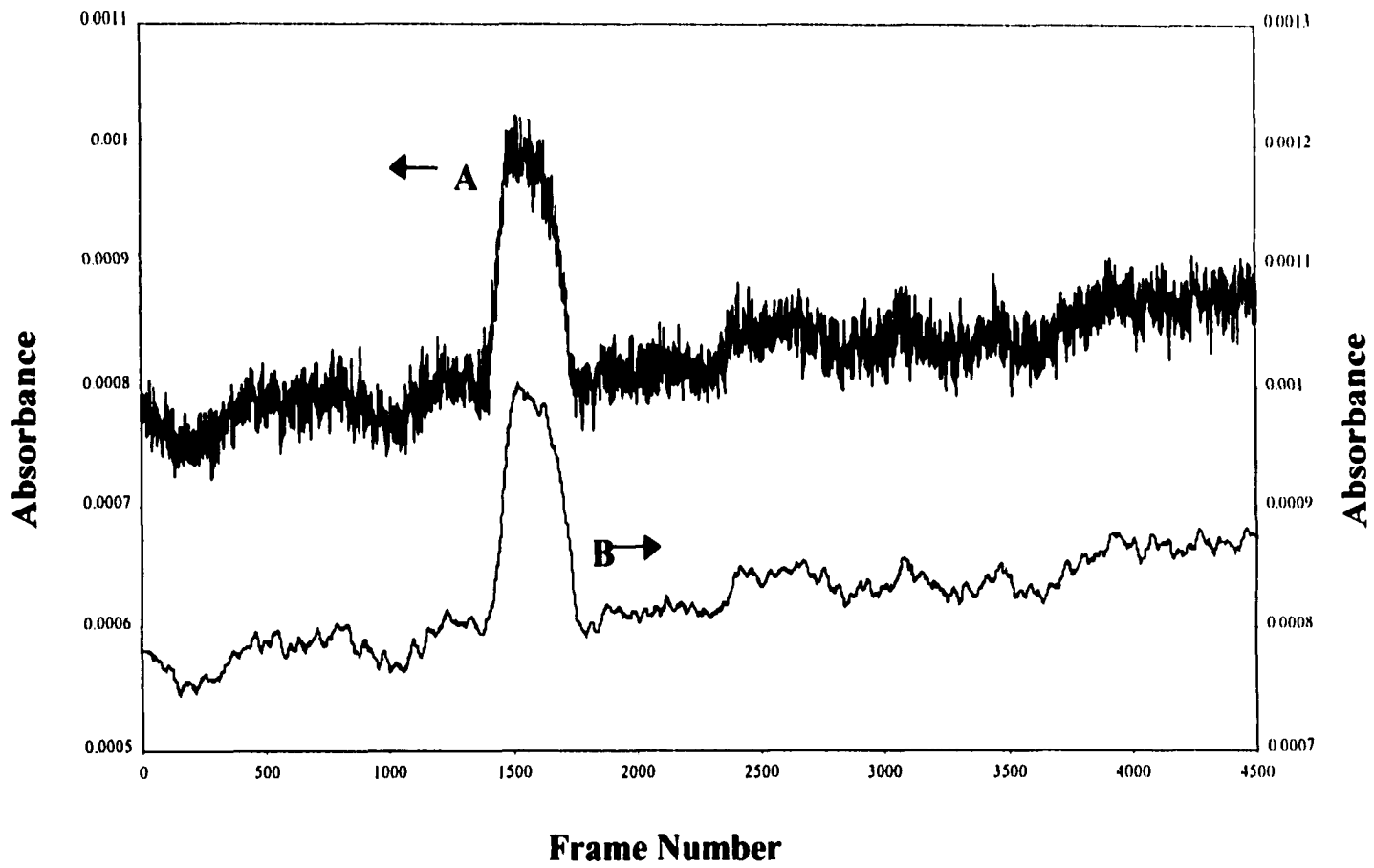


FIGURE 2



**FIGURE 3**

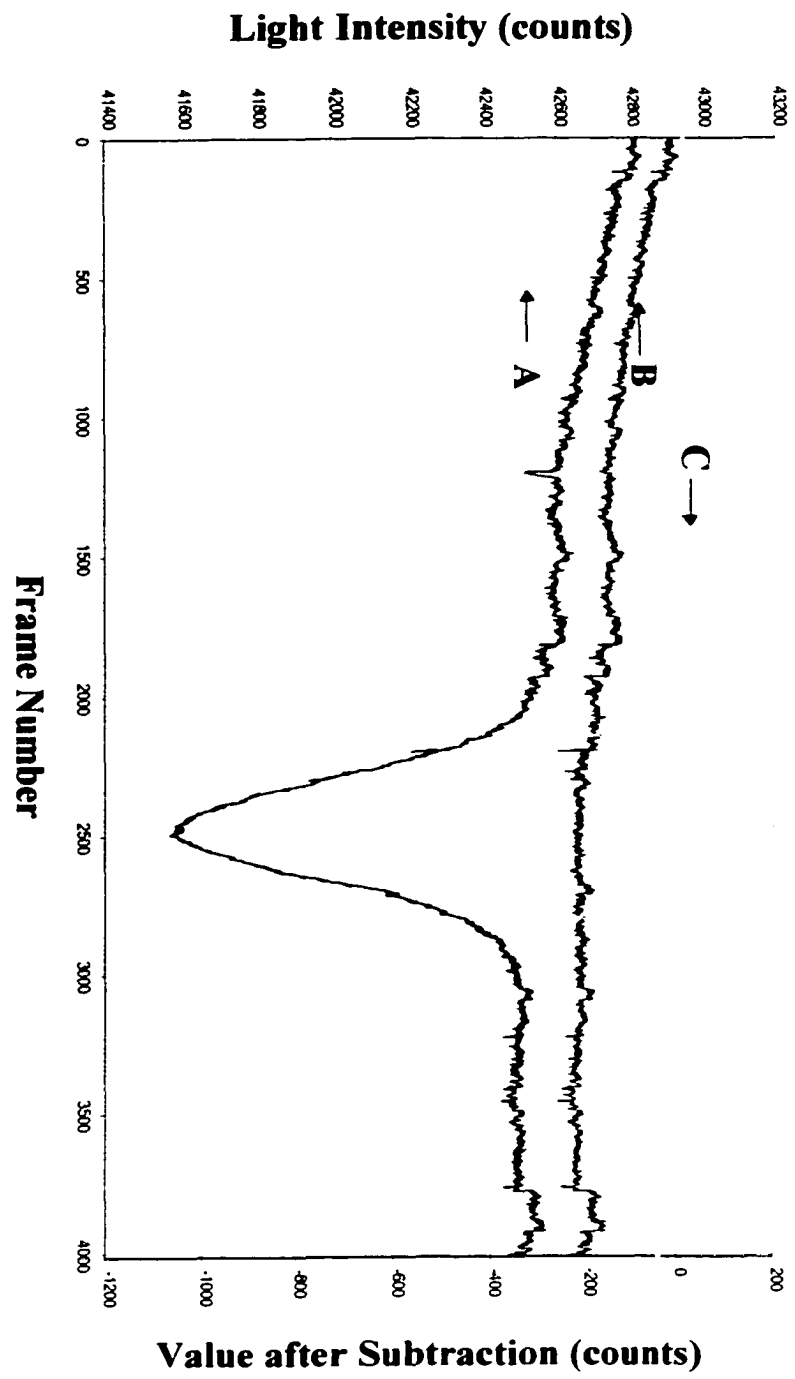
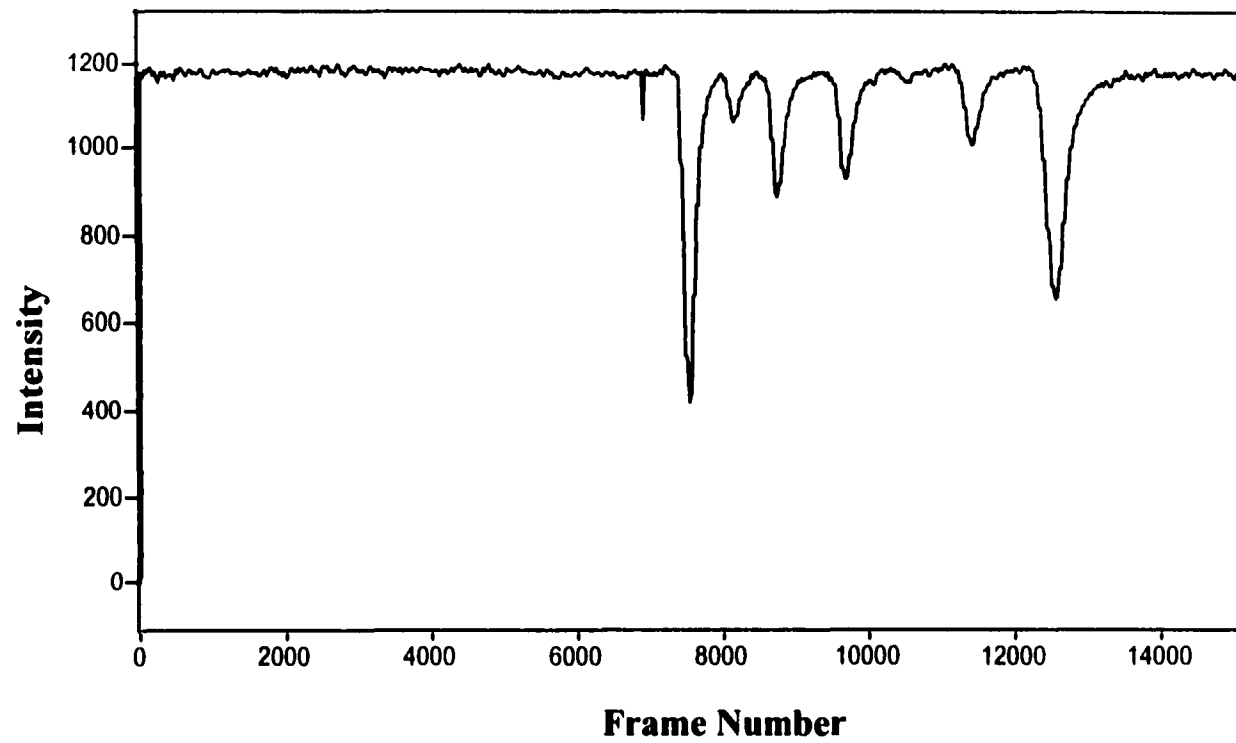


FIGURE 4



**FIGURE 5**

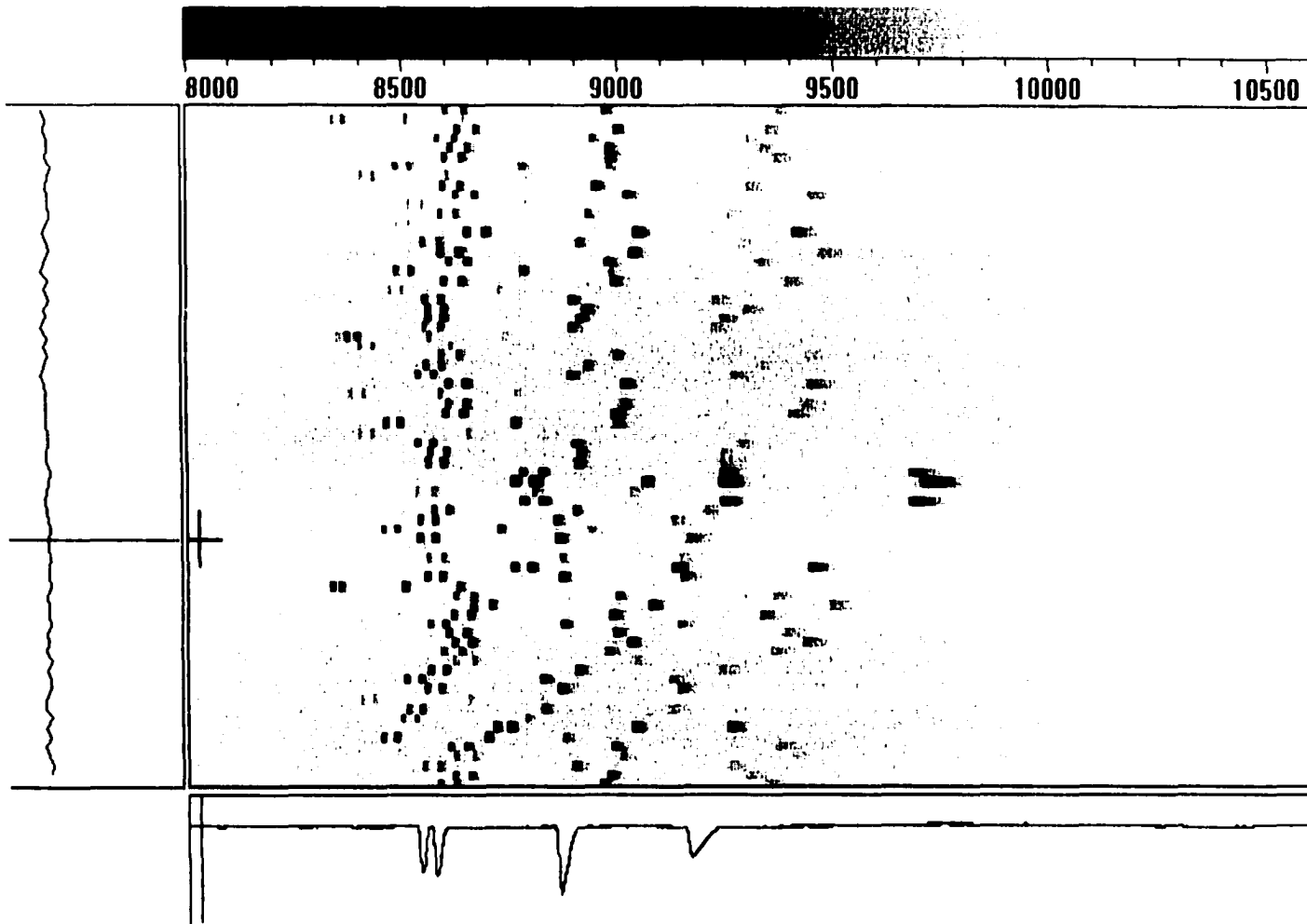


FIGURE 6

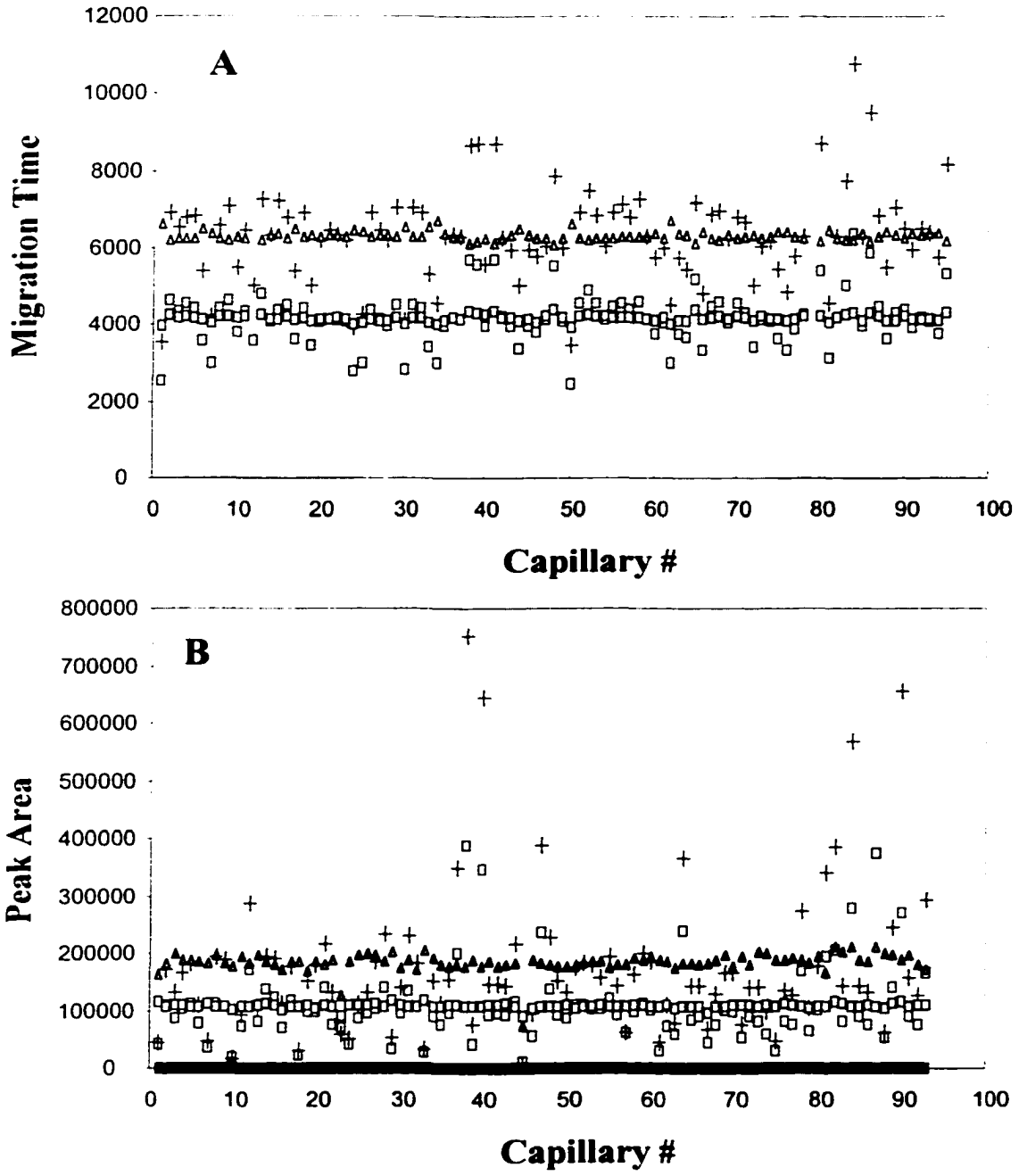


FIGURE 7

**CHAPTER 3. GENETIC TYPING AND HIV-1 DIAGNOSIS BY USING  
96 CAPILLARY ARRAY ELECTROPHORESIS  
AND UV ABSORBANCE DETECTION**

A paper published in *Journal of Chromatography B*\*

Xiaoyi Gong and Edward S. Yeung

**Abstract**

Current high-throughput approaches to the analysis of PCR products are based primarily on electrophoretic separation and laser-excited fluorescence detection. We show that capillary array electrophoresis can be applied to HIV-1 diagnosis and D1S80 VNTR genetic typing based simply on UV absorption detection. The additive contribution of each base pair to the total absorption signal provides adequate detection sensitivity for analyzing most PCR products. Not only is the use of specialized and potentially toxic fluorescent labels eliminated, but also the complexity and cost of the instrumentation are greatly reduced.

**Introduction**

Since the invention of the polymerase chain reaction (PCR) in 1985 by Kary Mullis, the ultimate in sensitivity, together with increasing ease in implementation, have placed this

---

\* Reprint with permission from *Journal of Chromatography*, 2000, 741, 15

technique in a central position in molecular biology research and in clinical diagnosis.<sup>1</sup> In the last ten years, PCR has stimulated numerous investigations in genetic analysis, and is even being used to determine the genetic basis of complex diseases.<sup>2</sup> There is no need to reiterate the development of capillary electrophoresis (CE) as a powerful analytical tool in post-PCR analysis. A large amount of research has been done to explore the advantages of CE over traditional slab gel electrophoresis, including high-speed, high-resolution restriction fragments analysis,<sup>3-8</sup> high-speed, high-throughput DNA sequencing,<sup>9-15</sup> rapid and precise DNA typing and sizing,<sup>16-22</sup> single-base mutation analysis<sup>23-28</sup> and the analysis of disease causing genes.<sup>29-33</sup> In particular, capillary array electrophoresis along with other micro-fabricated devices<sup>34-36</sup> are promising methods for the purpose of achieving high-throughput DNA analysis.

The conventional protocol for DNA analysis calls for labeling with radionuclides or fluorescent tags before, during or after size-based separation in slab gel electrophoresis or in capillary gel electrophoresis (CGE). This derivatization process involves expensive reagents and raises safety concerns for the operator and for waste disposal because of the toxic nature of these labeling reagents. Single capillaries have been utilized for DNA analysis.<sup>3</sup> Recently, a 96-capillary array electrophoresis system based on a novel absorption detection approach using a single linear photodiode array has been invented in our lab.<sup>37</sup> Based on this system, we are able to design DNA analysis protocols to take advantage of capillary array gel electrophoresis and absorption detection based on the inherent spectral properties of the DNA bases. The fact is that a 100-bp DNA contains 100 absorbing units that can provide excellent net absorptivity for sensitive detection. No special labeling reactions are required.

The method was tested on two broadly used PCR protocols using typical concentrations of starting materials. We show that as low as 50 copies of HIV-1 *gag* fragment can provide a positive diagnosis. Also, the human D1S80 VNTR region can be used to provide a DNA (genetic) fingerprint following the same method. Best of all, since the novel absorption detector involves no lasers and is suitable for simultaneously monitoring 96 capillaries (and scalable eventually to 1000 capillaries), high throughput can be achieved in a low-cost rugged instrument.

## **Experimental Section**

### **Reagents and Materials**

1×TBE buffer was prepared by dissolving pre-mixed TBE buffer powder (Amersco, Solon, OH) in deionized water. Poly(vinylpyrrolidone) (PVP) was obtained from Sigma (St. Louis, MO). The coating matrix was made by dissolving 2% (w/v) of 1,300,000 MW PVP into the buffer, shaking for 2 min and letting it stand for 1 h to get rid of bubbles. Poly(ethylene oxide) (PEO) was obtained from Aldrich Chemical (Milwaukee, WI). The sieving matrix was made by dissolving 2% (w/v) 600,000 MW PEO into the buffer. The solution was stirred vigorously overnight until all the material was dissolved and no bubbles could be observed. Ethidium bromide (EtBr) was obtained from Molecular Probes Inc. (Eugene, OR). 50-bp and 100-bp DNA ladders were purchased from Life Technologies (Gaithersburg, MD).

## Sample Preparation

### *Polymerase chain reaction*

#### 1. Multiplexed PCR for variable number of tandem repeats (VNTR) loci

AmpliFLP D1S80 PCR amplification kit was purchased from Perkin-Elmer (Foster City, CA). The kit included D1S80 PCR Reaction Mix (containing two D1S80 primers, AmpliTaq DNA polymerase and dNTPs in buffer), MgCl<sub>2</sub> solution and Control DNA 3 (human genomic DNA of D1S80 type 18, 31 in buffer). The PCR mixtures used are described as follows:

Positive Control: 20 µl of D1S80 PCR Reaction Mix, 10 µl of MgCl<sub>2</sub> solution and 20 µl of Control DNA3.

Negative Control: 20 µl of D1S80 PCR Reaction Mix, 10 µl of MgCl<sub>2</sub> solution and 20 µl of autoclaved DI H<sub>2</sub>O.

The polymerase chain reactions were performed with the following parameters: 30 cycles of denaturation at 95 °C for 15 s, annealing at 66 °C for 15 s, and extension at 72 °C for 40 s. The thermal cycler used was a Perkin-Elmer GeneAmp PCR system 2400.

#### 2. PCR for human immunodeficiency virus (HIV)

The HIV testing kit (Perkin-Elmer) included positive control DNA that includes all parts of the HIV-1 genome, negative control DNA, HIV primers, AmpliTaq DNA polymerase, dNTPs, PCR reaction buffer and MgCl<sub>2</sub> solution. The PCR mixtures used are listed in Table

1. The protocol for the Perkin-Elmer GeneAmp thermal cycler is 40 cycles of denaturation at 95 °C for 30 s, annealing and extension at 62 °C for 1 min. The annealing and extension temperatures were the same for this amplification.

### ***DNA purification***

All PCR products were purified with Microcon YM-30 centrifugal filter devices (Millipore, Bedford, MA). After the purification, salts, dNTPs and most HIV-1 primers were eliminated from the DNA samples.

### **Capillary Array Electrophoresis**

The 96 capillary array electrophoresis system with photodiode array absorption detection has been detailed before.<sup>37</sup> A DC-powered mercury lamp (UVP Inc., Upland, CA) was used as the light source, which gave lower noise levels than the AC-powered mercury lamp used in previous work. The absorption wavelength was set at 254 nm by an interference filter (Oriel, Stamford, CT). The total length of the capillaries was 55 cm, with 35-cm effective length. The capillary array was first flushed with deionized water and then with 1 ml of 2% PVP at a pressure of 100 psi. While the injection ends were immersed in the buffer reservoir, 0.5 ml of 2% PEO (600,000 MW) sieving matrix was pushed into the capillary bundle at 100 psi. The procedure roughly took 20 min. After the gel filling, ethidium bromide was added to the buffer reservoirs at the concentration of 1  $\mu\text{g/ml}$ . The system was then pre-run for 10 min with the electric field strength at 150 V/cm. After the pre-run, ethidium bromide should have spread out evenly in the sieving matrix through electrical migration. Ethidium bromide is known to make the DNA fragments more rigid, thereby leading to sharper bands in CGE. It is not expected to significantly alter the absorption strength of the DNA fragments in this study. The samples were injected electrokinetically at 150 V/cm for 15 s. 150 V/cm field strength was employed for the separation. The total current was about 620  $\mu\text{A}$

during the separation process. 12 different samples were used in the 96-capillary array electrophoresis experiment, which are detailed in Table 2. Each type of sample was injected into and run in eight different capillaries in the 96-capillary array.

### **Results and Discussion**

Figure 1 shows the result of the capillary array gel electrophoresis for DNA analysis as a reconstructed “gel” image. The vertical direction represents the capillary array arrangement while the horizontal direction represents the migration time. All separations were finished within 25 min. Capillary #84 (Sample type 11, see Table 2) showed bad separation resolution after 350 base pairs. The other 95 capillaries all gave reasonable separation and good signal-to-noise ratios. The migration times and peak intensities were highly non-uniform among the capillaries. This is to be expected from the absence of temperature regulation and variations in the column surfaces. We have demonstrated that an internal standardization scheme can be employed to normalize the results among the capillaries so the migration times and the peak areas are reliable enough for high-throughput applications.<sup>38</sup>

Actual electropherograms were extracted from capillaries #3, 9, 17, 25, 33, 41, 49, 57, 65, 73, 85 and 89, to represent each type of sample described in Table 2, and are shown in Figure 2. In capillaries #9-16 and #17-24, negative and positive HIV-1 PCR products were injected respectively. The positive and negative results can be easily differentiated through the HIV-1 *gag* fragment peak (triangle) which appeared only in the electropherograms from capillaries #17-24. Both the positive and negative HIV-1 PCR samples also contained the excess primers (circle) and the primer dimers (cross). To provide an even higher level of confidence for identification despite the variation of migration times among capillaries, the

HIV-1 *gag* fragments, primers and primer dimers can be sized by mixing the PCR products with 100-bp DNA ladders (capillaries #25-32), and injecting them into capillaries #33-40 and #41-48. The electropherograms from the latter two groups of capillaries showed that the HIV-1 *gag* fragment is about 115 bp and the primer dimer is about 60 bp.

In the electropherograms from capillaries #1-8, the HIV-1 primers gave broad peaks, which we believe are due to sample overloading. Deionized H<sub>2</sub>O was injected into capillaries #89-96, which gave blank electropherograms. These electropherograms served as blank references and were subtracted from the signals in the other capillaries to cancel out the flicker noise from the mercury lamp, as reported before.<sup>37</sup> The electropherograms from capillaries #49-56 showed negative D1S80 PCR results, where only the primer peaks can be observed. The electropherograms from capillaries #57-64 showed positive D1S80 genotyping PCR results. Two component peaks (D1S80 type 18 and 31) can be observed as expected from the heterozygous samples in addition to the very broad primer peaks. Again, to increase the confidence level for identification, the two D1S80 components as well as the primer were roughly sized by mixing each PCR product with a 50-bp ladder (capillaries #65-72) and injecting them into capillaries #73-80 (negative) and #81-88 (positive). The results showed the two D1S80 components to be about 400-bp and 600-bp.

### **Conclusions**

We designed DNA analysis protocols to take advantage of high-throughput capillary array gel electrophoresis and simple UV absorption detection based on the inherent spectral properties of the DNA bases. UV absorption detection of DNA products reduces the cost of analysis since it does not require labeling. 96-capillary array electrophoresis analysis of two

typical PCR products was demonstrated. 12 different samples were successfully analyzed simultaneously. The capillary array was flushed with water in between runs and did not show any degradation over tens of runs in a one-month period. Since the sample injection can be fully automated, this work demonstrated that it should be possible to obtain a true DNA analysis throughput that is 100 times (scalable to 1000 times) higher than what commercial single capillary gel electrophoresis systems can achieve, at relatively low cost.

### **Acknowledgement**

The authors thank Dr. H.-M. Pang for assistance in setting up the 96-capillary array. The Ames Laboratory is operated for the U.S. Department of Energy by Iowa State University under Contract No. W-7405-Eng-82. The instrumentation was developed with support from the Director of Science, Office of Basic Energy Sciences, Division of Chemical Sciences. This work was supported by the Director of Science, Office of Biological and Environmental Research and by the National Institutes of Health.

### **References:**

1. A. Rolf, I. Schuller, U. Finckh and I. Weber-Rolfs, *PCR: Clinical Diagnostics and Research*, 1992, Springer-Verlag, Berlin and Heidelberg.
2. R. K. Sacki, S. Scharf, F. Faloona, K. B. Mullis, G. T. Horn, H. A. Erlich and N. Arnheim, *Science*, 1985, 230, 1350.
3. A. Guttman, B. Wanders and N. Cooke, *Anal. Chem.* 1992, 62, 2348.
4. R. E. Milofsky and E. S. Yeung, *Anal. Chem.*, 1993, 63, 153.
5. P. E. Williams, M. A. Marino, S. A. Del Rio, L. A. Turni and J. M. Devaney, *J. Chromatogr. A*, 1994, 680, 525.

6. H. T. Chang and E. S. Yeung, *J. Chromatogr. B*, **1995**, 669, 113.
7. A. E. Barron, W. M. Sunada and H. W. Blanch, *Electrophoresis*, **1995**, 16, 64.
8. P. G. Righetti and C. Gelfi, *Anal. Biochem.*, **1997**, 244, 195.
9. M. C. Ruiz-Martinez, J. Berka, A. Belenkii, F. Foret, A. W. Miller and B. L. Karger, *Anal. Chem.*, **1993**, 65, 2851.
10. H. Lu, E. Arriaga, D. Y. Chen and N. J. Dovichi, *J. Chromatogr. A*, **1994**, 680, 497.
11. H. Lu, E. Arriaga, D. Y. Chen, D. Figeys and N. J. Dovichi, *J. Chromatogr. A*, **1994**, 680, 503.
12. E. N. Fung and E. S. Yeung, *Anal. Chem.*, **1995**, 67, 1913.
13. J. Zhang, Y. Fang, J. Y. Hou, H. J. Ren, R. Jiang, P. Roos and N. J. Dovichi, *Anal. Chem.*, **1995**, 67, 4589.
14. E. Carrilho, M. C. Ruiz-Martinez, J. Berka, I. Smirnov, W. Goetzinger, A. Miller, D. Brady and B. L. Karger, *Anal. Chem.*, **1996**, 68, 3305.
15. Y. Kim and E. S. Yeung, *J. Chromatogr.*, **1997**, 781, 315.
16. Y. Baba, R. Tomisaki, C. Sumita, I. Moromoto, S. Sugita, M. Tsuhako, T. Miki and T. Ogihara, *Electrophoresis*, **1995**, 16, 1437.
17. D. Noble, *Anal. Chem.*, **1995**, 67, 613A.
18. N. Zhang and E. S. Yeung, *Anal. Chem.*, **1996**, 68, 2927.
19. A. R. Isenberg, B. R. McCord, B. W. Koons, B. Budowle and R. O. Allen, *Electrophoresis*, **1996**, 17, 1505.
20. N. Zhang and E. S. Yeung, *J. Chromatogr. A*, **1997**, 768, 135.
21. J. M. Butler, B. R. McCord, J. M. Jang, J. A. Lee, B. Budowle and R. O. Allen, *Electrophoresis*, **1995**, 16, 974.
22. Y. Wang, J. Ju, B. A. Carpenter, J. M. Atherton, G. F. Sensabaugh and R. A. Mathies, *Anal. Chem.*, **1995**, 67, 1197.

23. M. A. Marino, K. R. Weaver, L. A. Tully, J. E. Girard and P. Belgrader, *Electrophoresis*, **1996**, 17, 1499.
24. H. Arakawa, K. Uetanaka, M. Maeda and A. Tsuji, *J. Chromatogr. A*, **1994**, 664, 89.
25. K. Hebenbrock, P. M. Williams and B. L. Karger, *Electrophoresis*, **1995**, 16, 1429.
26. A. W. H. M. Kuypers, P. C. M. Linssen, P. M. W. Willems and E. J. B. M. Mensink, *J. Chromatogr. B*, **1996**, 675, 205.
27. J. Cheng, K. Kasuga, N. D. Watson and K. R. Mitchelson, *J. Cap. Elec.*, **1995**, 2, 24.
28. J. Ren, A. Ulvik, P. M. Ueland and H. Refsum, *Anal. Biochem.*, **1997**, 245, 79.
29. W. Lu, D. Han, J. Yuan and J. M. Andrieu, *Nature*, **1994**, 368, 269.
30. T. A. Felmlee, P. S. Mitchell, K. J. Ulfelder, D. A. Persing and J. P. Landers, *J. Cap. Elec.*, **1995**, 2, 125.
31. C. Gelfi, A. Orsi, F. Leoncini, P. G. Righetti, I. Spiga, P. Carrera and M. Ferrari, *Bio-Techniques*, **1995**, 19, 254.
32. P. D. Grossman, W. Bloch, E. Brinson, C. Z. Chang, F. A. Eggerding, S. Fung, D. A. Iovannisci, S. Woo and E. S. WinnDeen, *Nucleic Acids Res.*, **1994**, 22, 4527.
33. P. G. Righetti and C. Gelfi, *Electrophoresis*, **1997**, 18, 1709.
34. K. Ueno and E. S. Yeung, *Anal. Chem.*, **1994**, 66, 1424.
35. S. Takahashi, K. Murakami, T. Anazawa and H. Kambara, *Anal. Chem.*, **1994**, 66, 1021.
36. T. Anazawa, S. Takahashi and H. Kambara, *Anal. Chem.*, **1996**, 68, 2699.
37. X. Gong and E. S. Yeung, *Anal. Chem.*, **1999** in press.
38. G. Xue, H.-M. Pang and E. S. Yeung, *Anal. Chem.*, **1999**, 71, 2642.

**TABLE CAPTIONS**

TABLE 1: PCR Mixtures for HIV Amplification.

TABLE 2: Sample description in the capillary array electrophoresis

**TABLE 1: PCR mixtures for HIV amplification**

Component	Addition Order	Volume	Final Concentration
Autoclaved, deionized water	1	32.8 $\mu$ l	
10 $\times$ PCR buffer II	2	5 $\mu$ l	1 $\times$
DNTPs	3	1 $\mu$ l each	200 $\mu$ M each dNTP
HIV-1 primer 1 (SK38)	4	1 $\mu$ l	0.5 $\mu$ M
HIV-1 primer 2 (SK39)	5	1 $\mu$ l	0.5 $\mu$ M
AmpliTaq DNA polymerase	6	0.2 $\mu$ l	1 unit
25 mM MgCl <sub>2</sub> solution	7	5 $\mu$ l	2.5 mM
Positive Control DNA or Negative Control DNA	8	1 $\mu$ l	0.5 $\mu$ g human placental DNA

**TABLE 2: Sample description in the capillary array electrophoresis**

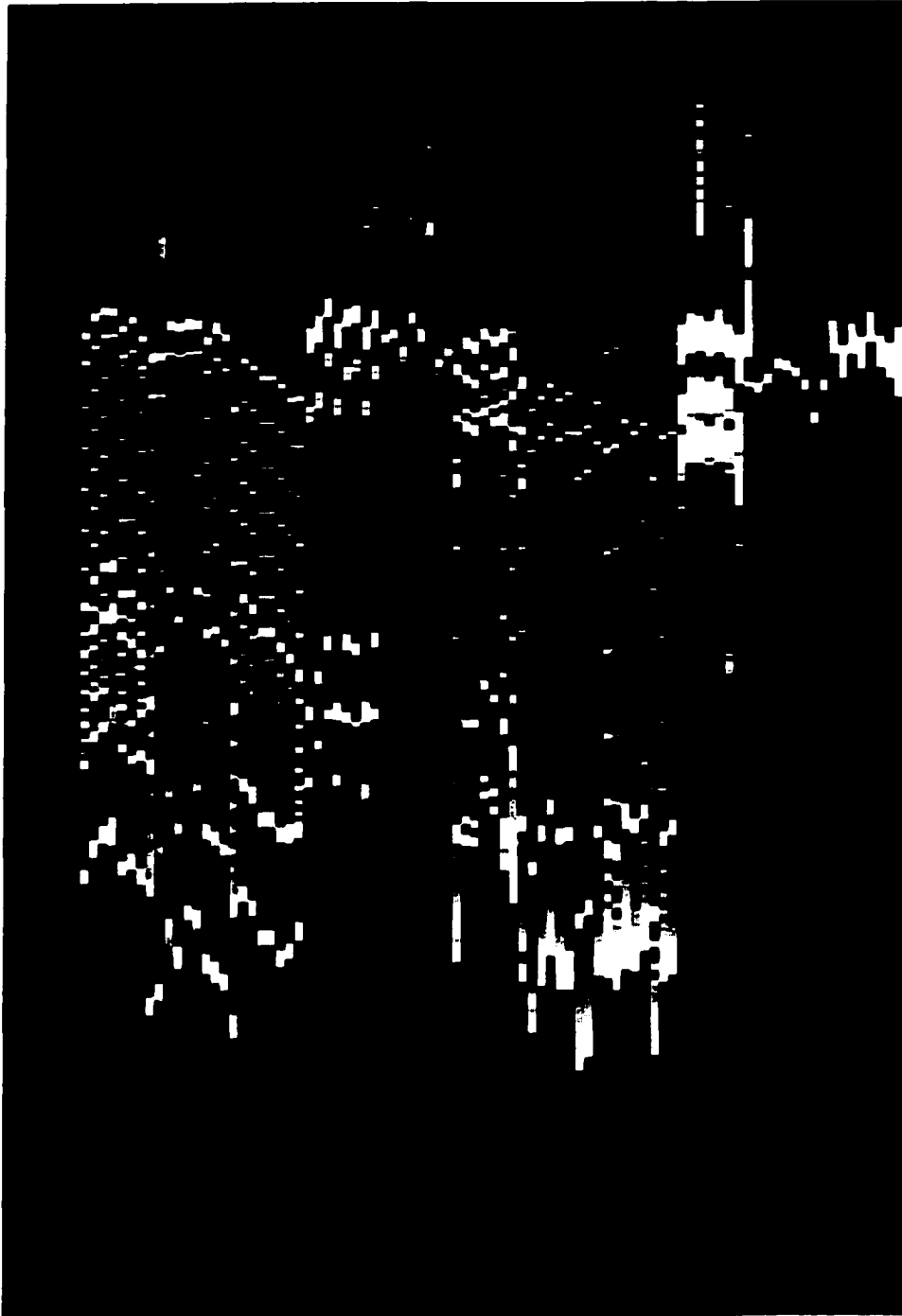
Sample No.	Description
1	4 $\mu$ l of HIV-1 primer-1 (SK38)
2	4 $\mu$ l of purified HIV-1 negative PCR product
3	4 $\mu$ l of purified HIV-1 positive PCR product
4	4 $\mu$ l of 100 bp ladder
5	3 $\mu$ l of purified HIV-1 negative PCR product with 1 $\mu$ l of 100-bp ladder
6	3 $\mu$ l of purified HIV-1 positive PCR product with 1 $\mu$ l of 100-bp ladder
7	4 $\mu$ l of purified D1S80 negative PCR product
8	4 $\mu$ l of purified D1S80 positive PCR product
9	4 $\mu$ l of 50-bp ladder
10	3 $\mu$ l of purified D1S80 negative PCR product with 1 $\mu$ l of 50-bp ladder
11	3 $\mu$ l of purified D1S80 positive PCR product with 1 $\mu$ l of 50-bp ladder
12	4 $\mu$ l of DI H <sub>2</sub> O

**FIGURE CAPTIONS**

FIGURE 1. Reconstructed two-dimensional electropherogram for capillary array electrophoresis. The 96 capillaries are aligned vertically and the migration time direction is from left to right. The samples are described in Table 2.

FIGURE 2. Selected extracted electropherograms for capillary array electrophoresis. From top to bottom are capillaries #3, 9, 17, 25, 33, 41, 49, 57, 65, 73, 85 and 89. O, primer; ∇, primer dimer; Δ, HIV-1 *gag* PCR product; and □, D1S80 PCR product.

**Capillary #**



**Time**

**FIGURE 1**

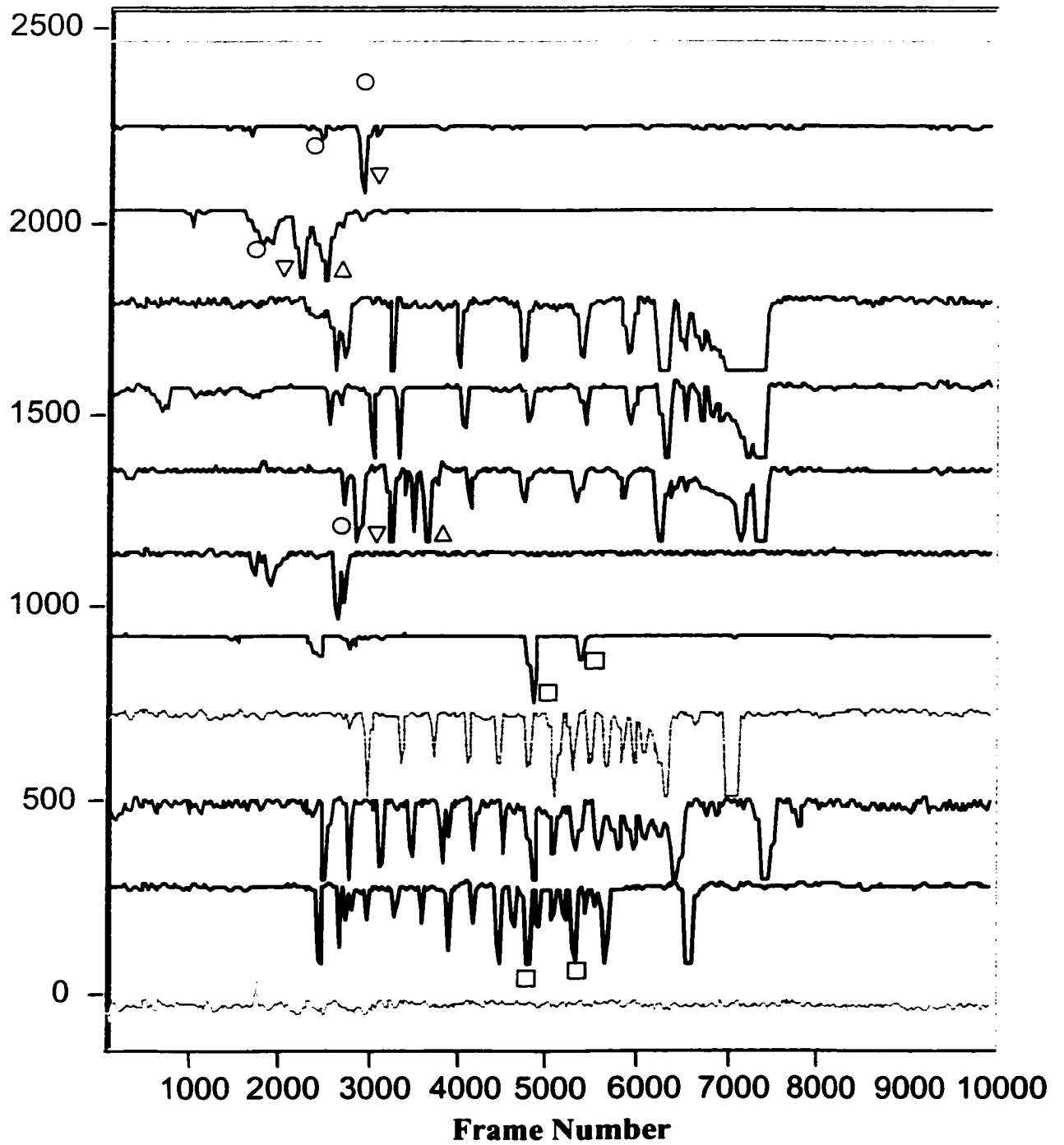


FIGURE 2

## **CHAPTER 4. COMBINATORIAL SCREENING OF ENZYME ACTIVITY BY USING MULTIPLEXED CAPILLARY ELECTROPHORESIS**

A paper accepted by Analytical Chemistry

Lianjia Ma, Xiaoyi Gong and Edward S. Yeung

### **Abstract**

Efficient and comprehensive screening of enzyme activity was accomplished in a combinatorial array of 96 reaction microvials. Quantitation of the extent of the reaction at well-defined time intervals was achieved by using 96-capillary array electrophoresis coupled with a multiplexed absorption detector. Capillary electrophoresis provides high separation resolution to isolate the product from the reactants. Absorption detection provides universal applicability to combinatorial screening. For the conversion of NADH to NAD<sup>+</sup>, the catalytic activity of LDH was confirmed to be the highest at pH 7. This scheme should be useful for high-throughput drug discovery, clinical diagnosis, substrate binding as well as combinatorial synthesis.

### **Introduction**

Combinatorial screening has attracted much attention recently because of its ability to efficiently and reliably zero in and identify the best solution to a chemical or biochemical question.<sup>1</sup> In chemical synthesis, optimization of the reaction yield can be achieved by si-

multaneously exploring all possible reaction conditions, catalysts and reagents. In drug discovery, all related structural variants of a given candidate can be tested against the target. However, screening must be comprehensive so that there is no chance of missing the best combination. This dictates having a large number of experiments to cover many parameters and to extend the range of each of these parameters. High throughput is a requirement in order to produce a timely result. It is primarily because of the advances in high-throughput technologies and automation that combinatorial screening became practical. Still needed are general and rugged analytical methodologies that can keep up with the large number of reactions that can be performed in any given time. Another issue is miniaturization of the entire operation. This impacts the cost of reagents, proper disposal of solvents, space for manipulation and storage, etc.

A highly successful format for combinatorial screening is that of DNA chips.<sup>2-4</sup> A comprehensive set of oligonucleotides immobilized within a small area is used to identify specific target sequences by hybridization. Oligonucleotide chips have also been used to develop aptamers that exhibit specific protein-nucleotide binding.<sup>5</sup> Such heterogeneous screening assays have benefited from sensitive detection based on laser-induced fluorescence (LIF), either by selective labeling or by selective quenching. For homogeneous assays, the 96-well microtiter plate is a popular format. Fluidic operations, plate readers and auto-samplers to interface to standard analytical instruments have all been developed for this format. When there is a color (absorption) change or fluorescence change, detection and quantitation is straightforward. In many situations, however, the reaction mixture is complex and some degree of separation or purification is needed before measurement. Multiple liquid

chromatographs or single instruments with several columns can in principle be used for analysis of the reaction mixtures. Still, much higher throughput and much smaller sample sizes are desirable.

Characterization of enzymes has been very important in the clinical and biochemical laboratory. The determination of enzyme activities can provide disease diagnosis or direct the development of new pharmaceutical products. Lactate dehydrogenase (LDH) has been found to be associated with different kinds of diseases, such as liver disease, myocardial infarction, etc.<sup>6</sup> Both the LDH activity and the LDH isoenzyme patterns in serum are potential biomarkers for different cancers. Published reports have pointed to the possibility of using LDH activity to classify leukemia.<sup>7</sup> Regnier and coworkers utilized capillary electrophoresis (CE) to perform enzyme assays and showed that CE could be a powerful tool for measuring enzyme activity.<sup>8-10</sup> We have previously demonstrated that CE-LIF can be used for LDH enzyme assay.<sup>11, 12</sup> Even single molecules have been detected in this manner.<sup>13, 14</sup> We therefore chose LDH as an example to demonstrate combinatorial screening by multiplexed CE.

Recently, 96-capillary electrophoresis has become a very powerful tool for analyzing large numbers of samples in very short time. Originally developed for DNA sequencing, capillary arrays have been utilized for zone electrophoresis and micellar electrokinetic chromatography as well.<sup>15</sup> Fluorescence-based instrumentation is already commercially available. However, fluorescence limits the scope of applicability to fluorescent compounds. One high-throughput 96-capillary array electrophoresis system using UV absorption detection

has also been reported.<sup>16</sup> With such instruments, 96 different reaction conditions can be tested in a standard microtiter plate to perform simultaneous enzyme assays. In this demonstration, the differences in LDH activity as a function of the pH of the reaction buffer and the concentration of LDH are monitored as a function of time. This simulates a drug-screening or substrate-binding protocol in the pharmaceutical industry.

## **Experimental Section**

### **Instrumentation**

The multiplexed capillary system has been described before<sup>16</sup>. A total of 96 fused-silica capillaries (50- $\mu\text{m}$  i.d., 150- $\mu\text{m}$  o.d.; Polymicro Technologies, Phoenix, AZ) packed side by side with 50-cm effective length and 70-cm total length were used for separating reactants, products and enzymes. 0.2 ml 96-well preloaded plates were used as reactors for carrying out the enzyme reactions. A 254-nm mercury lamp was used for UV absorption detection. A voltage of +11 kV ( $\sim 157$  V/cm) was applied across the capillaries for separation.

### **Reagents**

Sodium pyruvate (99+%) was obtained from Sigma (St. Louis, MO, USA).  $\beta$ -Nicotinamide adenine dinucleotide, reduced form ( $\beta$ -NADH) was also obtained from Sigma. Both solutions were freshly prepared and kept in a refrigerator before the experiment. The NADH solution was covered by black tape to prevent exposure to light. L-lactate dehydrogenase (LDH-5(M<sub>4</sub>) 98+% isoenzyme, suspension in 2.1 M  $(\text{NH}_4)_2\text{SO}_4$ ) was also purchased from Sigma. Bacteria-free 0.2 ml 96-well preloaded plates were obtained from Marsh

Biomedical Products, Inc., (Rochester, NY, USA). Sodium phosphate monobasic ( $\text{NaH}_2\text{PO}_4 \cdot \text{H}_2\text{O}$ ) was purchased from Fisher (Fair Lawn, NJ, USA). All water used in this experiment was purified by a Millipore water purification system to make sure that there was no enzyme contamination. During the period of incubation, the plates were covered by plastic film to minimize evaporation of the reaction solution. This allowed the concentrations of enzyme and substrate to remain as stable as possible.

### Detection Method

Because of the inhibition of pyruvate on the catalysis of LDH, an optimal concentration of pyruvate is important. At pH 7.2 and 25 °C, 2 mM pyruvate is normally suitable for the  $M_4$  isoenzyme. So, in the reaction buffers (20 mM phosphate, pH ranges from 5.8 ~ 8.0), 2.0 mM NADH and ~2.0 mM pyruvate were added as the substrates for the enzymatic reaction. The direction of reaction was chosen as follows:



The reaction was allowed to proceed for a fixed period prior to hydrodynamic injection of the reactants, products and enzymes into the capillaries. A solution of 10 mM phosphate with pH of 8.0 was used as the separation buffer. After applying voltage, we can readily separate all components due to different mobilities. Since we used low concentrations of enzyme ( $5 \times 10^{-10} \sim 1 \times 10^{-8}$  M) (pseudo-first-order reaction), the amount of  $\text{NAD}^+$  formed

during a given period of time at a fixed temperature is linearly proportional to the LDH activity. Therefore, the LDH activity can be quantified by measuring the peak area of  $\text{NAD}^+$  formed during the fixed incubation period. In this work, we integrated the areas of the  $\text{NAD}^+$  peak and the NADH peak. Because  $\text{NAD}^+$  and NADH both absorb at 254 nm while the enzyme does not contribute much to the background at this wavelength, a 254-nm mercury lamp was used. By measuring the absorption coefficients of  $\text{NAD}^+$  and NADH at 254 nm in a conventional spectrophotometer, we converted the peak areas to amounts. The ratio between the  $\text{NAD}^+$  amounts formed and the original NADH amounts was calculated. Since a small background reaction exists, we also monitored blank reactions and subtracted the effect of the background reaction.

### **Sample Preparation and Injection**

We prepared separate 20 mM phosphate buffers with pH values of 5.8, 6.3, 6.5, 6.7, 7.0, 7.3, 7.6 and 8.0. We added 175  $\mu\text{l}$  buffer solution, 10  $\mu\text{l}$  enzyme solution, 10  $\mu\text{l}$  40 mM NADH and 5  $\mu\text{l}$  90 mM pyruvate into 96 wells for reaction. Reactions progressed at room temperature. The various final concentrations of enzyme in those solutions were  $5 \times 10^{-10}$  M,  $2 \times 10^{-9}$  M,  $3 \times 10^{-9}$  M,  $4 \times 10^{-9}$  M,  $5 \times 10^{-9}$  M,  $6 \times 10^{-9}$  M,  $7 \times 10^{-9}$  M,  $8 \times 10^{-9}$  M and  $1 \times 10^{-8}$  M. Thus, for every concentration of enzyme, we have eight different buffer solutions. At the same time, for every buffer solution with a different pH value, we have 9 different concentrations of the enzyme. We incubated the reaction mixtures for 30 min, 78 min, 128 min, 180 min, 308 min, 420 min, 480 min and 1477 min. After each incubation

period, we used hydrodynamic injection to initiate CE analysis. The volumes withdrawn each time from the reaction vials are negligible compared to the starting volumes. Therefore, essentially non-intrusive monitoring is achieved.

## **Results and Discussion**

### **Sample Injection**

The reason for using hydrodynamic injection is that electrokinetic injection would have caused serious errors. This is because of different surface conditions from capillary to capillary, different compositions of the buffer solutions, different capillary temperatures, and different migration velocities of NADH and NAD<sup>+</sup>.<sup>17</sup> The effect is obvious from Figure 1.

There, a solution with 1 mM NADH and 1 mM NAD<sup>+</sup> was prepared and injected separately by hydrodynamic injection and electrokinetic injection into 9 different capillaries. A 5 cm difference in height was maintained for 60 s for the former and +11 kV was applied for 30 s for the latter. By applying +11 kV to the capillaries, the NADH and NAD<sup>+</sup> sample zones were separated and driven across the detection windows. Since all the solutions had the same NADH and NAD<sup>+</sup> concentrations, identical peak areas were expected for the NADH peaks and NAD<sup>+</sup> peaks. According to Figure 1, hydrodynamic injection only caused a very small standard deviation (SD), which was about 0.027 with a mean of 0.817, while electrokinetic injection caused serious errors, with SD of 0.483 with a mean of 3.66. Such an injection problem is more serious in capillary arrays compared to repeated injections in a single capillary because of surface heterogeneity.

## Quantitation

The migration times varied from capillary to capillary, because the conditions of the capillaries were different. Despite the different migration times, the NADH and NAD<sup>+</sup> peaks are easily identified in this simple mixture. These peak areas are used for quantitation. After each incubation period, the fraction of NADH converted to NAD<sup>+</sup> was calculated using the following equations:

$$\text{amount of NADH (reacted)} = \text{NAD}^+ \text{ area} \times \frac{\epsilon_{\text{NADH}}}{\epsilon_{\text{NAD}^+}}$$

$$\text{fraction of NADH (reacted)} = \frac{\text{amount of NADH (reacted)}}{\text{amount of NADH (reacted)} + \text{NADH area}}$$

As stated before, we could use the fraction of NADH (reacted) to represent the activity of the enzyme whenever this reaction is pseudo-first-order. The use of a ratio avoids problems with variations in detection sensitivity and injected amounts among capillaries. Additional corrections for the different speeds of the analytes passing the detector were made since hydrodynamic injection was employed.<sup>17</sup> In this way, it is not necessary to first renormalize the migration times in Fig. 2-4.

## Combinatorial Screening

Since 8 pH conditions and 9 enzyme concentrations were screened, there are a total of 72 channels (capillaries) where products are detected. In addition 16 channels of background reaction (8 pH conditions with substrates but no enzymes) were monitored. The

other 8 channels in the array were filled with the buffer (no substrate and no enzyme) as the absorption reference. The entire data set for the 96-capillary array is shown as a reconstructed image in Figure 2. As expected, there are substantial variations in migration times among the different channels.<sup>15</sup> The change in electroosmotic flow from one capillary to the next and temperature variations are the main reasons. Here, even larger variations are expected because the sample pH and sample ionic strengths are all different. The capillary walls will become dynamically altered as a result of injection. Internal standards can be employed to normalize the migration times,<sup>15</sup> but were not needed for the simple electropherograms in this study. The intensity variations in Figure 2 are partly due to uneven illumination but mostly due to the expected variations in the extents of reaction in each channel. Uneven illumination does not affect quantitation here, since each capillary has its own well defined 0% and 100% intensity points for calculating the absorbance.

Extracted electropherograms for activity screening are shown in Figures 3 and 4. At a constant pH (Figure 3), it is easy to see that the extent of reaction increases with LDH concentration. At a fixed LDH concentration (Figure 4) it can be seen that there is an optimum pH where the LDH activity is the highest.

The quantitative optimization results shown in Figure 5 indicate that in all cases the highest activity for LDH is obtained at pH 7. This agrees with the known properties of the enzyme.<sup>6</sup> The activities were then examined more carefully by repeated sampling of the reaction mixture at well defined time intervals. For a 30-min reaction time (Figure 6), there is a roughly linear increase in the extent of reaction as a function of LDH concentration for all

pH conditions. The measured rates correspond to those found in standard experiments.<sup>6</sup> This approximates ideal behavior. For a 24-h reaction time (Figure 7), nonlinearity is observed, especially when the fraction reacted exceeds 0.6. The reason for this is saturation of the reaction. As is well known, when a significant fraction of the reagent (NADH) is consumed, the pseudo-first-order reaction description fails. The remedy is to use higher reagent concentrations or to stay with short reaction times. This feature shows the importance of monitoring the full kinetics of reactions as opposed to single-point monitoring. Figure 7 by itself would have led to the incorrect conclusion that there is not much difference in enzymatic activity over a broad pH range.

The above results clearly show the utility of capillary array electrophoresis for combinatorial screening. Since only 10-100 nL is required for each analysis, repeated sampling from 1-10  $\mu$ L sample vials can be accomplished without disturbing the reactions. Unlike plate readers, CE separation provides for selectively quantifying the reagents and the products. Absorption detection has adequate sensitivity for enzyme assays and binding assays, and is broadly applicable if, e.g., 214-nm light is employed. The separation times here are limited by the length of the capillaries in this particular instrument. For a simple chemical system such as the one used here (Fig. 3 and 4), 5-min run times in shorter capillaries should be adequate. The capillary format allows one-step injection and analysis from 96-well microtiter plates, a feature that is not yet available in microfluidic devices. Besides, 96-channel absorption detection has yet to be demonstrated in microchips. When kinetic studies require experiment times longer than separation times, the capillary format has the additional benefit of staggering multiple 96-sample trays for an even higher throughput.

### Acknowledgement

The Ames Laboratory is operated for the U.S. Department of Energy by Iowa State University under Contract No. W-7405-Eng-82. This work was supported by the Director of Science, Office of Basic Energy Sciences, Division of Chemical Sciences.

### References:

1. Borman, S., *C&E News*, **1999**, 33-60.
2. Southern, E. M., *Electrophoresis*, **1995**, *16*, 1539-1542.
3. Chee, M. et al., *Science*, **1996**, *274*, 610-614.
4. Winzeler, E. A. et al., *Science*, **1998**, *281*, 1194-1197.
5. Weiss, S., Proske, D., Neumann, M., Groschup, M. H., Kretzschmar, H. A., Famulok, M., and Winnacker, E.-L., *J. Virol.*, **1997**, *71*, 8790-8797.
6. Kaplan, A., Szabo, L. L., and Ppheim, K. E., *Clinical Chemistry*, 3rd ed., Philadelphia: Lea & Febiger, 1988.
7. Bottomley, R. H., Locke, S. J., and Ingram, H. C., *Blood*, **1966**, *29*, 182-195.
8. Wu, D., and Regnier, F. E., *Anal. Chem.*, **1993**, *65*, 2029-2035.
9. Bao, J. and Regnier, F. E., *J. Chromatogr.*, **1992**, *608*, 217-224.
10. Yao, X. W., Wu, D., and Regnier, F. E., *J. Chromatogr.*, **1993**, *636*, 21-29.
11. Xue, Q., and Yeung, E. S., *Anal. Chem.*, **1994**, *66*, 1175-1178.
12. Xue, Q., and Yeung, E. S., *J. Chromatogr. B*, **1996**, *677*, 233-240.
13. Xue, Q., and Yeung, E. S., *Nature*, **1995**, *373*, 681-683.
14. Tan, W., and Yeung, E. S., *Anal. Chem.*, **1997**, *69*, 4242-4248.

15. Xue, G., Pang, H.-M., and Yeung, E. S., *Anal. Chem.*, **1999**, *71*, 2642-2649.
16. Gong, X., and Yeung, E. S., *Anal. Chem.*, **1999**, *71*, 4989-4996.
17. Lee, T. T. and Yeung, E. S., *Anal. Chem.*, **1992**, *64*, 1226-1231.

**FIGURE CAPTIONS**

- FIGURE 1. Comparison of quantitative reproducibility in a capillary array for electrokinetic injection (top trace) vs. hydrodynamic injection (bottom trace) for identical concentrations of  $\text{NAD}^+$  and  $\text{NADH}$  in the samples.
- FIGURE 2. Reconstructed absorption image of combinatorial screening of enzyme activity in a 96-capillary array. The capillaries (1-96) are arranged from top to bottom. Migration time (0 to 33 min) is plotted from left to right.
- FIGURE 3. Electropherogram of products after 180 min reaction for different LDH concentrations at  $\text{pH} = 7$ . Decreases in transmitted intensity correspond to increases in absorbance when the components elute. Left peak:  $\text{NAD}^+$  (product); right peak:  $\text{NADH}$  (reactant). From top to bottom, the concentrations are 0, 0.5 nM, 2 nM, 3 nM, 4 nM, 5 nM, 6 nM, 7 nM, 8 nM and 10 nM. The enzyme is not detected at this concentration.
- FIGURE 4. Electropherogram of products after 180 min reaction for different pH at a LDH concentration of  $5 \times 10^{-9}$  M. Decreases in transmitted intensity correspond to increases in absorbance when the components elute. Left peak:  $\text{NAD}^+$  (product); right peak:  $\text{NADH}$  (reactant). From top to bottom, the pH are 5.8, 6.3, 6.5, 6.7, 7.0, 7.3, 7.6 and 8.0.
- FIGURE 5. Combinatorial optimization of LDH activity as a function of pH. The plots are for different LDH concentration as indicated in the inset. The incubation time is 180 min. Only one experiment is needed.

FIGURE 6. Fraction of NADH reacted as a function of LDH concentration. The plots are for different pH conditions. The reaction time is 30 min.

FIGURE 7. Fraction of NADH reacted as a function of LDH concentration. The plots are for different pH conditions. The reaction time is 24 h.

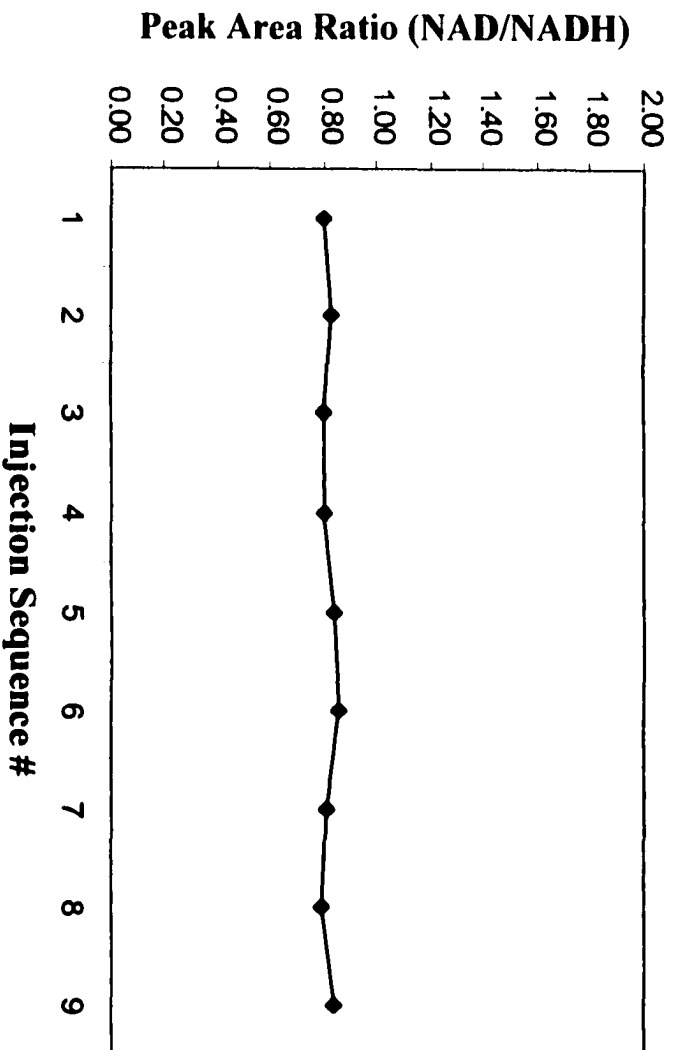
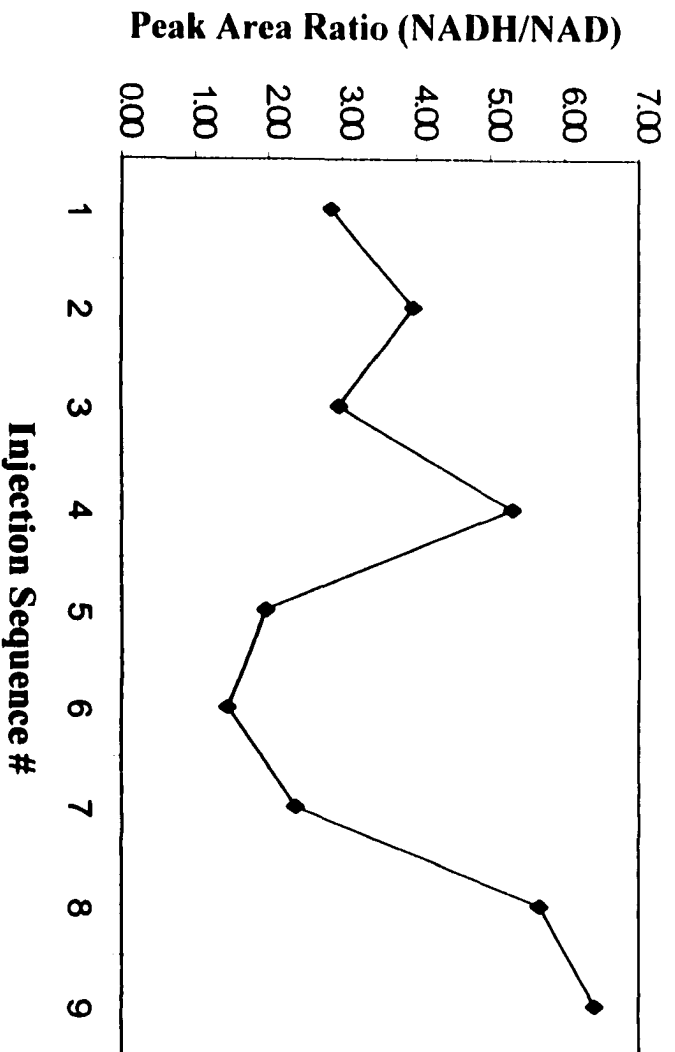
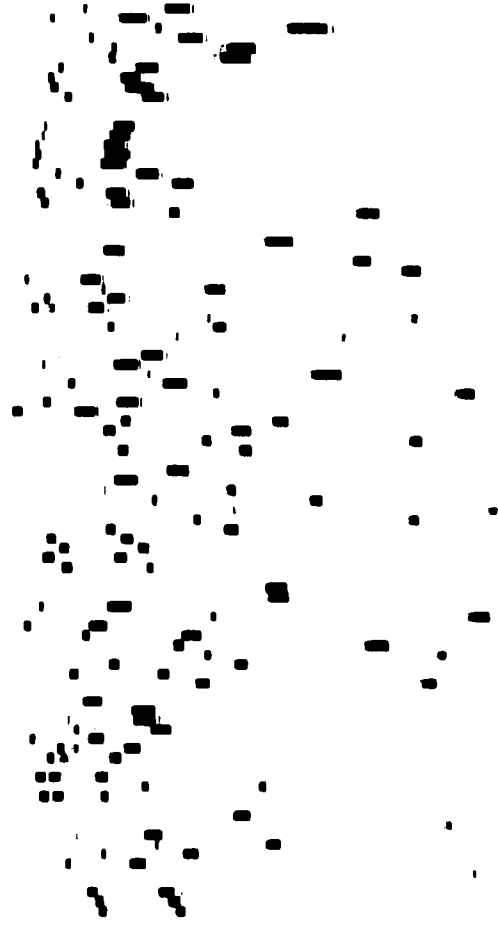


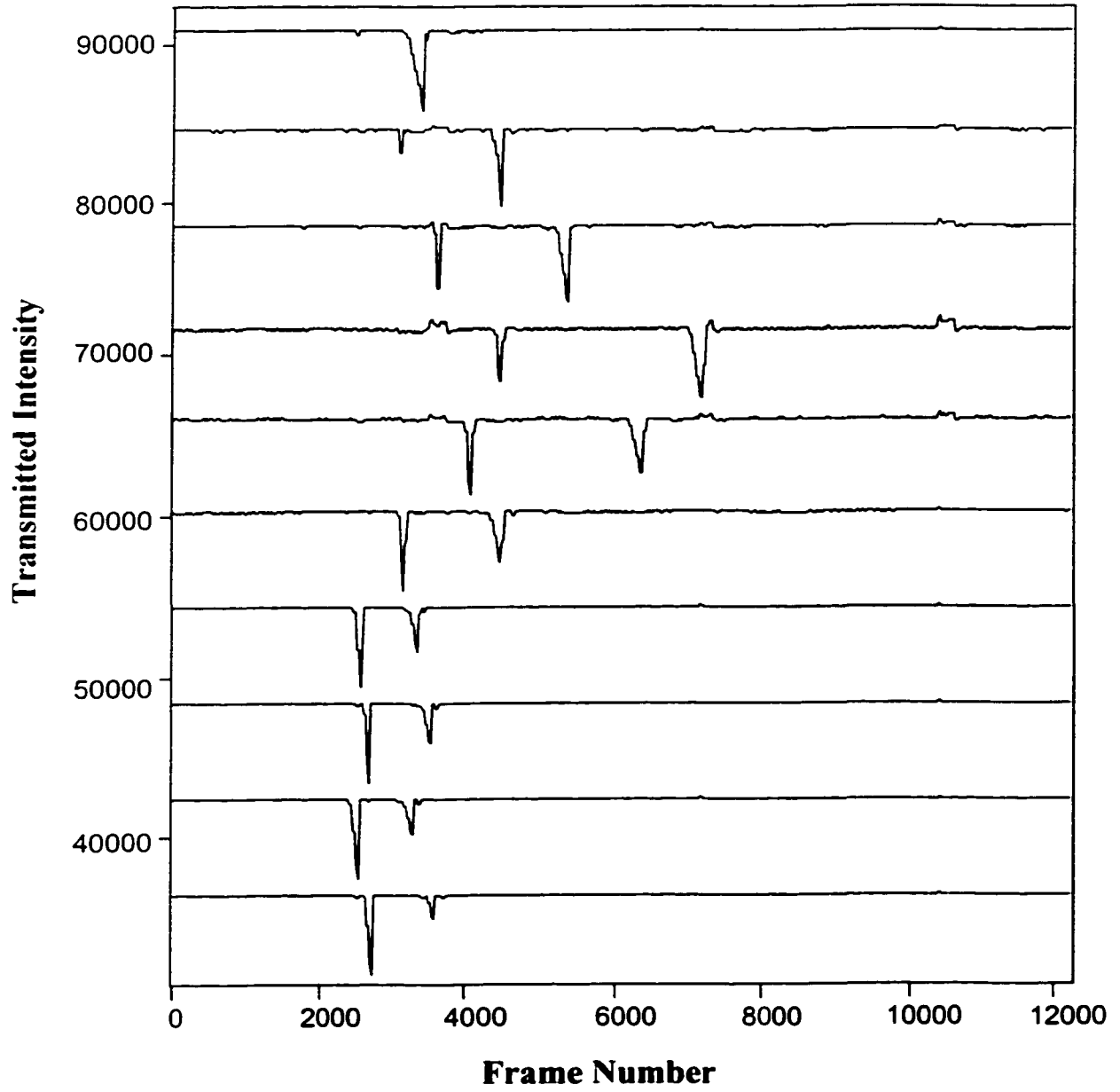
FIGURE 1

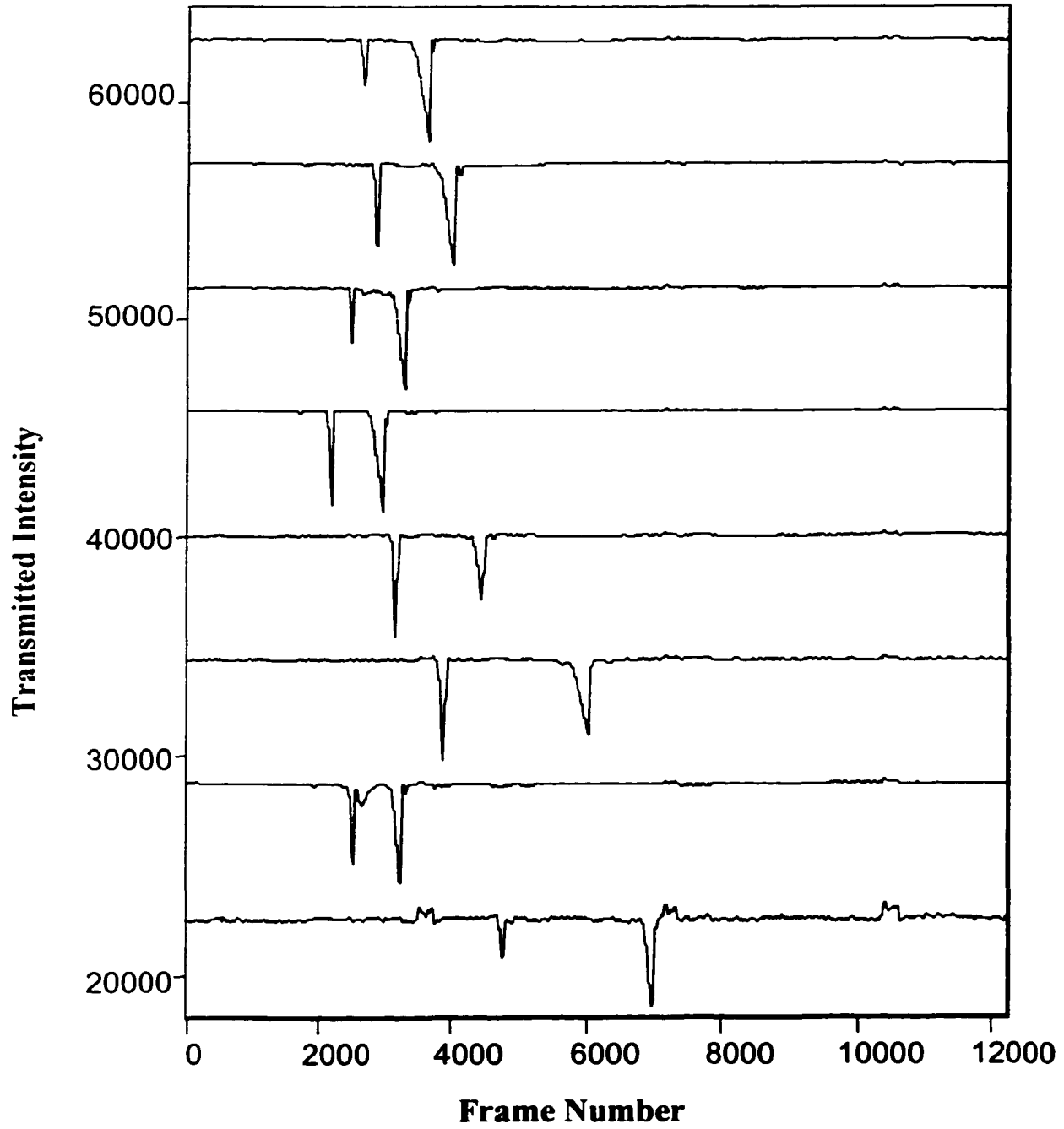
**Capillary #**



**Time**

**FIGURE 2**

**FIGURE 3**

**FIGURE 4**

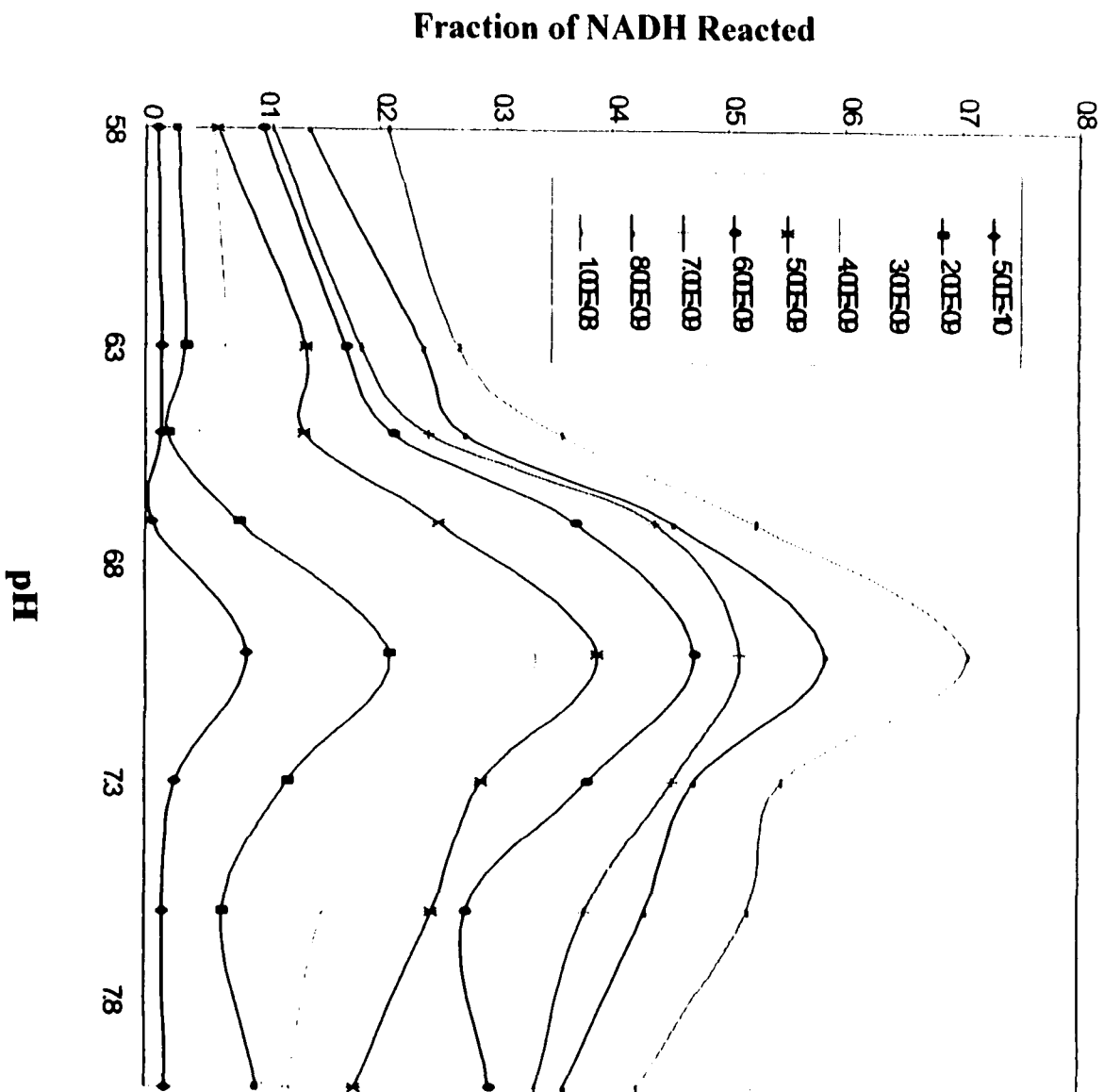


FIGURE 5

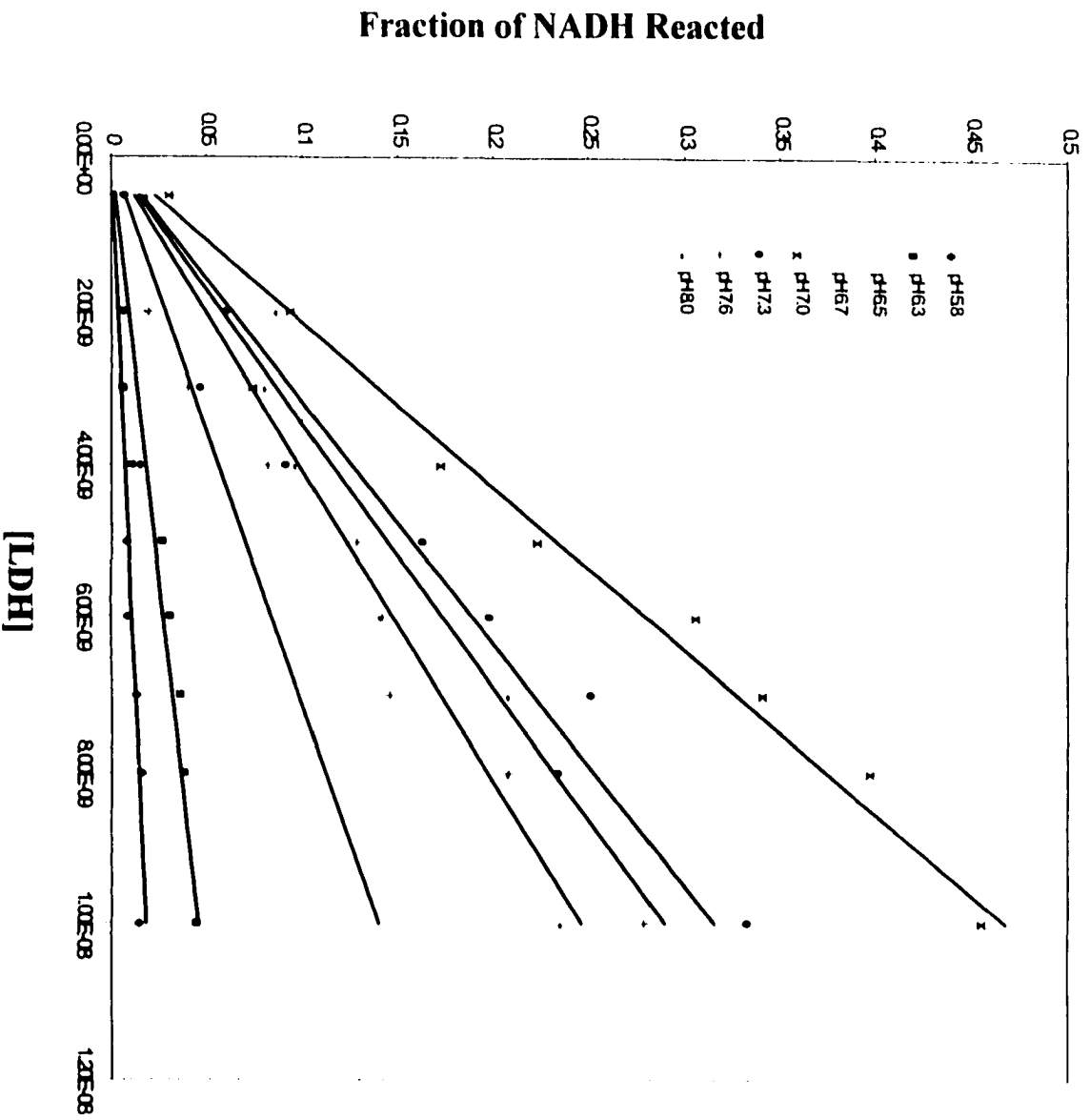


FIGURE 6

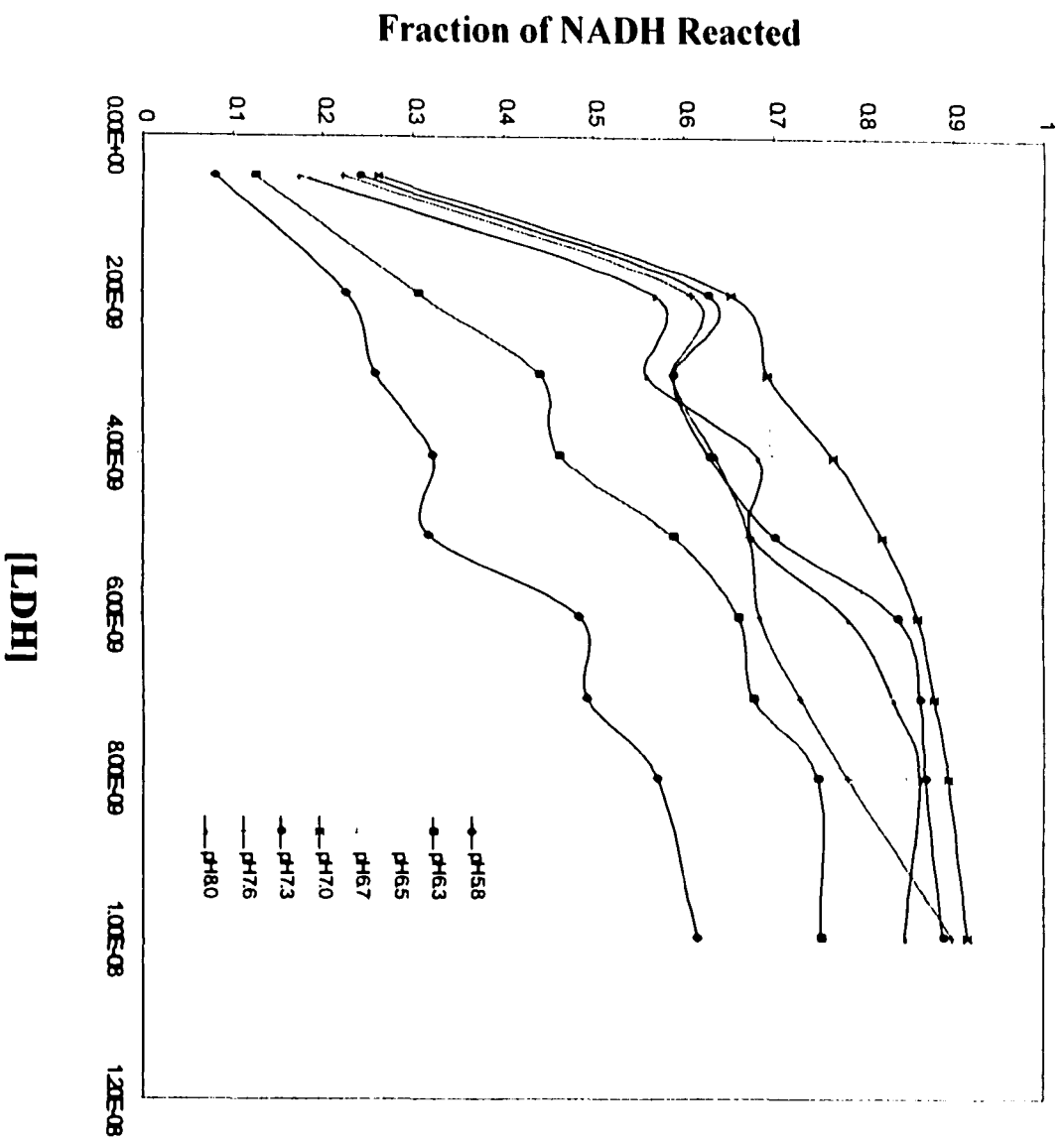


FIGURE 7

## **CHAPTER 5. HIGH-THROUGHPUT COMPREHENSIVE PEPTIDE MAPPING OF PROTEINS BY MULTIPLEXED CAPILLARY ELECTROPHORESIS**

A paper accepted by Analytical Chemistry

Seong Ho Kang, Xiaoyi Gong, and Edward S. Yeung

### **Abstract**

A novel multi-modal method for peptide mapping of proteins by multiplexed capillary electrophoresis (CE) is presented. By combining charge to size separations in four different channels and micellar electrokinetic chromatography for hydrophobicity-based separations in two different channels in a 96-capillary array, peptide fragments of digested proteins were readily resolved and showed unique fingerprints. Each capillary spanned several diodes in a photodiode array (PDA) for absorption measurement. The 96 capillaries were monitored simultaneously at 214 nm by a single PDA element with 1024 diodes and analysis was completed within 45 min. This demonstrates that it is possible to rapidly screen biotechnological products as well as to efficiently optimize separation conditions in CE by a combinatorial approach.

### **Introduction**

Peptide mapping represents one of the most powerful and successful tools available for the characterization of proteins.<sup>1-2</sup> Although less informative than protein sequencing, it allows rapid analysis with simple instrumentation. In peptide mapping, a sample protein is selectively cleaved by enzymes or by chemical digestion.<sup>3-6</sup> This peptide map then serves as a unique fingerprint of the protein and can accurately reveal very subtle differences

among individual variants. Trypsin is by far the most widely used proteolytic enzyme in peptide mapping. Its desirable features are that cleavage at the C-terminal side of lysine and arginine is generally quantitative under proper conditions and that trypsin tolerates concentrations of urea as high as 4 M.<sup>4</sup> The disadvantage is that the fragments formed may be too small, averaging 7-12 amino acid residues, resulting in very complex tryptic maps. After tryptic digestion, the digest is typically analyzed by various methods such as slab gel electrophoresis,<sup>7</sup> thin-layer chromatography (TLC),<sup>8</sup> high-performance liquid chromatography (HPLC) with or without mass spectrometry (MS),<sup>9-15</sup> and capillary zone electrophoresis (CZE)<sup>16-23</sup> to yield a peptide map. Gradient reversed-phase HPLC is the most common form of peptide mapping in use today.<sup>13-15</sup> Although these methods are useful for characterizing proteins, there are still some problems such as the relatively large amount of sample required, long analysis time, and efficiency of the derivatization reaction. Also, a typical map contains 20-150 peaks, all of which should ideally be totally resolved and identified by MS.<sup>4</sup> Therefore, a high degree of column resolution and system precision are required to accurately reproduce the maps, preferably starting with subnanomolar quantities.

Capillary electrophoresis (CE) has become an important tool for the separation of a wide variety of biological substances including peptides, proteins, nucleic acid fragments, and oligosaccharides because of its high speed, simplicity, small sample requirement, and high efficiency. In particular, CZE has received considerable attention as a complementary method to reversed-phase liquid chromatography in peptide mapping efforts.<sup>16-23</sup> Separation of various peptides can be optimized through pH adjustments. Through the addition of micelle-forming surfactants to the running buffer, a dynamic partition mechanism (i.e., hydrophobicity) of peptide separation can also be established for the neutral fragments. Although CE is quite efficient and fast for analyzing peptide fragments, the complete separation of peptides in a digest of e.g. high molecular mass proteins is not possible by using a single buffer condition. Unlike HPLC, the implementation of gradient separation in CE

is not trivial.<sup>24-25</sup>

A multiplexed CE method can help to overcome this difficulty. The applications of multiplexed CE have mainly been limited to DNA sequencing and genetic analysis in support of the Human Genome Project.<sup>26-33</sup> Recently, our group applied multiplexed CE to assay four kinds of fluoresceins and six polyaromatic hydrocarbons using MEKC and CZE.<sup>34</sup> An absorbance detection approach for multiplexed CE using a single linear photodiode array (PDA) detector was also reported.<sup>35</sup> At 214 nm, CE essentially offers universal detection. In this study, we present a novel multi-dimensional and multiplexed CE method for peptide mapping of proteins using a 96-capillary array. As model proteins, we selected two variants of  $\beta$ -lactoglobulin. Trypsin was used to digest  $\beta$ -lactoglobulin A and B. Four different CZE conditions and two different MEKC conditions were simultaneously applied to separate and detect the peptide fragments. The peptide map obtained using this method can serve as a unique fingerprint of the protein. The results show that reliable high-throughput analyses can be performed based on multi-modal CE and a single prescribed experimental protocol.

## **Experimental Section**

### **Reagents and Chemicals**

$\beta$ -lactoglobulin A and B (BLGA and BLGB), L-1-tosylamide-2-phenylethyl chloromethyl ketone (TPCK)-treated trypsin, CHES (2-[N-cyclohexylamino]ethanesulfonic acid), Tricine (N-tris[hydroxymethyl]methylglycine), Trizma<sup>®</sup>-Base (tris[hydroxymethyl]aminomethane), ammonium acetate, CaCl<sub>2</sub>, and sodium dodecyl sulfate (SDS) were purchased from Sigma Chemical Co. (St. Louis, MO). Tween 20 was purchased from Aldrich Chemical Co. (Milwaukee, WI). All buffers were filtered through a Corning<sup>®</sup> Filter System, 0.22- $\mu$ m cellulose acetate filters (Corning, NY) or  $\mu$ Star LB<sup>™</sup>, 0.22- $\mu$ m cellulose acetate non-pyrogenic filters (Coaster, Cambridge), and degassed prior to

use. The water used to prepare solutions was deionized with a Milli-Q water purification system (Millipore, Worcester, MA).

### **96-Capillary Array Electrophoresis System**

The experimental CE setup for multi-dimensional 96-capillary array electrophoresis is similar to that described in ref. 35. Briefly, a total of 96 fused-silica capillaries (Polymicro Technologies, Inc., Phoenix, AZ), 50- $\mu\text{m}$  i.d. and 360- $\mu\text{m}$  o.d., with 50-cm effective length and 70-cm total length were packed side by side at the detection window and clamped between two flat surfaces of a plastic mount. The window was created after packing by using an excimer laser beam to burn off the polyimide coating. At the ground end (outlet), every 12 capillaries were bundled together to allow simultaneous filling of six-different buffers for six-dimensional peptide mapping as shown in Figure 2. At the injection end, the capillary array was spread out and mounted on a copper plate to form an  $8 \times 12$  format with dimensions to fit into a 96-well microtiter plate for sample introduction. 96 gold-coated pins (MillMax Mfg. Corp.) were mounted on the copper plate near each capillary tip to serve as individual electrodes, with the capillary tips slightly extended ( $\sim 0.5$  mm) beyond the electrodes to guarantee contact with small-volume samples. A high-voltage power supply (Glassman High Voltage, Inc., Whitehorse Station, NJ) was used to drive the electrophoresis.

The light source, filter, capillary array holder, and PDA detector were all contained in a light-tight metal box attached to an optical table. As the light source, a 213.9-nm zinc lamp (model ZN-2138, Cole-Parmer) was used for UV absorption detection. The transmitted light from the capillary array passed through an interference filter (Oriel) and a quartz lens (Nikon; f.l. = 105 mm;  $F = 4.5$ ). An inverted-image of the capillary array at a nominal magnification factor of 1.2 was created by the quartz lens on the face of the PDA. The PDA (Hamamatsu model S5964, Hamamatsu, Japan) incorporated a linear image sensor chip

(1024 diodes, 25- $\mu\text{m}$  in width, 2500- $\mu\text{m}$  in height), a driver/amplifier circuit, and a temperature controller. The built-in driver/amplifier circuit was interfaced to an IBM-compatible computer (233-MHz Pentium, Packard Bell) via a National Instrument PCI E Series multifunction 16-bit I/O board. All codes used to operate the PDA and to acquire the data were written in house using Labview 5.0 software (National Instruments, Austin, TX).

The raw data sets were converted into single-diode electropherograms by another in-house Labview program. Data treatment and analysis were performed using Microsoft Excel 97 and GRAMS/32 5.05 (Galactic Industries).

### **Separation Conditions**

In the multi-modal CE experiments, the capillary array was first flushed with methanol and then water for cleanup. The six running buffers used for four-dimensional CZE separations and two-dimensional MEKC separations were as follows: (1) 50 mM Trizma<sup>®</sup>-Phosphate buffer (pH 2.5 with  $\text{H}_3\text{PO}_4$ ), (2) 50 mM sodium acetate buffer (pH 5.0 with acetic acid), (3) 0.1 M Trizma<sup>®</sup>-Base/0.1 M Tricine buffer (pH 8.1), (4) 0.1 M CHES/0.1 M NaOH (pH 9.3), (5) 0.1% Tween 20 in 50 mM sodium acetate buffer (pH 5.0 with acetic acid), and (6) 7% Tween 20 and 10 mM SDS in 0.1 M Trizma<sup>®</sup>-Base/0.1 M Tricine buffer (pH 8.1). The samples were put into a 96-well microtiter sample plate (1  $\mu\text{l}$ /well) and gravity injected at the anode for 60 s at 8-cm height. The applied electric field was +157 V/cm and electrophoresis was performed at ambient temperature. After each run, the capillaries were rinsed with 0.1 M NaOH, water, and running buffer for 5 min each.

### **Single-Capillary Electrophoresis System**

All CE separations for CZE and MEKC analyses were optimized on an ISCO (Lincoln, NE) Model 3140 Electropherograph System before the multi-dimensional multiplexed CE runs. Bare fused-silica capillaries (Polymicro Technologies, Inc., Phoenix, AZ) with 50-

cm effective length and 75-cm total length (50- $\mu$ m i.d. and 361- $\mu$ m o.d.) were used. Four different buffer systems were investigated for CZE separations and two different buffer systems were also investigated for MEKC separations. The optimal compositions are described above. The samples were introduced with hydrodynamic flow by placing the inlet of the capillary into the sample vial and raising the sample vial 30 cm above the exit vial and allowing the sample to siphon into the capillary for 10 s. The applied electric field was +227 V/cm and electrophoresis was performed at ambient temperature. The detection wavelength was set at 214 nm for monitoring peptide fragments. After each run, the capillary was rinsed in the following sequence; 0.1 M NaOH, water, and running buffer for 5 min respectively.

### **Tryptic Digestion**

Tryptic digestion of BLGA and BLGB was carried out according to the procedure of Cobb et al.<sup>36</sup> without the dialysis and lyophilization steps. A mixture of 2 mg/ml BLG and trypsin was prepared with a 10 mM Trizma<sup>®</sup>-Base and 50 mM ammonium acetate buffer (pH 8.2) containing 0.1 mM calcium chloride. Trypsin was added at a trypsin-protein ratio of 1:50 (w/w), and the digestion mixture was incubated at 37 °C for 5 h. The digest was directly injected into the separation CE system without filtration.

## **Results and Discussion**

### **Tryptic Digestion of BLGA and BLGB**

Our model protein, bovine  $\beta$ -lactoglobulin (BLG) is the major whey protein of cow's milk. Mature bovine BLG has 162 residues as shown in Figure 2. Three variants of BLG, labeled as A, B, and C, commonly occur in cow's milk. Variants A and B differ at two sites: Aspartic acid (D) 64 in BLGA is changed to glycine (G) in BLGB, and valine (V) 118 in BLGA is changed to alanine (A) in BLGB. Variants B and C differ at one site: Glutamine (Q) 59 in BLGB is changed to histidine (H) in BLGC.<sup>37</sup> Tryptic digestion is quantitative

and very specific because trypsin cleaves only at the C-terminal side of lysine and arginine residues. The theoretical fragments are listed in Table I. In the case of BLG, seventeen different peptides exist after tryptic digestion.

### **Peptide Mapping with the Commercial CE System**

Since peptides are polymers of amino acids, they typically have a limited number of charged states in their structure depending on the presence of amino acid moieties with ionizable side chains.<sup>38</sup> This determines the pH ranges for CE separations beyond which no theoretical optimization can be performed. At  $\text{pH} < 2$ , all ionizable groups of peptides will be protonated. The number of basic residues in the peptide chain will determine the overall charge-state of the molecule. At  $\text{pH} > 10$ , all ionizable groups will be de-protonated, resulting in a negatively charged peptide. At these extreme pH conditions, the separation of peptides cannot be adjusted. At intermediate pHs, partly ionized termini and side chain residues allow optimization of the peptide separation. So we selected four different pH conditions, pH 2.5, 5.0, 8.1, and 9.3, for the separation of peptide fragments. We note that ionization of peptides generally occurs over a pH range of 2.5-8.0. So, these pHs are sufficiently far apart to give independent electropherograms but are close enough to form a continuous (combinatorial) set of conditions.

Figure 3 shows typical peptide maps of BLGA and BLGB at four pH conditions for CZE using a single capillary after tryptic digestion. The peptide peaks at the four different separation conditions were well resolved within about 30 min. Each condition revealed different peptide maps. The separation of peptides above pH 5.0 were completed quickly and efficiently within 15 min (Fig. 3A, B and C). The electropherograms at pH 2.5 showed good resolution in spite of a relatively long analysis time (Figure 3D). Adsorption of the proteins on the capillary wall in CE can be a serious problem. This can lead to variable migration times, band broadening, and peak tailing. At pH 2.5, much of the negative charge had been

titrated off the silica walls of the capillary such that there was little coulombic interaction between the peptide and the wall. This is not true of other pH conditions. We therefore used high ionic strengths in the running buffers to provide efficient separations because of reduced interaction between the peptide fragments and the capillary wall.

Figure 3 shows the differences in the peptide maps of BLGA and BLGB at four different CZE conditions. Although the amino acid sequences of bovine BLGA and BLGB differ only at two sites (64 and 118, Figure 2) among the 162 amino acids, we can clearly identify the differences in the peptide fragments of BLGA and BLGB. Peptide mapping by CE is increasingly being utilized as a complement, if not a viable substitute, for the already established technique of HPLC. CE has several advantages over HPLC, including much higher efficiency and a smaller sample requirement. Moreover, CE also offers a straightforward correlation of migration time with physio-chemical properties. According to the dependence on pH, the net charges of each peptide fragment can be confirmed. Interpretation of the combined peptide maps at the four different conditions (Figure 3A-D) showed comprehensive data with overlapping redundancy for the peptides that cannot be obtained using only one separation condition.

The addition of surfactants to the running buffer can add several new aspects to the separation mechanism. Above their critical micelle concentration, the surfactants form micelles, introducing a pseudo-stationary phase into the running buffer. Figure 4 shows MEKC peptide maps of BLGA and BLGB obtained at two different MEKC conditions using a nonionic surfactant, Tween 20 (Figures 4A and 4B), and/or the combination of nonionic and anionic surfactant, Tween 20 + SDS (Figures 4C and 4D). The use of the surfactants in the intermediate-pH range was appropriate because more neutral peptides should exist there than at the extreme pHs such as pH 2 or 10.

In the MEKC I condition (Figures 4A and 4B), the electropherograms showed similar resolution compared to the electropherograms obtained using CZE conditions (Figure

3C). There are some minor shifts in relative peak positions, mostly for the early eluting components. At pH 5.0, as the concentration of the nonionic surfactant Tween 20 is increased, the resolution of peptide fragments increased without an increase in the current. Although all of the peptide fragments showed baseline separation above 0.3% Tween 20, the analysis time was approximately 1 h. Under the applied electric field of +227 V/cm, 0.2% Tween 20 was selected so that the analysis time can be kept under 20 min.

In the MEKC II condition (Figures 4C and 4D), the higher concentration of Tween 20 and the anionic surfactant SDS were needed to increase the resolution. Because higher pH caused larger mobilities for the peptide fragments in solution, a lower frequency of dynamic partition into the micelles resulted. However, as the concentration of surfactants in the running buffer is increased to favor partition, the analysis time also increased and the sensitivity decreased. So, we chose 7% Tween 20 and 10 mM SDS as an optimal surfactant concentration for MEKC II. The unique advantage of combining Tween 20 and SDS led to the full resolution of all peptide fragments, enabling higher resolution for both neutral peptides and same-charged peptides. Figure 5 shows the effect of Tween 20 at pH 8.1. It is clear that both resolution and selectivity are affected by the surfactant. The patterns of the peptide maps obtained at the six different CE conditions above (Fig. 3 and 4) were reproducible as judged by comparing the results of five repeated injections in each case.

### **Multi-dimensional CE with a 96-capillary Array**

A multiplexed capillary array system allowed high-throughput characterization and generation of peptide maps of proteins, after enzymatic digestion, using capillary electrophoresis at six different conditions at a constant applied electric field. Figure 6 shows the 96-capillary array image obtained using a zinc lamp and the PDA. As shown in Figure 6B, the center of each capillary corresponds to a “peak” in the image. Between every two center “peaks”, there is a “valley” which corresponds to the wall of the capillary. When the capil-

lary array image was well focused onto the PDA, the intensities of these valleys became minimized. This feature was used to produce the best focusing. Comparing the capillary array image with what we reported before,<sup>35</sup> those “spacing peaks” were eliminated in this study. This results from a special treatment on the window of the capillary array whereby epoxy glue was applied between the capillaries on the detection window. The epoxy glue greatly strengthened the window area of the capillary array and minimized movement of the capillaries in the electric field. Because the epoxy glue is not UV transparent, it absorbed all of the light that would have passed through the spacing of the capillaries and eliminated the “spacing peaks”. This further reduced stray light for absorption detection. The zinc lamp provided 213.9-nm light that is well suited for the absorption detection of peptides. The emitting length of the zinc lamp is about 2 cm, which is long enough for uniform illumination of the entire capillary array (1.5 cm). Figure 6A shows less than 2× variation in optical throughput from the center to the edge of the array. This means the detection limit will vary by less than  $\sqrt{2}$  × across the array. The zinc lamp was very stable and produced negligible flicker noise, so no double-beam subtraction was necessary in this experiment.

Up to the present, peptide mapping of proteins is primarily based on the cleavage of proteins with enzyme or chemical agents followed by a one- or two-dimensional separation of the resulting peptide fragments. While the resolution of peptide fragments achieved by one-dimensional separation is often insufficient to resolve the complex mixture of peptides, the conventional two-dimensional techniques suffer from the difficulty of efficiently recovering uncontaminated peptides from the first dimension to transfer to the second dimension. Also, two-dimensional separation conditions have to be changed according to the sample protein. To overcome these problems we used a six-modal system. By combining four different CZE conditions at different pHs and two different MEKC conditions, we can quickly obtain comprehensive and complementary information about the peptides of arbitrary proteins. As shown in the results of single-capillary runs (Figures 3 and 4), the peptide frag-

ments at different separation conditions showed different but related peptide maps. Figure 7 shows the results of the six-modal separations of tryptic digests of BLGA and BLGB in the 96-capillary array. The vertical direction represents the capillary array arrangement while the horizontal direction represents the migration time.

In the single-capillary CE system, when the electric field of +227 V/cm was applied to the 50- $\mu$ m i.d. capillary the current was below 20  $\mu$ A at ambient temperature. However, the capillaries were packed side by side in the 96-capillary array system and the dense packing generated a much higher temperature at the same separation condition. Consequently, some of the capillaries can lose current during the separation because of the formation of bubbles. So we applied a lower electric field of +157 V/cm in spite of an increased analysis time. All separations were still completed within 45 min. Although capillaries 87 and 88 showed unusually long separation times and much lower signal levels, all of the other 94 capillaries gave comparable separation times and good signal-to-noise ratios. As shown in the reconstructed image, even for the same separation condition, the migration times and peak intensities were not uniform among the capillaries. This phenomenon is to be expected from the absence of temperature control in the experiment.<sup>34,35</sup> However, we have demonstrated that an internal standardization scheme can be applied to normalize the results among the capillaries<sup>34,35</sup> so that the corrected migration times and peak areas are of sufficient reliability for high-throughput applications.

Figures 8 and 9 show the extracted electropherograms of BLGA and BLGB derived from the six-dimensional data in Figure 7. The individual maps are virtually identical to the single-capillary results. The peptide patterns of BLGA and BLGB can be easily differentiated in each of the six-modal separation conditions. Compared with the single-capillary run, 0.1% Tween 20 in 50 mM sodium acetate buffer (pH 5.0) gave slower migration times in the 96-capillary array. In part, this was due to the lower applied electric field (+157 vs. +227 V/cm). 0.1% Tween 20, instead of 0.2% Tween 20, at the MEKC condition was used in the

array because the latter would have resulted in even longer analysis times. The presence of the surfactant resulted in a larger change in selectivity for multiple capillaries (Figures 8C and 9C) compared to single capillaries (Figure 4) due to the higher operating temperature in the former case. The higher temperature and longer migration times for the array also explain the loss in efficiency at pH 2.5.

### **Conclusions**

A new high-throughput multi-modal method for peptide mapping of proteins has been demonstrated by using multiplexed capillary electrophoresis. Unique fingerprints of closely related sample proteins, BLGA and BLGB, on a 96-capillary array with six different separation conditions were obtained within 45 min. The 214-nm monitoring of peptide bonds is universal but also very complex because a typical map generally contains 20-150 peaks<sup>4</sup> and all of the fragments should ideally be totally resolved and identified by MS. Maps of unknown proteins are not unambiguous by using only one- or two-dimensional separation. With six complementary separation conditions, there is no need to reoptimize the protocol for each new sample. The instrumental set-up is simplified and automation of the method becomes possible. Most importantly, this multi-modal and multiplexed peptide mapping technique is inherently a small-volume and high-throughput approach. For example, although only two proteins are studied here, sixteen different proteins can be mapped at the same time starting with  $\mu\text{L}$  samples. Alternatively, different enzymes or chemical agents can be employed to provide complementary sets of peptide maps for further confirmation. In this study, the peptide fragments are known and interpretation is straightforward. For complex unknown samples, internal standards can be used to normalize the migration times and peak areas.<sup>34,35</sup> The six separation conditions can then be used to rank order the peptide fragments with respect to their pIs very much like a high-resolution gradient elution. The use of different sets of buffer systems in each capillary in the array is in effect a combinatorial

approach to developing the best separation conditions for a given group of analytes. This last feature should be generally useful in all applications of CE. Finally, capillary arrays are compatible with on-column digestion of proteins<sup>39</sup> so that full automation in multiple channels<sup>25,27,40</sup> is possible with sub-microliter volumes of samples and reagents. Unlike DNA analysis where viscous separation matrices are used,<sup>26,31,33</sup> little degradation of the capillary array was observed over a one-month period.

### Acknowledgement

The Ames Laboratory is operated for the U.S. Department of Energy by Iowa State University under Contract No. W-7405-Eng-82. This work was supported by the Director of Science, Office of Basic Energy Sciences, Division of Chemical Sciences.

### References

1. Garnick, R. L., Solli, N. J., and Papa, P. A., *Anal. Chem.*, **1988**, *60*, 2546-2557.
2. Borman, S., *Anal. Chem.*, **1987**, *59*, 969A-973A.
3. Tarr, G. E., and Crabb, J. W., *Anal. Biochem.*, **1983**, *131*, 99-107.
4. Dong, M. W., *Advances in Chromatography*, Marcel Dekker, Inc.: New York, **1992**, Vol. 32, p. 22-51.
5. Geisow, M. J., and Beaven, G.H., *Biochem. J.*, **1977**, *161*, 619-625.
6. Ward, L. D., Ried, G., Moritz, R. L., and Simpson, R. J., *J. Chromatogr.*, **1990**, *519*, 199-216.
7. Cleveland, D. W., Fisher, S. G., Kirschner, M. W., and Laemmli, U. K., *J. Bio. Chem.*, **1977**, *252*, 1102-1106
8. Stephens, R. E., *Anal. Biochem.*, **1978**, *84*, 116-126.

9. Hancock, W. S., Bishop, C. A., Prestidge, R. L., and Hearn, M. T. W., *Anal. Biochem.*, **1978**, *89*, 203-212.
10. Cox, M. J., Shapira, R., and Wilkinson, K. D., *Anal. Biochem.*, **1986**, *154*, 345-352.
11. Fullmer, C. S., and Wasserman, R. H., *J. Biol. Chem.*, **1979**, *254*, 7208-7212.
12. Vensel, W. H., Fujita, V. S., Tarr, G. E., Margoliash, E., and Kayser, H., *J. Chromatogr.*, **1983**, *266*, 491-500
13. Leadbeater, L., and Ward, F. B., *J. Chromatogr.*, **1987**, *397*, 435-443.
14. Dong, M. W., and Tran, A. D., *J. Chromatogr.*, **1990**, *499*, 125-139.
15. Hartman, P. A., Stodola, J. D., Harbour, G. C., and Hoogerheide, J. G., *J. Chromatogr.*, **1986**, *360*, 385-395.
16. Jorgenson, J. W., and Luckacs, K. D., *HRC CC, J. High Resolut. Chromatogr. Chromatogr. Commun.*, **1981**, *4*, 230-231.
17. Cobb, K. A., and Novotny, M., *Anal. Chem.*, **1989**, *61*, 2226-2231.
18. Chang, H. T., and Yeung, E. S., *Anal. Chem.*, **1993**, *65*, 2947-2951.
19. Nashabeh, W., and Rassi, Z. E., *J. Chromatogr.*, **1991**, *536*, 31-42.
20. Ward, L. D., Reid, G. E., Moritz, R. L., and Simpson, R. J., *J. Chromatogr.*, **1990**, *519*, 199-216.
21. Janini, G. M., Metral, C. J., Issaq, H. J., and Muschik, G. M., *J. Chromatogr. A*, **1999**, *848*, 417-433.
22. Frenz, J., Wu, S. L., and Hancock, W. S., *J. Chromatogr.*, **1989**, *480*, 379-391.
23. Grossman, P. D., Colburn, J. C., Lauer, H. H., Nielsen, R. G., Riggin, R. M., Sittampalam, G. S., and Rickard, E. C., *Anal. Chem.*, **1989**, *61*, 1186-1194.
24. Whang, C.-W., and Yeung, E. S., *Anal. Chem.*, **1992**, *64*, 502-506.
25. Chang, H.-T., and Yeung, E. S., *J. Chromatogr. B*, **1992**, *608*, 65-72.
26. Gao, Q., Pang, H., and Yeung, E. S., *Electrophoresis*, **1999**, *20*, 1518-1526.
27. Zhang, Y., Tan, H., and Yeung, E. S., *Anal. Chem.*, **1999**, *71*, 5018-25.

28. Kheterpal, I., and Mathies, R. A., *Anal. Chem.*, **1999**, *71*, 31A-37A.
29. Tan, H., and Yeung, E. S., *Anal. Chem.*, **1998**, *70*, 4044-4053.
30. Ueno, K., and Yeung, E. S., *Anal. Chem.*, **1994**, *66*, 1424-1431.
31. Kambara, H., and Takahashi, S., *Nature*, **1993**, *361*, 565-566.
32. Taylor, J. A., and Yeung, E.S., *Anal. Chem.*, **1993**, *65*, 956-960.
33. Huang, X. C., Quesada, M. A., and Mathies, R. A., *Anal. Chem.*, **1992**, *64*, 2149.
34. Xue, G., Pang, H-M., and Yeung, E. S., *Anal. Chem.*, **1999**, *71*, 2642-2649.
35. Gong, X., Yeung, E. S., *Anal. Chem.*, **1999**, *71*, 4989-4996.
36. Cobb, K. A., and Novotny, M., *Anal. Chem.*, **1989**, *61*, 2226-2231.
37. Bin, B. Y., Bewley, M. C., Creamer, L. K., Baker, E. N., and Jameson, G. B., *Protein Science*, **1999**, *8*, 75-83.
38. Landers, J. P., *Handbook of Capillary Electrophoresis*, CRC Press, 1997, p. 219-221.
39. Chang, H.-T., and Yeung, E. S., *Anal. Chem.*, **1993**, *65*, 2947-2951.
40. Zhang, N, Tan, and H., Yeung, E. S., *Anal. Chem.*, **1999**, *71*, 1138-1145.

**TABLE 1. Theoretical products of tryptic digest of BLGA and BLGB**

Expected fragment	Sequence	Residues
1	L-I-V-T-Q-T-M-K	1-8
2	G-L-D-I-Q-K	9-14
3	V-A-G-T-W-Y-S-L-A-M-A-A-S-D-I-S-L-L-D-A-Q-S-P-L-R	15-40
4	V-Y-V-E-E-L-K-P-T-P-E-G-D-L-E-T-L-L-Q-K	41-60
5	W-E-N-D-E-C-A-Q-K (W-E-N-G-E-C-A-Q-K) <sup>a</sup>	61-69
6	K	70
7	I-A-A-E-K	71-75
8	T-K	76-77
9	I-P-A-V-F-K	78-83
10	I-D-A-L-N-E-N-K	84-91
11	V-L-V-L-D-T-D-Y-K	92-100
12	K	101
13	Y-L-L-F-V-M-E-N-S-A-E-P-E-Q-S-L-V-C-Q-C-L-V-R (Y-L-L-F-V-M-E-N-S-A-E-P-E-Q-S-L-A-C-Q-C-L-V-R) <sup>a</sup>	102-124
14	T-P-E-V-D-D-E-A-L-E-K	125-135
15	F-D-K	136-138
16	A-L-K	139-141
17	A-L-P-M-H-I-R	142-148
18	L-S-F-N-P-T-Q-L-E-E-Q-C-M-I	149-162

<sup>a</sup>The peptides in parenthesis are fragments of BLGB.

**FIGURE CAPTIONS**

- FIGURE 1. Detailed configuration for sample introduction at a 96-microtiter plate for the multi-dimensional capillary array electrophoresis system. A, B, protein variants; C, zone electrophoresis; and M, MEKC.
- FIGURE 2. Amino acid sequence of bovine  $\beta$ -lactoglobulin B. Variants A and B (BLGA and BLGB) differ at two sites: Asp 64 in A is changed to Gly in B, and Val 118 in A is changed to Ala in B. Variants B and C (BLGB and BLGC) differ at one site: Gln 59 in B is changed to His in C.
- FIGURE 3. Differences in peptide maps of BLGA and BLGB obtained at four different conditions using a single capillary. CZE separation conditions: Running buffer, (A) 0.1 M CHES/0.1 M NaOH (pH 9.3). (B) 0.1 M Trizma<sup>®</sup>-Base/0.1 M Tricine buffer (pH 8.1), (C) 50 mM sodium acetate buffer (pH 5.0 with acetic acid), and (D) 50 mM Trizma<sup>®</sup>-Phosphate buffer (pH 2.5 with H<sub>3</sub>PO<sub>4</sub>). Applied electric field, +227 V/cm. Separation is at ambient temperature. Column, bare fused-silica capillary with effective/total length of 50/75-cm and 50- $\mu$ m i.d. Hydrodynamic injection for 10 s at 30-cm height.
- FIGURE 4. Peptide maps of BLGA and BLGB obtained at two different conditions using a single capillary. MEKC separation conditions: Running buffer, (A and B) 0.2% Tween 20 in 50 mM sodium acetate buffer (pH 5.0 with acetic acid), and (C and D) 7% Tween 20 and 10 mM SDS in 0.1 M Trizma<sup>®</sup>-Base/0.1 M Tricine buffer (pH 8.1). Other conditions are identical to those in Figure 3.
- FIGURE 5. Effect of Tween 20 concentration at pH 8.1 for BLGB. MEKC conditions: Running buffer, x% Tween 20 in 0.1 M Tris/0.1 M Tricine (pH 8.1). Other conditions are identical to those in Figure 3.

FIGURE 6. Image on the PDA of (A) the whole 96-capillary array and (B) one region of the 96-capillary array. C = center peak and V = valley.

FIGURE 7. Result of six-modal CE separation of BLGA and BLGB in the 96-capillary array. CE conditions: (A) 50 mM Trizma<sup>®</sup>-Phosphate buffer (pH 2.5 with H<sub>3</sub>PO<sub>4</sub>), (B) 50 mM sodium acetate buffer (pH 5.0 with acetic acid), (C) 0.1% Tween 20 in 50 mM sodium acetate buffer (pH 5.0 with acetic acid), (D) 0.1 M Trizma<sup>®</sup>-Base/0.1 M Tricine buffer (pH 8.1), (E) 7% Tween 20 and 10 mM SDS in 0.1 M Trizma<sup>®</sup>-Base/0.1 M Tricine buffer (pH 8.1), and (F) 0.1 M CHES/0.1 M NaOH (pH 9.3). Applied electric field, +157 V/cm. Column, bare fused-silica capillary with effective/total length of 50/70-cm and 50- $\mu$ m i.d. Hydrodynamic injection for 60 s at 8-cm height.

FIGURE 8. Selected electropherograms of BLGA extracted from the data in Figure 7.

FIGURE 9. Selected electropherograms of BLGB extracted from the data in Figure 7.

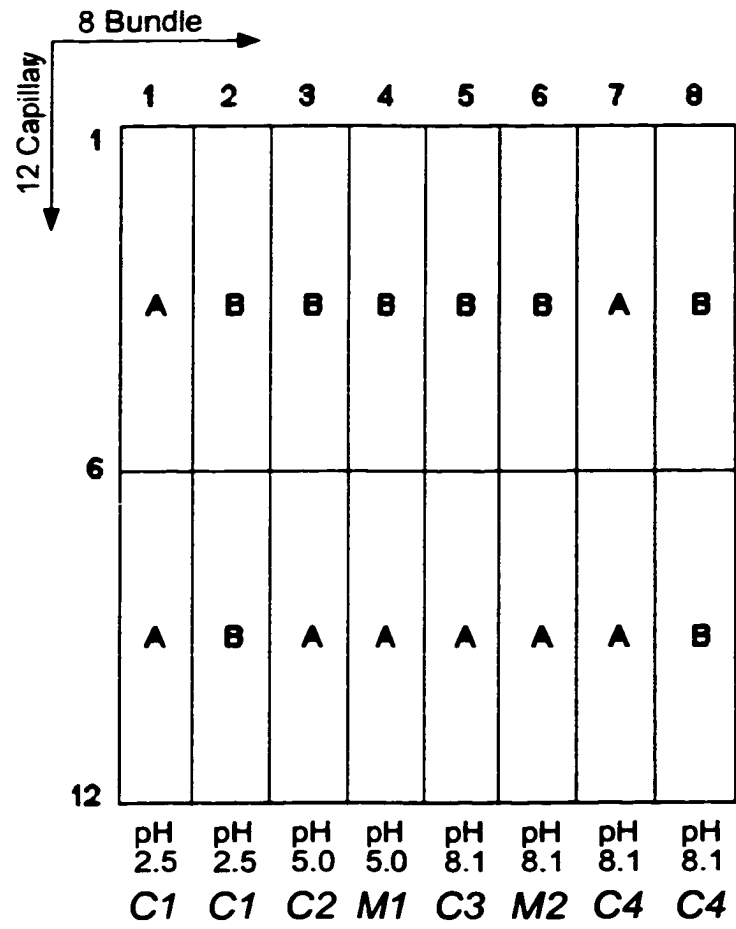
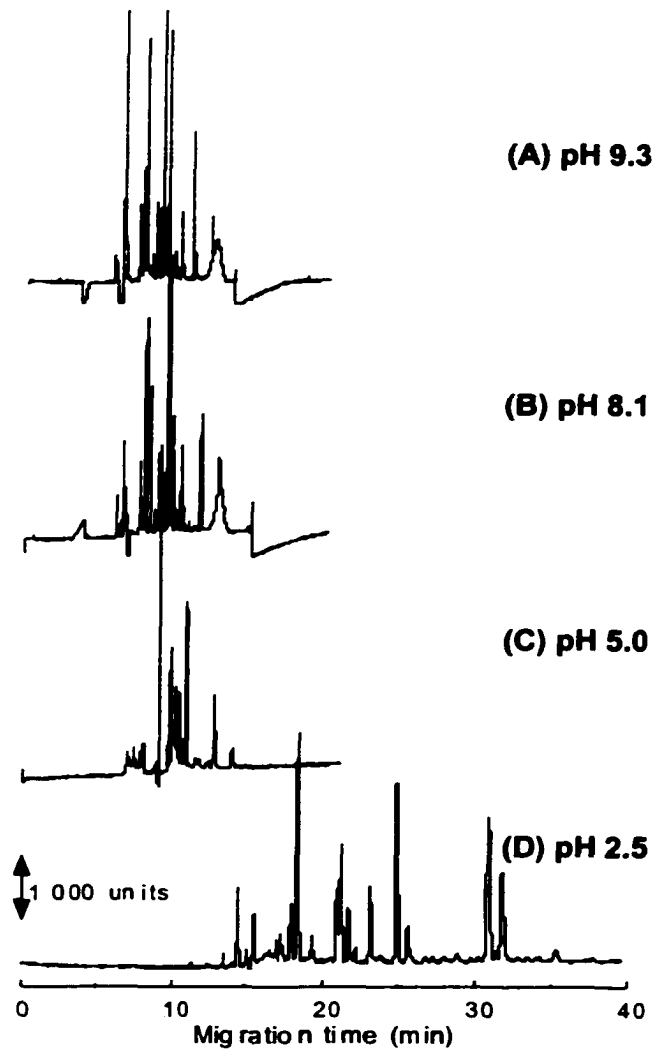


FIGURE 1



**FIGURE 3**

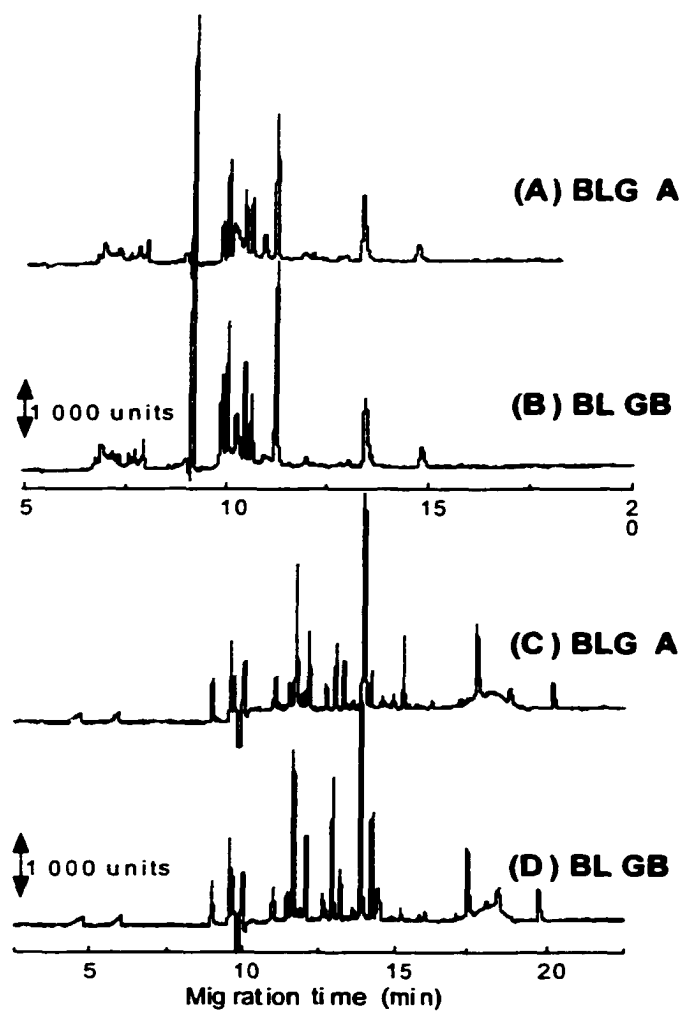
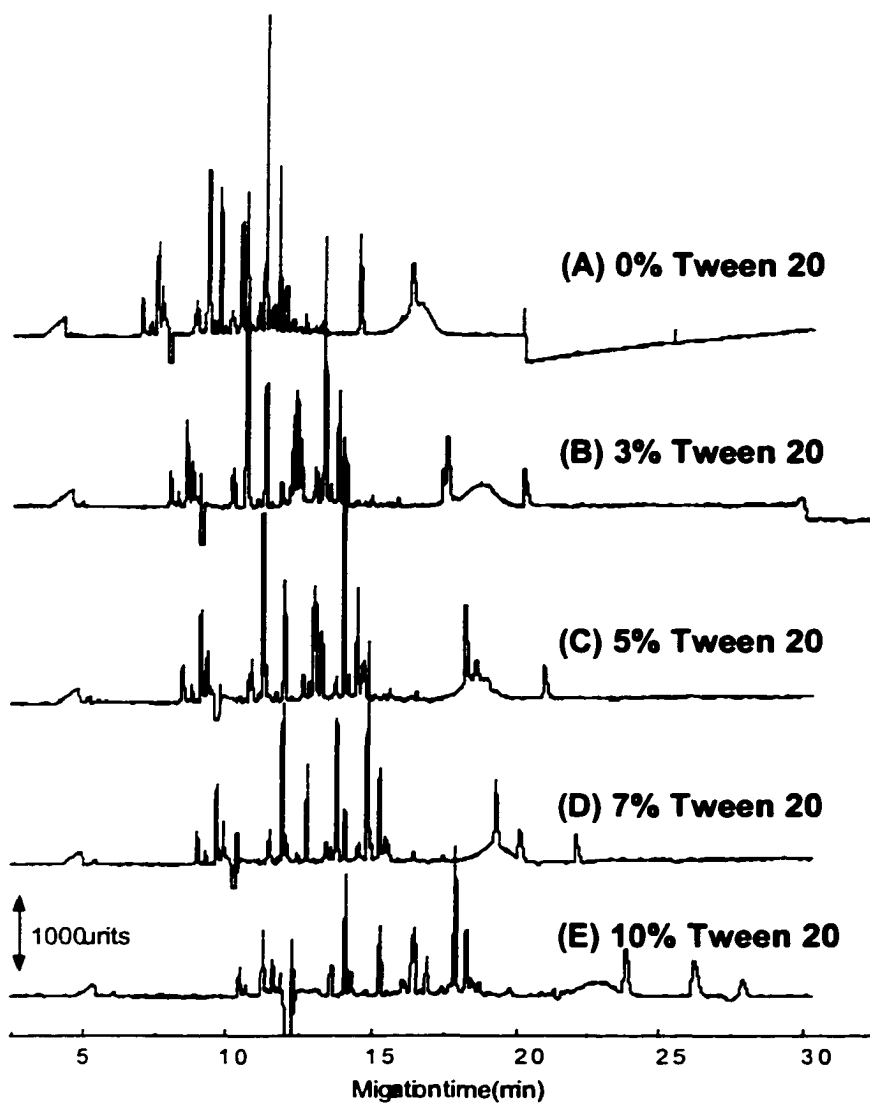
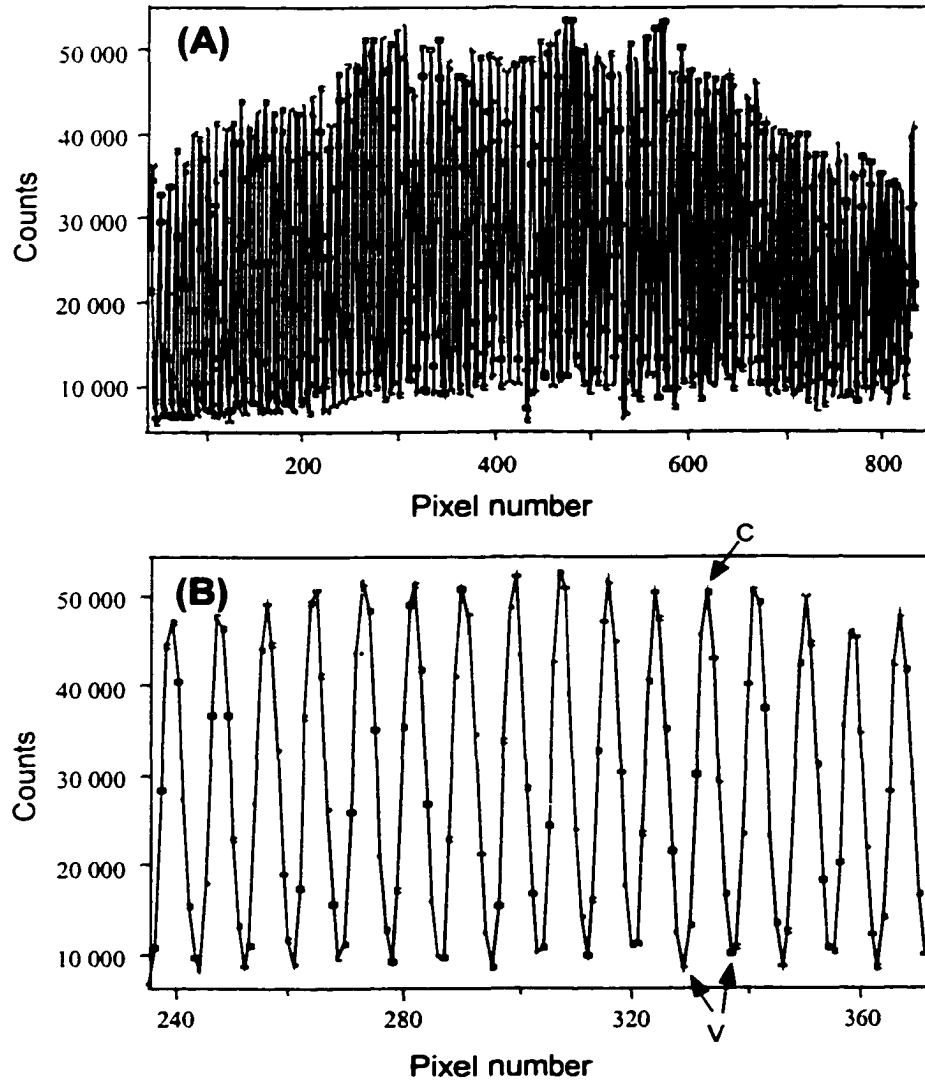


FIGURE 4

**FIGURE 5**

**FIGURE 6**

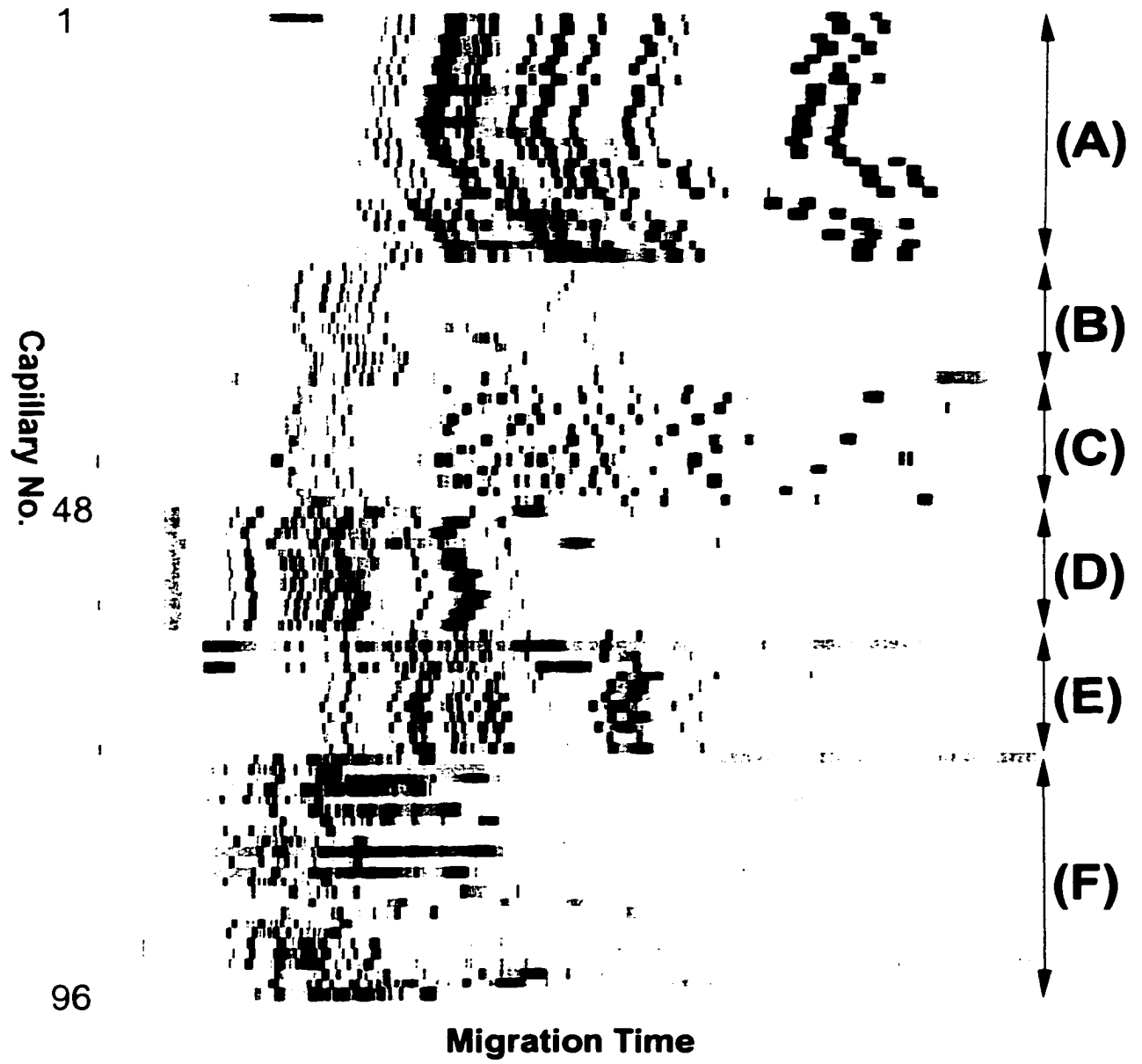
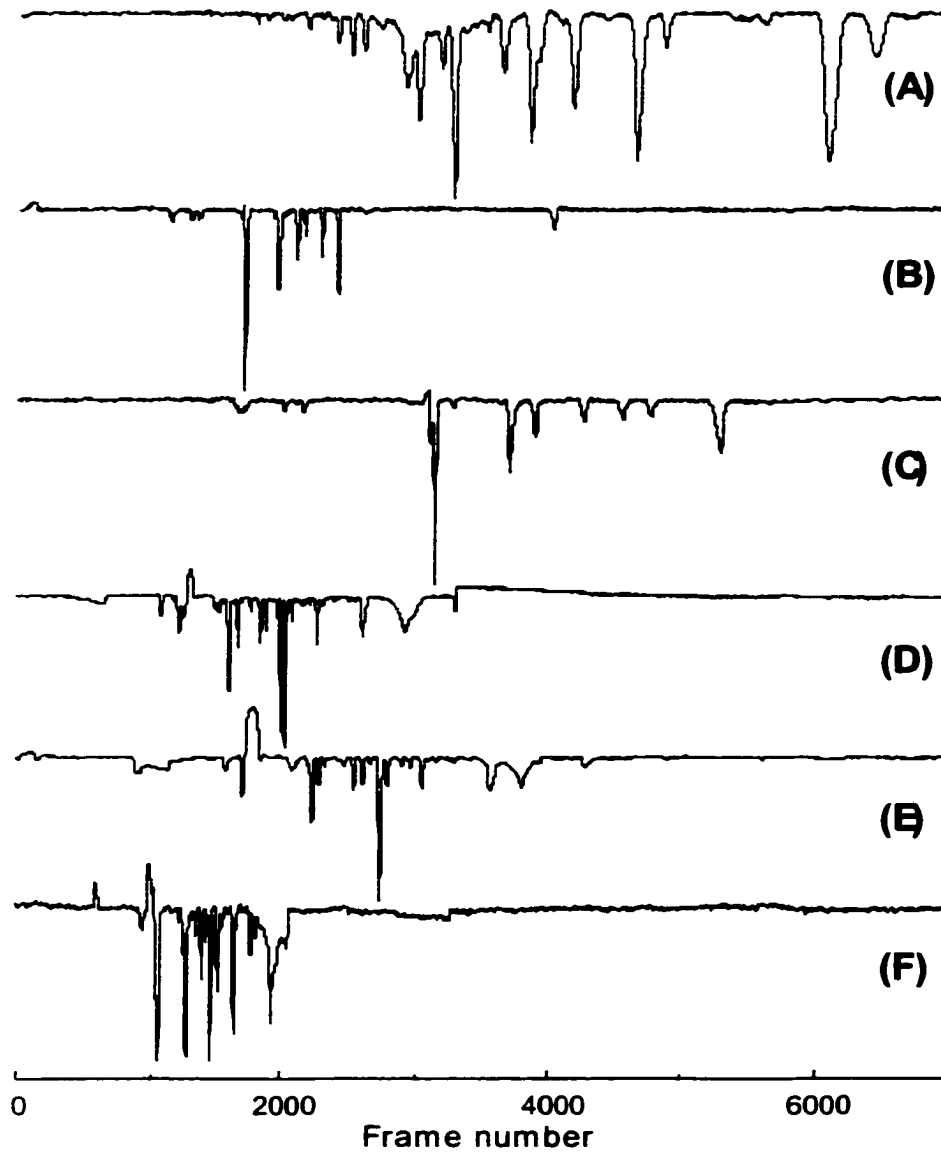
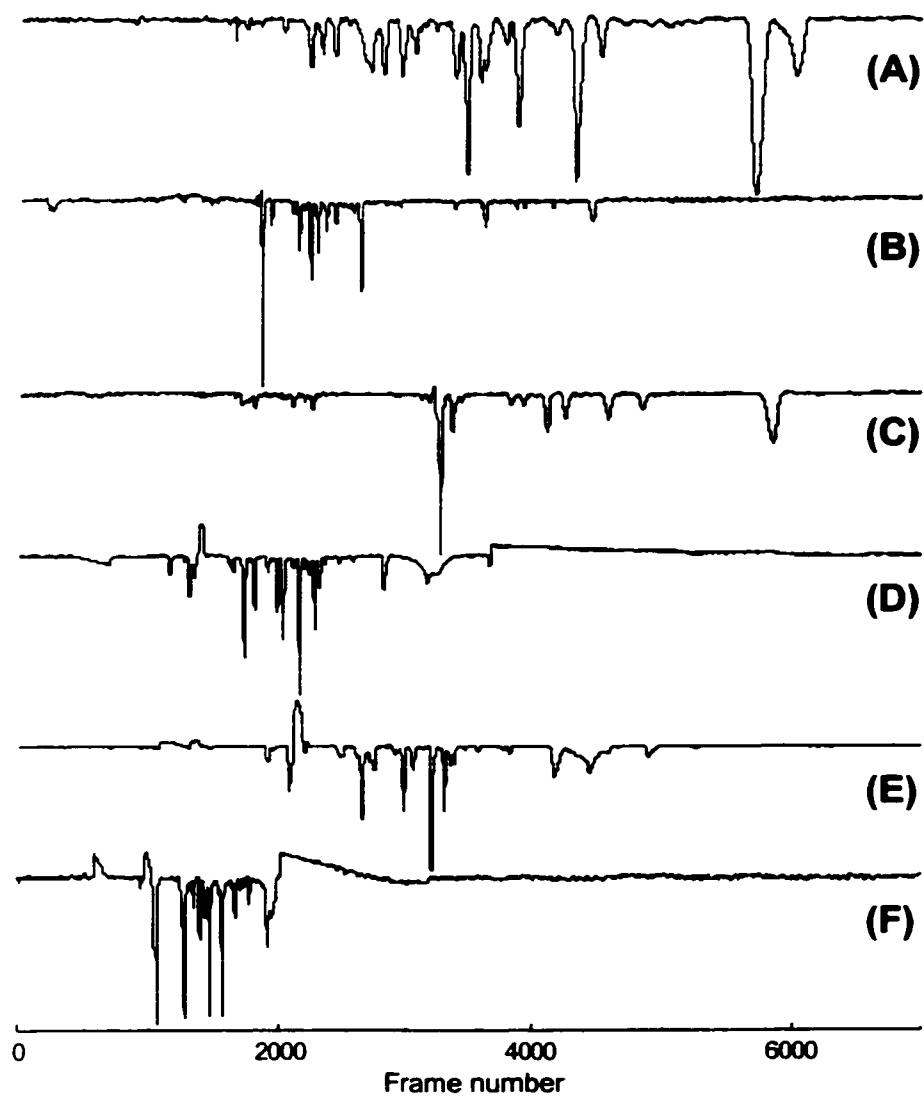


FIGURE 7

**FIGURE 8**

**FIGURE 9**

## CHAPTER 6. COMBINATORIAL SCREENING OF HOMOGENEOUS CATALYSIS AND REACTION OPTIMIZATION BASED ON MULTIPLEXED CAPILLARY ELECTROPHORESIS

A paper submitted to Journal of American Chemistry Society

Yonghua Zhang, Xiaoyi Gong, Haiming Zhang, Richard C. Larock and Edward S. Yeung

Combinatorial chemistry is revolutionizing the discovery of new drugs,<sup>1</sup> novel materials and efficient catalysts<sup>2</sup> by scanning and testing vast numbers of possibilities. In order to fully realize the potential of combinatorial chemistry, general and powerful schemes for high-throughput screening (HTS) are essential.<sup>3</sup> Capillary array electrophoresis (CAE), a high-throughput technique driven by the Human Genome Project, has taken a key role in genomic analysis<sup>4</sup> and potentially will contribute to proteomics as well.<sup>5</sup> We report here the use of CAE for the rapid screening of a homogeneous catalytic reaction in a combinatorial manner. This approach has allowed the effective optimization of a homogeneously catalyzed synthetic organic reaction and the discovery of conditions that produce yields superior to those obtained previously by a less systematic approach.

So far there are several parallel assays for screening homogeneous catalysts. Modifications in UV absorption,<sup>6</sup> fluorescence,<sup>7</sup> color<sup>8</sup> or temperature<sup>9</sup> induced by the catalytic reactions are indicators of catalytic activity. In these approaches, although the relative activity of the catalyst is determined quickly, no quantitative information about the overall yield or the regioselectivity and stereoselectivity of the process can be obtained. It is also necessary that the product exhibit very different measurable properties compared to the solvent or the

reagents. Most of the time, secondary screening is necessary. Mass spectrometry (MS),<sup>10</sup> which has also been widely used to screen catalysts, can provide selective detection. However, to address stereoselectivity, these procedures still tend to be laborious.<sup>11</sup> So far, MS is still a serial, rather than a parallel, approach although the analysis time is reasonably short. Application to the optimization of synthetic organic reactions will require the development of a high-throughput interface.

Separation-based techniques can solve the above problems. Serial methods, which include fast high performance liquid chromatography (HPLC) and capillary electrophoresis (CE), have been used to analyze asymmetric catalysis<sup>12</sup> and alkylation reactions.<sup>13</sup> The throughput that can be achieved with serial separation schemes is low even with special techniques, such as sequential sample injection<sup>14</sup> and sample multiplexing.<sup>15</sup> Multiplex HPLC is another interesting approach,<sup>16</sup> but achieving a high degree of multiplexing, such as 96 capillaries in CAE, is not trivial. Thin-layer chromatography and gel electrophoresis, on the other hand, are difficult to completely automate. The uniqueness of CAE with absorption detection<sup>17</sup> is the easy adaptation to large numbers of samples and near-universal UV detection. Also the injection volume is minimal (10-100 nL) and thus microreactors can be used to save reagent cost.

The model reaction we have used for demonstration of the unique capabilities of multiplexed CAE (Scheme 1) is a new palladium-catalyzed annulation reaction,<sup>18</sup> which readily affords  $\alpha$ -carboline, noteworthy for their biological activity. The optimal reaction conditions and the regiochemistry for this type of annulation are generally highly dependent on the nature of the palladium catalyst and the base employed. Previous efforts to optimize this process employed 5% Pd(OAc)<sub>2</sub>, 10% PPh<sub>3</sub> and Na<sub>2</sub>CO<sub>3</sub> as base and afforded a 1:1 ratio of isomers A/B in essentially a quantitative yield.

The nature of this and other catalytic reactions is that a lot of parameters can affect the yield and “optimum” conditions are often found by trial and error. The general scale on

which we have run the above reaction is 0.25 mmole in 5 mL of DMF. We have reduced the volume to 120  $\mu$ L by using 6 mm O.D. glass tubes sealed at one end arranged in a 96-well format. The individual components were added as a DMF solution or as a slurry by pipetting. Septums were used to cap the reaction tubes to prevent evaporation. All reactions were thus run on a 5  $\mu$ mole scale. Heating was provided by a dry heat bath kept at 110 °C. As an internal standard, 1  $\mu$ mole of norharman was added to the reaction mixture. We did not observe any catalytic effect on the system from the addition of the norharman in control experiments. The CAE experiment is similar to what we have reported before.<sup>5</sup> Organic-based buffers,<sup>19</sup> which are more appropriate for organic synthesis, have been used because of the low solubility of the products in water. Complete separation of the reactant, products (isomer A and B) and internal standard was achieved in 40 mM NH<sub>4</sub>OAc, 0.75% formic acid and 80% DMF with 20% H<sub>2</sub>O at an applied field of 140 V/cm in a fused-silica capillary with effective/total length of 50/75-cm, 50- $\mu$ m I.D. and hydrodynamic injection 15 s at 8-cm height (Fig. S1, Supporting Information).

One important feature of the experimental protocol is that we injected the reaction mixture into CAE without diluting or quenching before analysis. At predetermined times during the reaction, the reaction block was removed from the heating platform, quickly cooled and put under the injection ends of the capillary array. No deleterious effect on the catalytic system was observed by this operation. By avoiding sample manipulation (e.g. by pipetting out of the reaction vials), we can reduce errors associated with transfer and contamination. We also noted that the CAE running buffer should be compatible with the reaction buffer for hydrodynamic injection. When using methanol as the buffer, injection was not uniform. Only about half of the 96 capillaries had adequate signal. It was not possible to increase the injection time, because some capillaries then became overloaded. When DMF-based buffer was used, all 96 channels had uniform signal over three consecutive runs. This buffer compatibility issue for CAE may be attributed to the differences in solution properties,

such as viscosity and surface tension, and was not observed in single-capillary experiments. The total analysis time is typically 60 min, plus 30 min for capillary cleaning. Judging from the resolution, the capillaries could have been shortened to 25% to provide analysis times of 15 min.

By choosing 8 different Pd catalysts and 11 different bases, 88 different combinations have been tested (Fig. S2, Supporting Information). We can determine the total yield (Fig. 1), selectivity (Fig. 2) and reaction kinetics (see Supporting Information) from the electropherograms. Some of the conditions have been tested previously.<sup>18</sup> Our results agree well with those. One example is that by using Pd(OAc)<sub>2</sub> with the ligand PPh<sub>3</sub> as catalyst and Na<sub>2</sub>CO<sub>3</sub> as the base, a total yield of 84% was achieved with virtually no regioselectivity in the microreactor, compared with a quantitative conversion (90% after 17 hours) with no selectivity under the protection of N<sub>2</sub> in a 5 mL reaction. Among all of the bases, inorganic bases proved to be more effective in promoting the reaction. When pyridine or other organic bases were used, the yield was low and some side products appeared. The ability to detect side products is clearly an advantage of CAE. Our preliminary results also reveal several new conditions which are quite effective in this annulation reaction. They are Pd(PPh<sub>3</sub>)<sub>4</sub> with Na<sub>2</sub>CO<sub>3</sub> (C9, 74%), Pd(dba)<sub>2</sub> with K<sub>2</sub>CO<sub>3</sub> (E10, 72%), PdBr<sub>2</sub> plus 2PPh<sub>3</sub> with Na<sub>2</sub>CO<sub>3</sub> (G9, 88%) and PdBr<sub>2</sub> plus 2PPh<sub>3</sub> with K<sub>2</sub>CO<sub>3</sub> (G10, 96%). The latter two are in fact superior to our previous best catalytic condition.<sup>18</sup> Complete regioselectivity is not observed in any of the test conditions (Fig. 2), even though some prove to be better than other systems.<sup>20</sup> The conditions G2, H2, B1 and C1 have some selectivity, but unfortunately their yields are low. There are significant differences in the rates and the shapes of the rate plots (Fig. S3, Supporting Information). This illustrates the need to monitor the reactions at several points in time.

In summary, a new methodology, nonaqueous capillary array electrophoresis coupled with microreaction, is developed to address the throughput needs of combinatorial approaches to homogeneous catalysis and reaction optimization. Catalytic activity, selectivity

and kinetics of the various combinations are determined quickly. Other combinatorial applications that can be envisioned based on this method are screening for asymmetric catalysts and drugs, as well as combinatorial library synthesis.<sup>5</sup>

### Acknowledgement

The Ames Laboratory is operated for the U.S. Department of Energy by Iowa State University under Contract No. W-7405-Eng-82. This work was supported by the Director of Science, Office of Basic Energy Sciences, Division of Chemical Sciences. The Larock group gratefully acknowledges partial financial support from the Petroleum Research Fund, and Kawaken Fine Chemicals Co., Ltd. for some of the palladium reagents.

### Supporting Information

Figures of separations, result of CE separation and kinetics of reactions are shown in Appendix A of this dissertation.

### References

1. *A Practical Guide to Combinatorial Chemistry*, Czarnih, A. and Dewitt, S., Ed., American Chemical Society, Washington DC, 1997.
2. (a) Brocchini, S., James, K., Tangpasuthadol, V., and Kohn, J., *J. Am. Chem. Soc.*, 1997, 119, 4553-4554. (b) Jandeleit, B., Schaefer, D., Powers, T., Turner, H., and Weinberg, W., *Angew. Chem. Int. Ed.*, 1999, 38, 2494-2532.
3. Kyranos, J., and Hogan, J., *Anal. Chem.*, 1998, 389A-395A.

4. Collins, F., Patrinos, A., Jordan, E., Chakravarti, A., Gesteland, R., and Walters, L., *Science*, **1998**, 282, 682-689.
5. (a) Kang, S., Gong, X., and Yeung, E. S., *Anal. Chem.*, accepted. (b) Ma, L.: Gong, X., and Yeung, E. S., *Anal. Chem.*, accepted.
6. (a) Wagner, J., Lerner, R., and Barbas, C., *Science*, **1995**, 270, 1797-1800. (b) Menger, F., Ding, J., Barragan, V., *J. Org. Chem.*, **1998**, 63, 7578-7579.
7. (a) Cooper, A., McAlexander, L., Lee, D., Torres, M., and Crabtree, R., *J. Am. Chem. Soc.*, **1998**, 120, 9971-9972. (b) Shaughnessy, K., Kim, P., and Hartwig, J., *J. Am. Chem. Soc.*, **1999**, 121, 2123-2132. (c) Copeland, G., and Miller, S., *J. Am. Chem. Soc.*, **1999**, 121, 4306-4307.
8. Lavastre, O., and Morken, J., *Angew. Chem. Int. Ed.*, **1999**, 38, 3163-3165.
9. (a) Taylor, S., and Morken, J., *Science*, **1998**, 280, 267-270. (b) Reetz, M., Becker, M., Kuhling, K., and Holzwarth, A., *Angew. Chem. Int. Ed.*, **1999**, 37, 2647-2650.
10. Orschel, M., Klein, J., Schmidt, H., and Maier, W., *Angew. Chem. Int. Ed.*, **1999**, 38, 2791- 2794.
11. Reetz, M., Becker, M., Klein, H., and Stockigt, D., *Angew. Chem. Int. Ed.*, **1999**, 38, 1758-1761.
12. (a) Porte, A., Reibenspies, J., and Burgess, K., *J. Am. Chem. Soc.*, **1998**, 120, 9180-9187. (b) Ding, K., Ishii, A., and Mikami, K., *Angew. Chem. Int. Ed.*, **1999**, 38, 497-501.
13. Gaus, H., Kung, P., Brooks, D., Cook, D., and Cummins, L., *Biotech. & Bioeng.*, **1998/1999**, 61, 169-177.
14. Roche, M., Oda, R., Machacek, D., Lawson, G., and Landers, J., *Anal. Chem.*, **1997**, 69, 99-104.
15. Woodbury, C., Fitzloff, J., and Vincent, S., *Anal. Chem.*, **1995**, 67, 885-890.
16. Zeng, L., and Kassel, D., *Anal. Chem.*, **1998**, 70, 4380-4388.

17. Gong, X., and Yeung, E. S., *Anal. Chem.*, **1999**, 71, 4989-4996.
18. Zhang, H., and Larock, R., manuscript in preparation. For previous annulation chemistry of this type, see Larock, R. C., *J. Organometal. Chem.* **1999**, 576, 111-124.
19. Sahota, R., and Khaledi, M., *Anal. Chem.*, **1994**, 66, 1141-1147.
20. Larock, R. C., Yum, E., and Refvik, M., *J. Org. Chem.*, **1998**, 63, 7652-7662.

**FIGURE CAPTIONS**

FIGURE 1. Total yield of the reaction after 17 hr at 110 °C. dppe = bis(diphenylphosphino)ethane, TBAC = tetra-n-butylammonium chloride, DABCO = 1,4-diazabicyclo[2.2.2]octane. dba = trans, trans-dibenzylideneacetone.

FIGURE 2. Selectivity plot of the two isomers produced in the reactions. P1/P2 is the ratio of the two isomers A and B respectively.

SCHEME 1. The model reaction

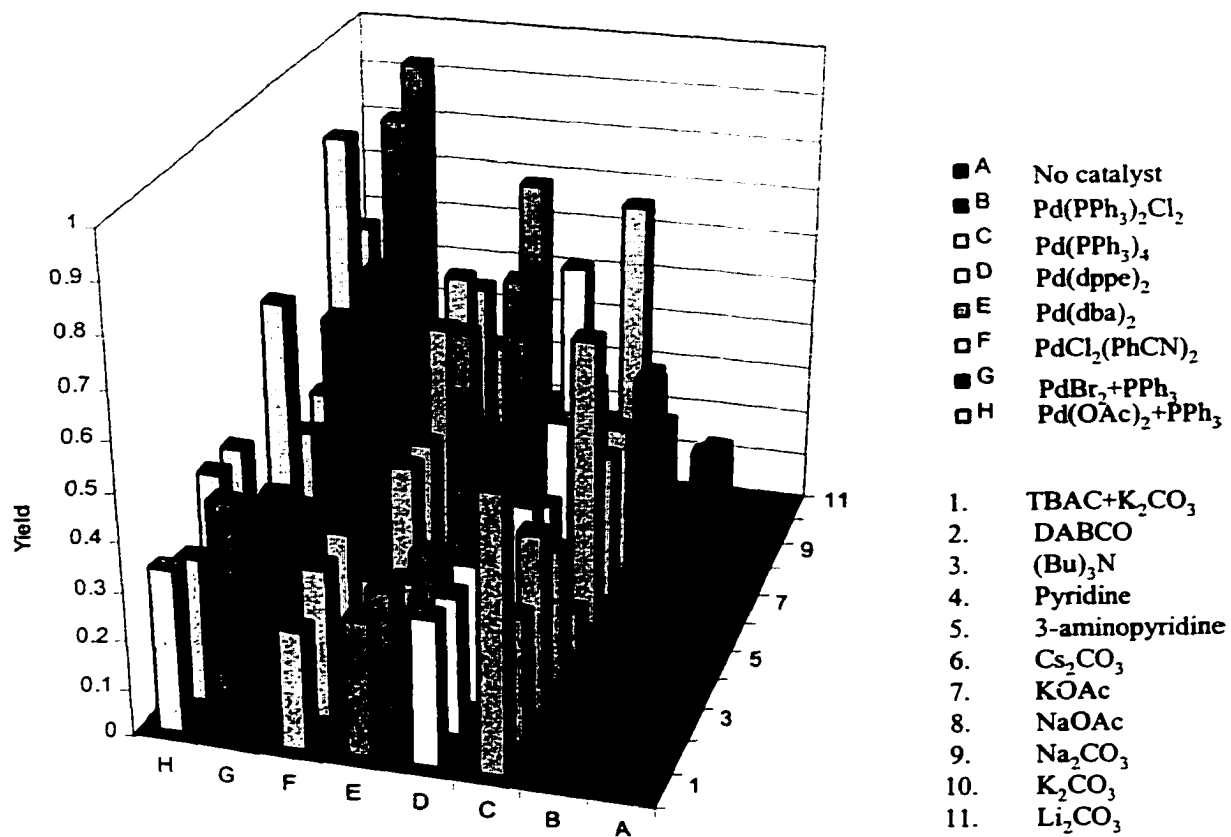


FIGURE 1

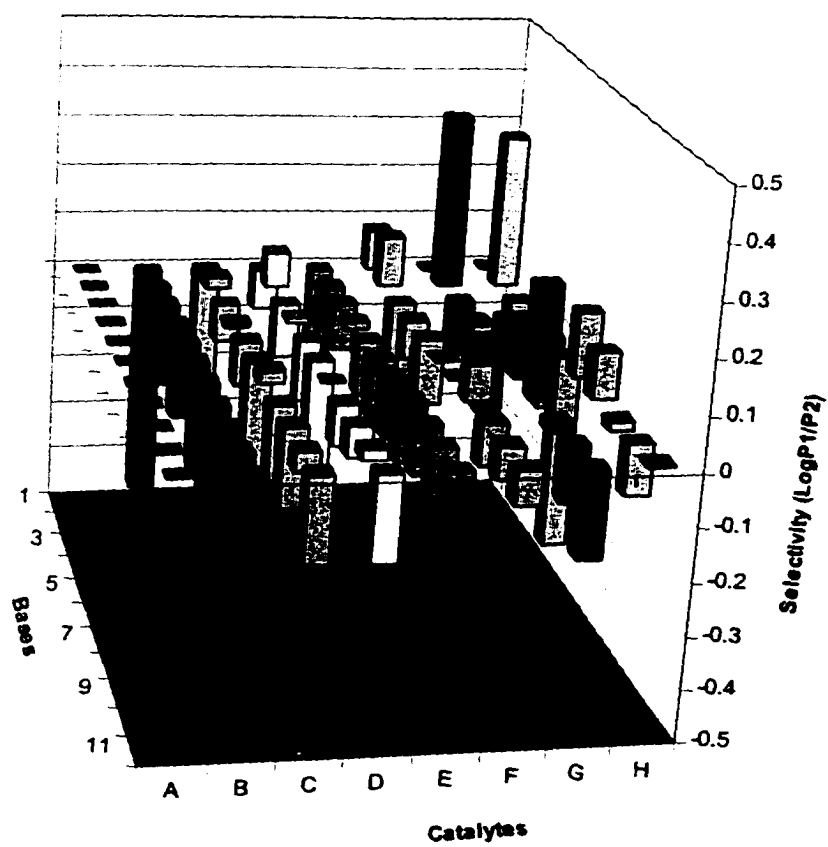
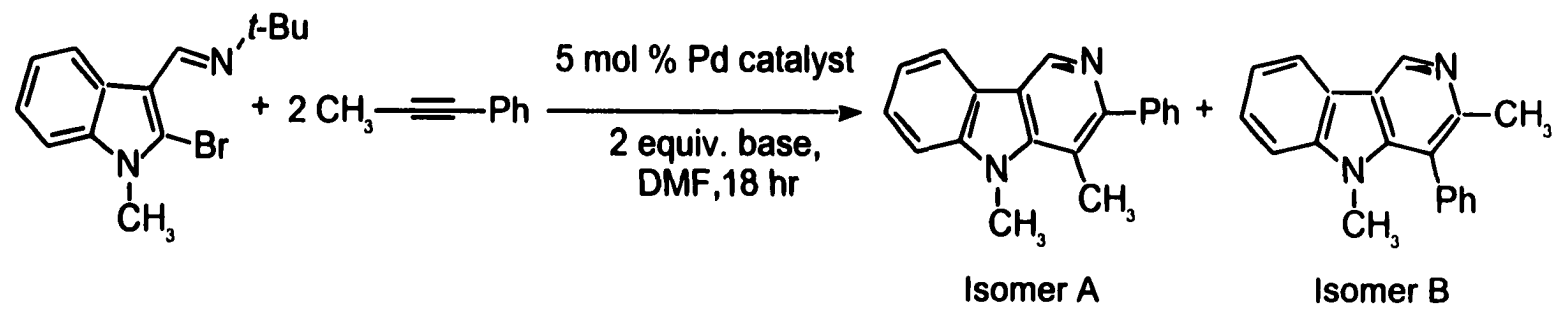


FIGURE 2



**SCHEME 1**

## CHAPTER 7. GENERAL CONCLUSIONS

Massively multiplexed capillary electrophoresis with laser induced fluorescence detection is a proven high-throughput analysis technique for DNA sequencing. To exploit its high-throughput ability in a wider field, we, however, need to develop a more universal detection approach because a variety of molecules of interest do not have strong enough native fluorescence for sensitive detection, and fluorescence labeling tends to be labor-intensive and environment-unfriendly. UV-vis absorbance detection is a natural choice for this purpose because of its ease of implementation and wide applicability for organic and biologically active molecules.

The work in this dissertation has described the development of a novel UV-vis absorbance detection approach for multiplexed capillary electrophoresis. CZE, MEKC, CGE and non-aqueous CE have been demonstrated on 96-capillary array electrophoresis systems using the new detection approach. Uniform separation efficiencies and signal to noise ratios were obtained. The detection limits achievable for this approach were comparable to those of commercial single-capillary electrophoresis instruments using absorption detection. Multiplexed capillary electrophoresis based on the new absorbance detection approach can do almost everything its single-capillary counterpart can do, only with much higher throughput.

Multiplexed capillary electrophoresis based on absorbance detection has been further applied successfully to high-throughput PCR analysis, enzyme assay, peptide mapping, and combinatorial screening of homogeneous catalytic reactions. It has also

been shown that the system can be used to perform high-throughput optimization of reaction and separation conditions.

For the future efforts, several other interesting applications can be envisioned based on multiplexed capillary electrophoresis using absorbance detection. Combinatorial library screening is one example. Based on the multi-modal CE separation of peptides and non-aqueous CE separation of organic molecules that are described in Chapter 4 and Chapter 5 respectively, both peptide libraries and organic libraries can be readily analyzed with high-throughput using our absorbance-detection based multiplexed capillary electrophoresis technique. By adding ligands into the separation buffer, we can adapt the technique into multiplexed affinity capillary electrophoresis, which can be employed to perform high-throughput binding assays for drug activity screening. From the point of view of instrumentation, further throughput improvement can be achieved by full automation and integration of microreaction and sample preparation techniques into multiplexed CE analysis systems. Even more highly multiplexed capillary electrophoresis systems could also be built base on absorbance detection if photodiode arrays with more pixels, light sources with larger emitting areas, and camera lenses with bigger apertures are available.

**APPENDIX A. SUPPORTING INFORMATION FOR CHAPTER 6**

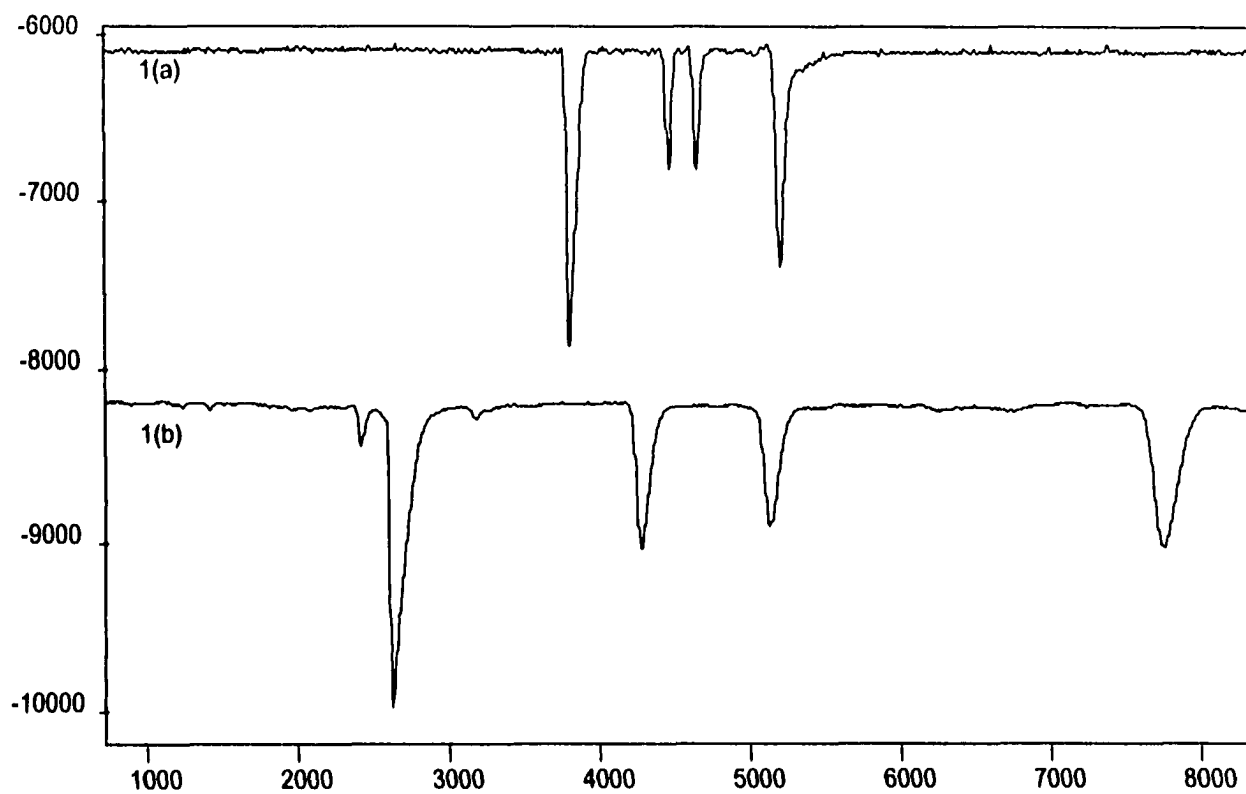


**FIGURE A1.** Separations of reactant, products (isomer A and B) and internal standard (Norharman) by two different solvents. Buffer, 40mM  $\text{NH}_4\text{Ac}$ , 0.75% formic acid in (a) MeOH (b) 80% DMF with 20%  $\text{H}_2\text{O}$ . Applied electric field, 140V/cm. Column, bare fused-silica capillary with effective/total length of 50/75-cm and 50- $\mu\text{m}$  I.D. Hydrodynamic injection 15s at 8-cm height.

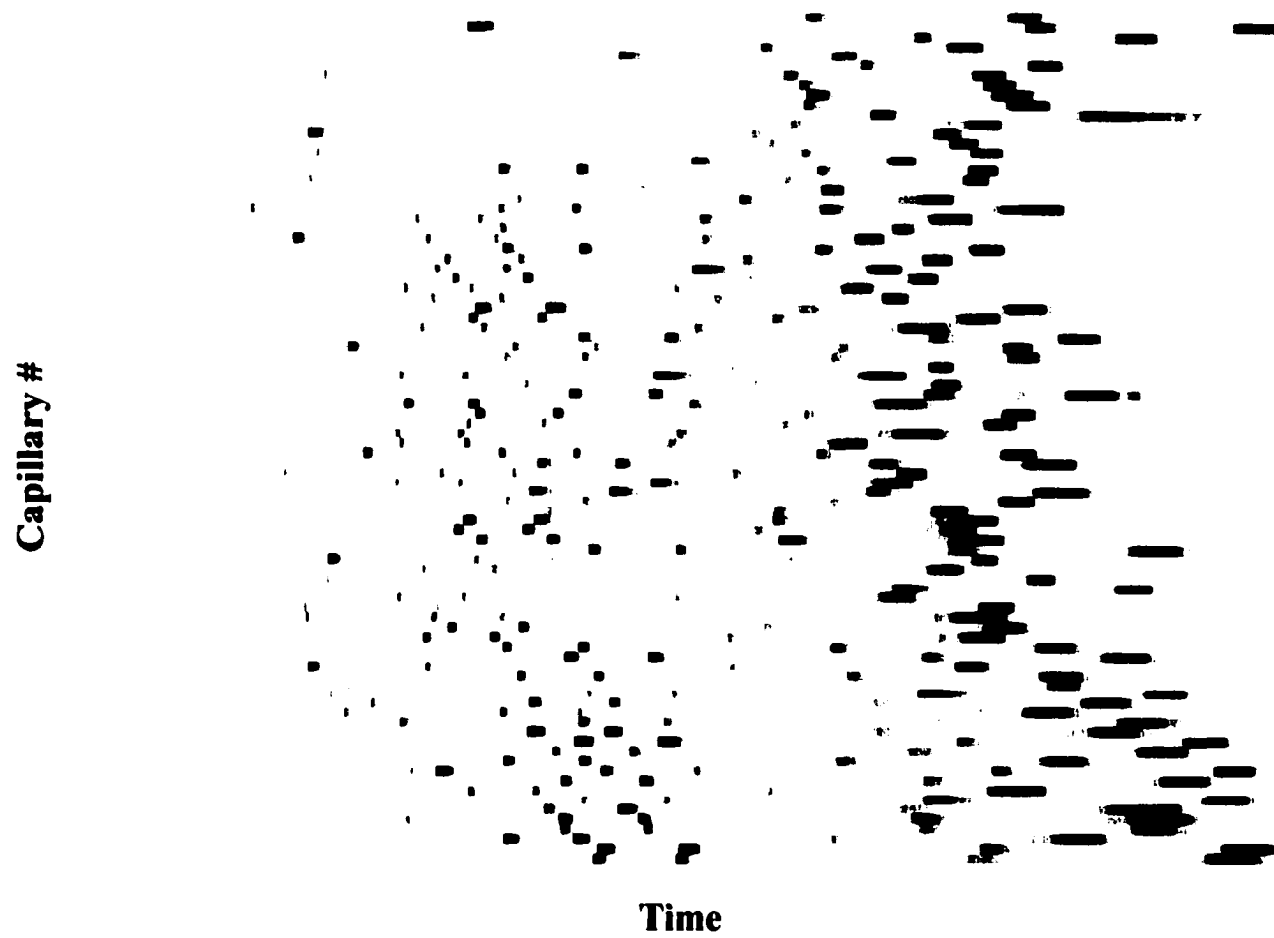


**FIGURE A2.** Result of CE separation of reaction mixtures in the 96-capillary array. Separation condition as in FigureA1 (b). Hydrodynamic injection 1 min.

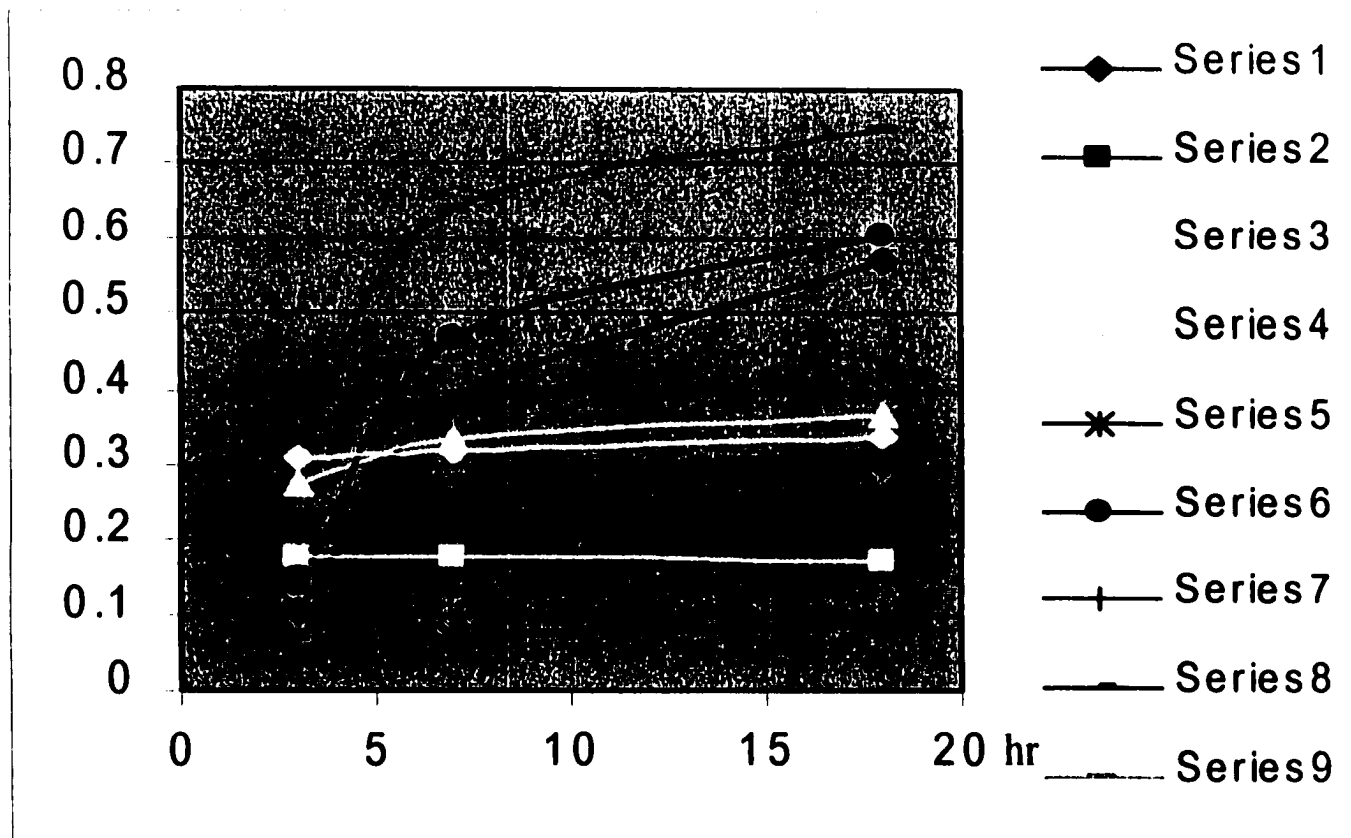


FIGURE A3. The kinetics of reactions using  $\text{Pd}(\text{PPh}_3)_4$  as catalyst and 11 different bases. Combination of bases can be found in FIGURE 1, Chapter 6 in this dissertation.

**APPENDIX B. DATA ACQUISITION AND PROCESSING SOFTWARE  
FOR PHOTODIODE ARRAY**

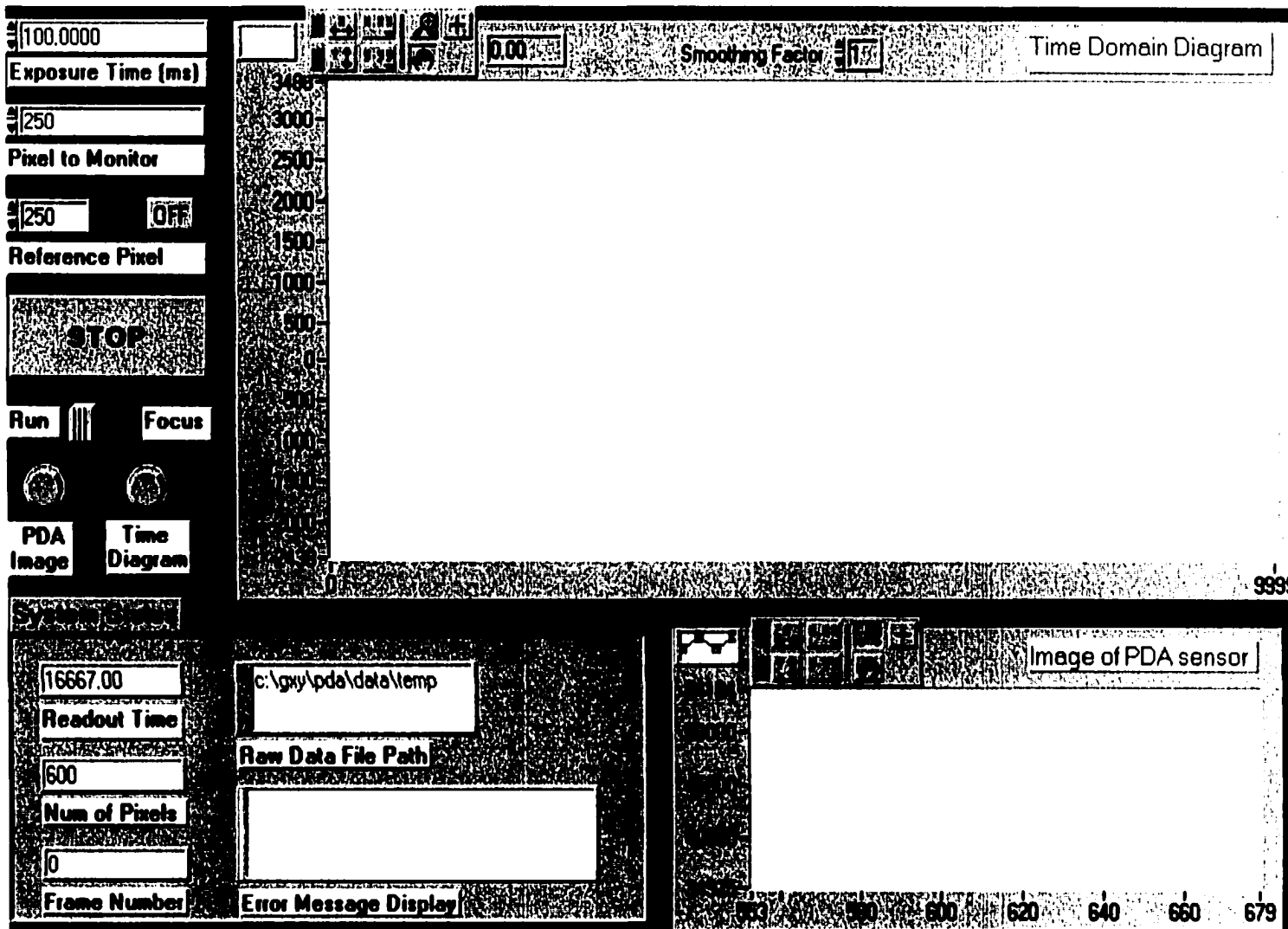


FIGURE B1. Front Panel of Data Acquisition Software for Photodiode Array

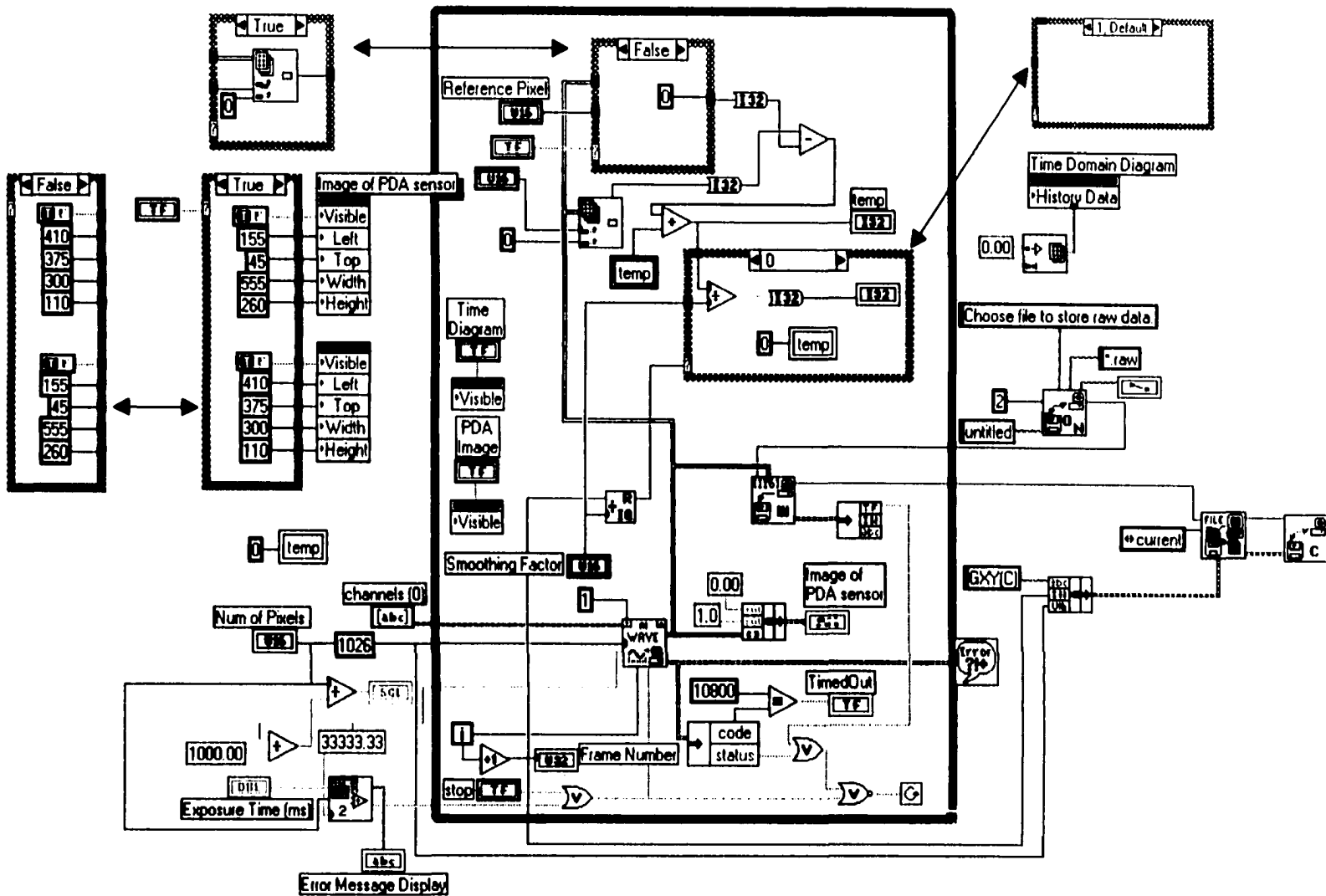


FIGURE B2. Block Diagram of Data Acquisition software for Photodiode Array

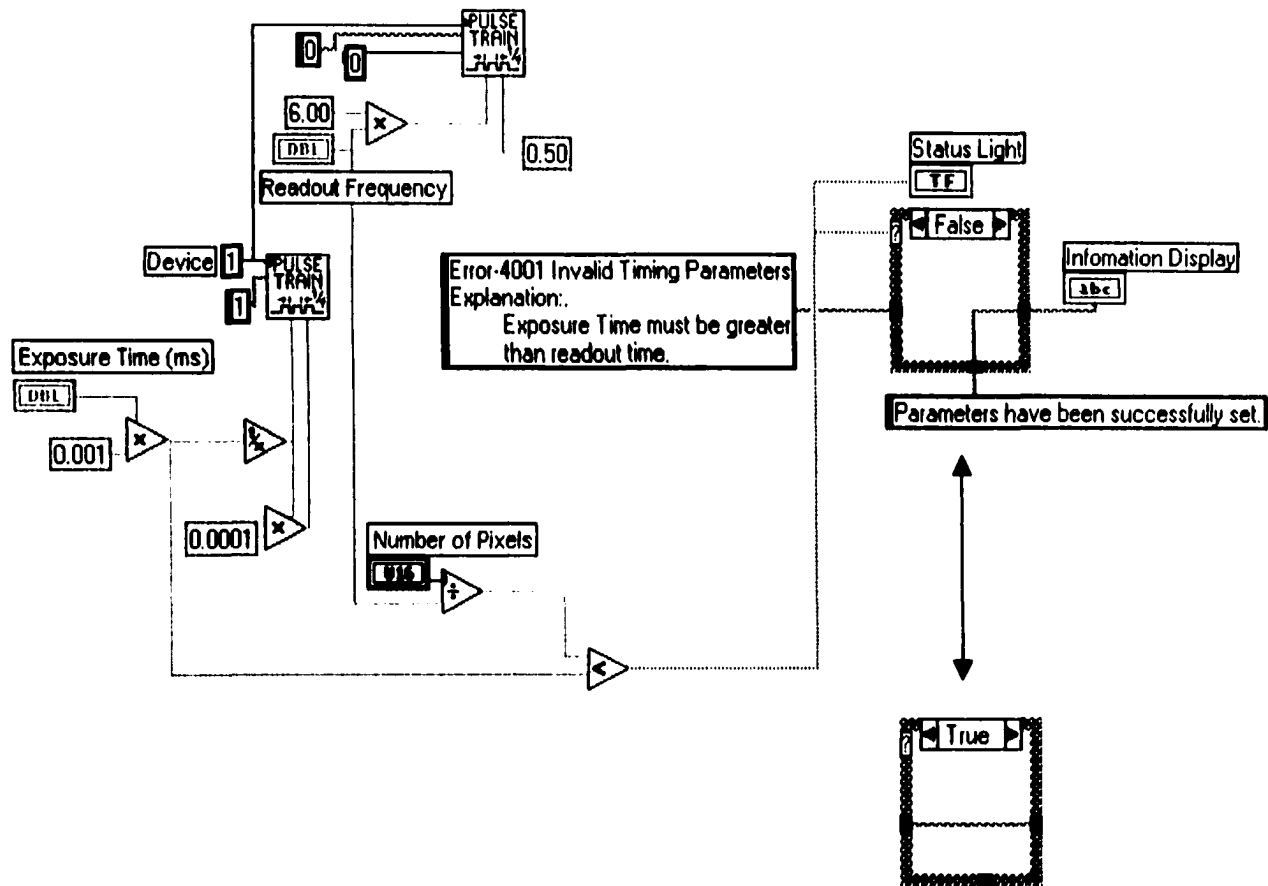


FIGURE B3. Block Diagram of Pulse Generation sub-VI for Photodiode Array Data Acquisition

Output File Path  
  
Frame to Begin  
  
Frames to Extract  
 (0: All)  
  OFF  
Reference Pixel

Scan to Perform

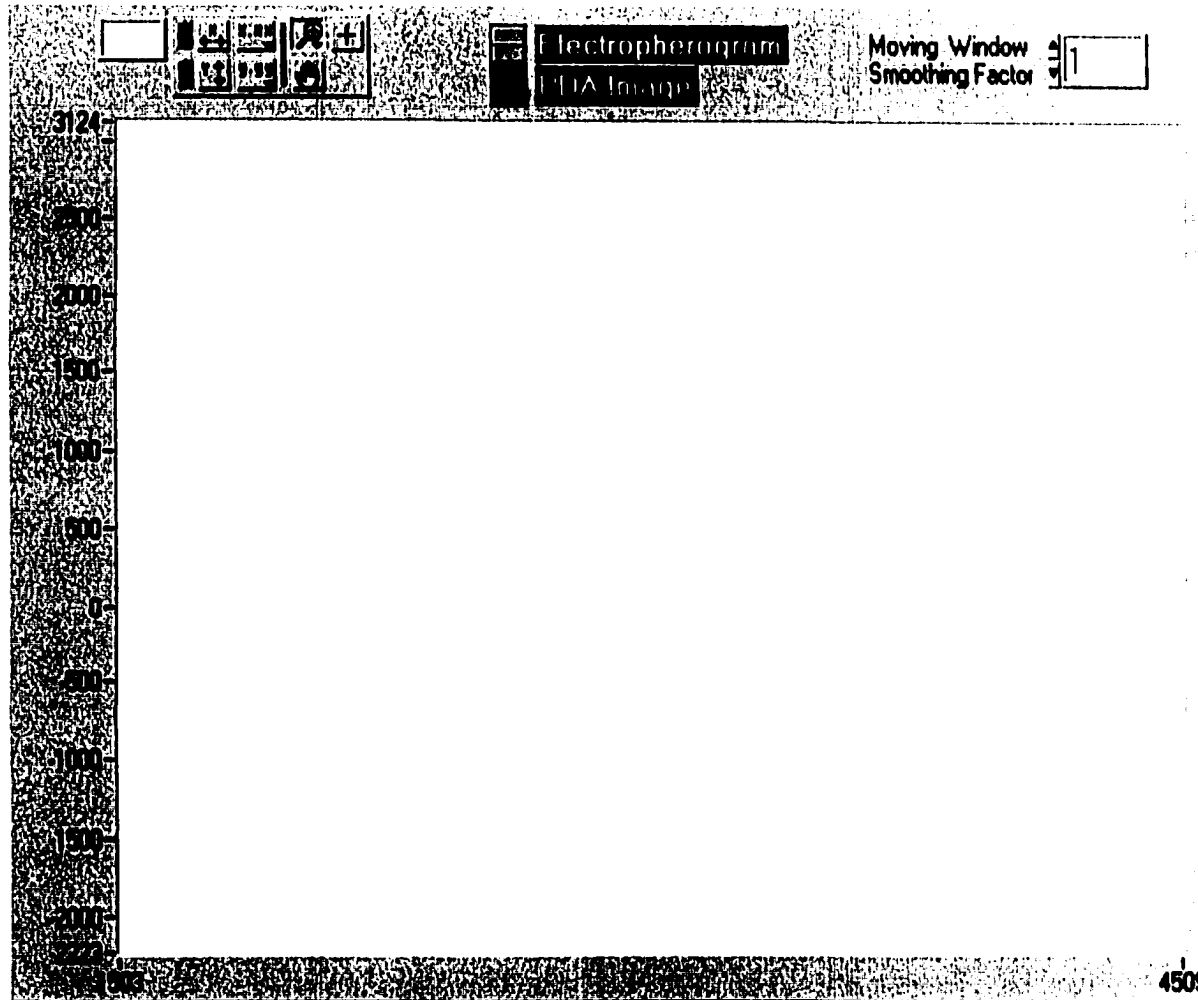
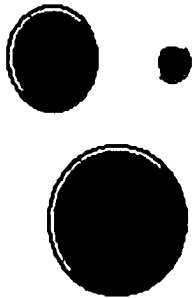


FIGURE B4. Front Panel of Data Processing Software for Photodiode Array

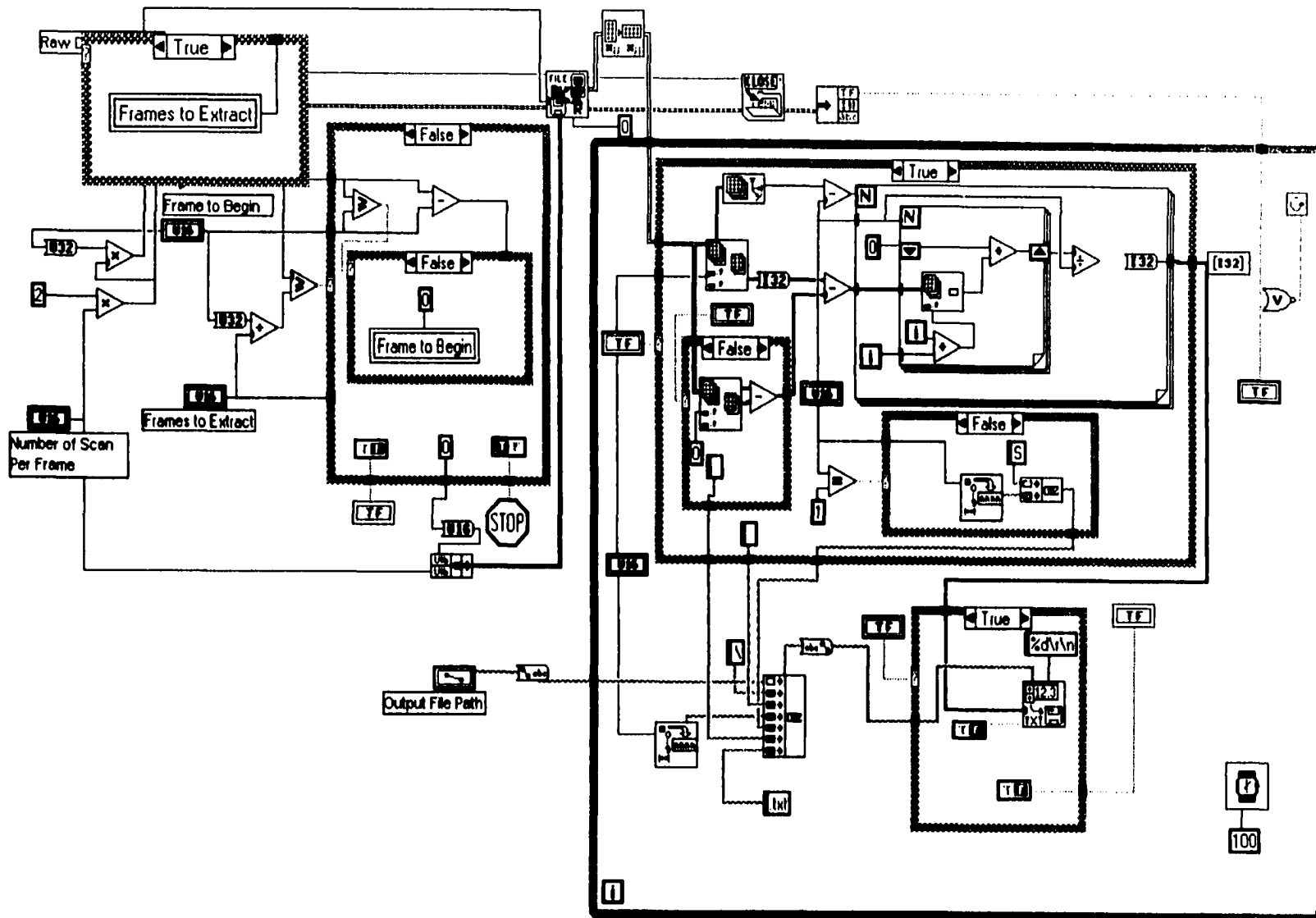


FIGURE B5 Block Diagram of Data Processing Software for Photodiode Array

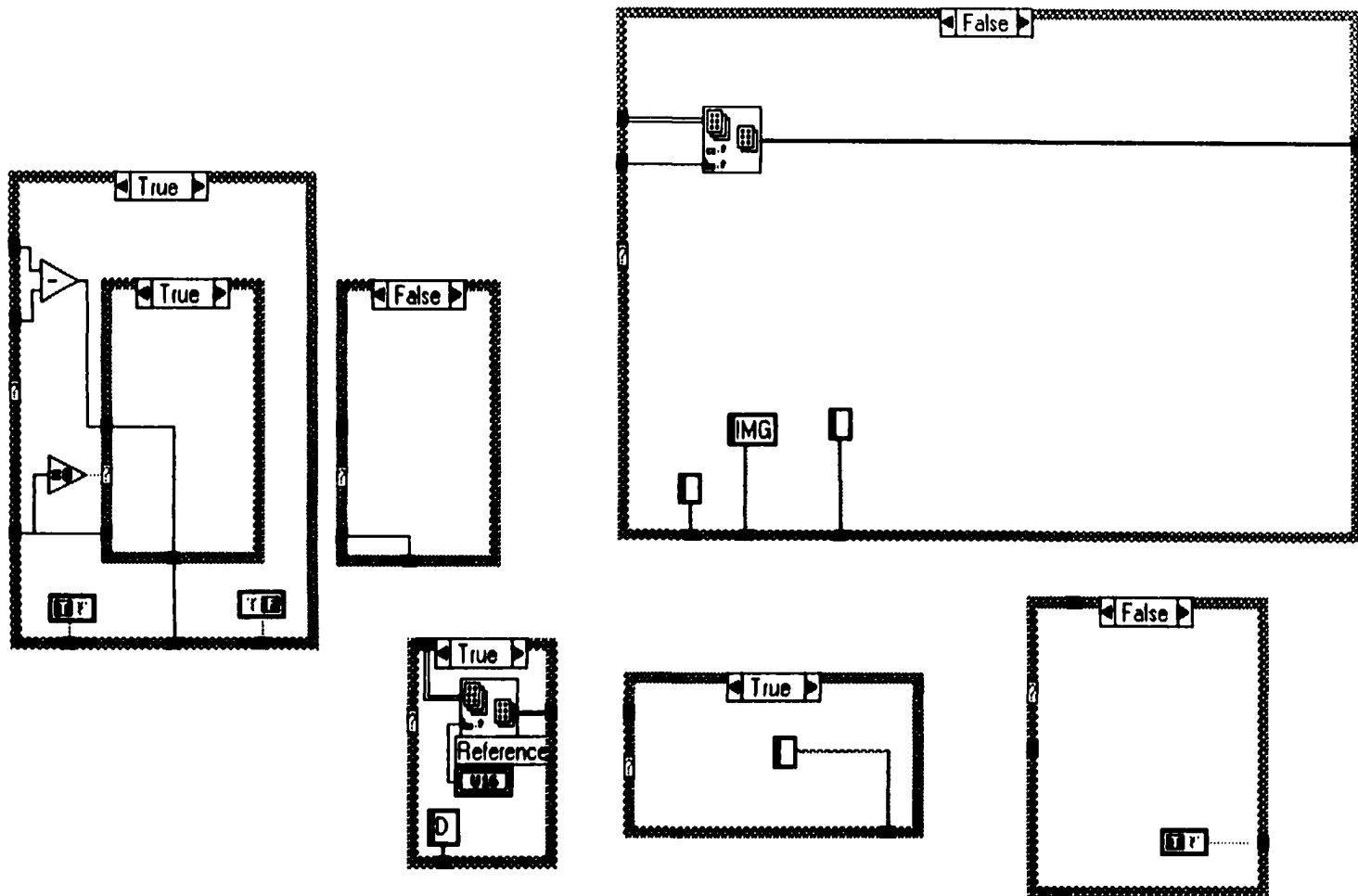


FIGURE B6. Hidden Frames in Figure 6

## ACKNOWLEDGEMENT

First of all, I would like to express my appreciation for Dr. Edward S. Yeung. As my doctoral advisor, he had provided me not only academic guidance but also spiritual encouragement through the four years when I was at Iowa State. More importantly, he stands as a brilliant scientist as well as a decent person whom I can look up to, which will be invaluable to me for the rest of my life.

I would also like to acknowledge the support of Dr. Porter, Dr. Johnson, Dr. Woo, Dr. Hargrove, and Dr. Thiel as my POS committee members.

I want to thank Yonghua, Lianjia and Dr. Kang for cooperating with me on different research projects. I also want to thank Homing Pang, Hongdong Tang, Michael Shortreed, Yingfa Ma, David Gao, Hui Su, and all the others who gave me a lot of help on my research. What's more, I want to thank all the Dr. Yeung's group members for the wonderful time I had with them in the Ames, Iowa, a Midwest American town where I knew nobody four years ago, but now my wife and I will remember forever as where our own first home is.

I feel deeply sorry that my late father could not make it to see me finishing my doctoral degree. I know that he would have been very proud of me, as he was always of his children. I would like to dedicate the dissertation to him, and I know in my heart that he knows how much I am proud of being his son.

I would also like to say thank you to my mom and my sister. Although we are separate physically for the time being, but in the bottom of our hearts we are always a family together, sharing the happiness and sadness in our lives.

Finally, I would like to thank my wife Yan, who was so brave to marry me when I was legitimately broke, who has been so patient and tolerant to me when I was stressed out, and with whom I am so fortunate to be able to share the rest of my life.